

5-2016

Role of microRNA-21 in atherogenesis.

Rihab Hamed-Berair
University of Louisville

Follow this and additional works at: <https://ir.library.louisville.edu/etd>

Part of the [Biochemistry Commons](#), [Medical Biochemistry Commons](#), and the [Molecular Biology Commons](#)

Recommended Citation

Hamed-Berair, Rihab, "Role of microRNA-21 in atherogenesis." (2016). *Electronic Theses and Dissertations*. Paper 2431.
<https://doi.org/10.18297/etd/2431>

This Doctoral Dissertation is brought to you for free and open access by ThinkIR: The University of Louisville's Institutional Repository. It has been accepted for inclusion in Electronic Theses and Dissertations by an authorized administrator of ThinkIR: The University of Louisville's Institutional Repository. This title appears here courtesy of the author, who has retained all other copyrights. For more information, please contact thinkir@louisville.edu.

ROLE OF MICRORNA-21 IN ATHEROGENESIS

By

Rihab Hamed-Berair

B.Sc., Alahlia University, Sudan, 1998

M.Sc. Khartoum University, Sudan, 2002

M.S., University of Louisville, 2013

A Dissertation

Submitted to the Faculty of the
School of Medicine of the University of Louisville
in Partial Fulfillment of the Requirements
for the Degree of

Doctor of Philosophy in Biochemistry and Molecular Biology

Department of Biochemistry and Molecular Genetics
University of Louisville
Louisville, Kentucky

May 2016

Copyright 2016 by Rihab E. Hamed-Berair

All rights reserved

ROLE OF MICRORNA-21 IN ATHEROGENESIS

By
Rihab Hamed-Berair
B.Sc., Alahlia University, Sudan, 1998
M.Sc. Khartoum University, Sudan, 2002
M.S., University of Louisville, 2013

A Dissertation Approved on
March 18, 2016

By the following Dissertation Committee:

Dissertation Director, Sanjay Srivastava, Ph.D.

Aruni Bhatnagar, Ph.D.

Russel Prough, Ph.D.

Kenneth S Ramos, Ph.D.

Yong Li, Ph.D.

Barbara J. Clark, Ph.D.

DEDICATION

This dissertation is dedicated to my wonderful husband, Dr. Yasier Basheer-Gowi, for his
endless support, encouragement, and love.

And to my
beautiful children Eltayeb, Ahmed, Reema, and Yusuf for surrounding me with love and
laughter.

It has always been fun surrounded by loved ones.

ACKNOWLEDGEMENTS

I am very grateful to my mentor Dr. Sanjay Srivastava for his valuable guidance and patience throughout this process. This dissertation would not have been possible without his encouragement and support. I would like to thank my committee members, Dr. Aruni Bhatnagar, Dr. Russel Prough, Dr. Kenneth Ramos, Dr. Barbara Clark, and Dr. Yong Li, for their valuable advice and directions in completing this project. I thank Dr. Srinivas Sithu for all his help and time, especially helping me format my dissertation. Many thanks to current and previous members of Srivastava's lab, Nalinie Wickramasinghe, Abhinav Agarwal, Millie Winner, Patrick Whang, Michelle Smith, Marina Malovichko for helping me throughout this project, and without them this would not have been possible. I am thankful to Dr. Marcin Wysoczynski for his assistance with the bone marrow transplant, which was crucial to my dissertation project. I thank Jasmit Shah for microarray data analysis and in helping me to understand our dataset. I am thankful to the Department of Biochemistry and Molecular genetics and special thanks to Dr. William Dean for believing in me.

I would like to give special recognition to my father who was a remarkable man and had the potential to do great things in the world. He will always be in our hearts. I would like to thank my mom, Mrs. Aisha Abdallah, for instilling in me the importance and power of hard work and higher education, for shaping me into the person I am today, and for taking care of my kids during this work. I would like to thank my in-laws Mrs. Suad

Ahmed and Mr. Awad Basheer-Gowi. Without their encouragement and help I would not have been able to balance a Ph.D. and family duties. Thanks to all my friends who encouraged me to keep going even during tough times. A special thanks to Sasha for her constant support, advice, and valuable friendship which made graduate school more joyful. I thank Shubha (Dr. Ghosh) for listening and always encouraging me. Finally thanks to all my community friends in Louisville for all the help and support.

ABSTRACT

ROLE OF MICRORNA-21 IN ATHEROGENESIS

Rihab Hamed-Berair

March 18, 2016

MicroRNA-21 (miR-21) is an evolutionarily conserved microRNA, abundant in most cardiovascular tissues. It has been implicated in the pathogenesis of several cardiovascular diseases including restenosis, myocardial infarction, and heart failure. However, little is known about the contribution of miR-21 in atherosclerosis. My data show that expression of miR-21 is increased by >1.5-fold in murine atherosclerotic lesions and by 1.5-2.0-fold in the macrophages of Western diet (WD)-fed LDLR-KO mice (for 12-20 weeks). *In vitro*, LDL, oxidized LDL, acetylated LDL and LPS induced miR-21 by 2-4-fold and down-regulated its target protein, PDCD4, in bone marrow-derived macrophages. Basally, macrophages isolated from miR-21-KO mice showed induction of several cytokines and chemokines, and significantly increased early and late apoptosis. Stimulation of miR-21-KO macrophages with interferon γ +LPS polarized the macrophages to the pro-inflammatory M1 phenotype (increased expression of CD11c and CD86). LPS increased the nuclear translocation of NF- κ B and increased the formation of several pro-inflammatory cytokines by 3-45-fold in miR-21-KO

macrophages. Staurosporine and 4-hydroxynonenal increased both early and late apoptosis of miR-21-KO macrophages (2-4-fold). This was accompanied by increased cleavage of caspase-3, caspase-7, and caspase-9. Transplantation of bone marrow cells from miR-21-KO to LDLR-KO mice, followed by 12 weeks of WD, increased the lesion formation (1.7-fold), apoptosis (3-fold) and necrosis (1.6-fold) in the aortic valve of miR-21-KO chimeric mice. This was accompanied by increased staining for IL-1 β , IL-12, cleaved caspase-3, and cleaved caspase-9 in the plaques of miR-21-KO chimeric mice. Collectively, these data suggest that miR-21 prevents atherosclerosis by inhibiting macrophage apoptosis, necrosis, and inflammation.

TABLE OF CONTENTS

	PAGE
DEDICATION.....	iii
ACKNOWLEDGEMENTS	iv
ABSTRACT	vi
LIST OF FIGURES	x
LIST OF TABLES	xiii
CHAPTERS 1: GENERAL INTRODUCTION	
ROLE OF MICRORNAS IN ATHEROSCLEROSIS.....	1
PROJECT OBJECTIVES.....	30
CHAPTERS 2: EXPRESSION OF MICRORNA-21 IN RESPONSE TO ATHEROGENIC AND INFLAMMATORY STIMULI, AND CONTRIBUTION OF MICRORNA-21 IN ATHEROGENESIS	
Introduction	31
Experimental procedures	32
Results	40
Discussion	88
CHAPTERS 3: CONTRIBUTION OF MICRORNA-21 IN REGULATING MACROPHAGE INFLAMMATION AND APOPTOSIS <i>IN VITRO</i> AND IN MURINE ATHEROSCLEROTIC PLAQUES	
Introduction	93
Experimental procedures	94

Results	98
Discussion	138
CHAPTERS 4: CONCLUSIONS AND FUTURE DIRECTIONS.....	143
REFERENCES	147
CURRICULUM VITAE.	160

LIST OF FIGURES

FIGURE	PAGE
1. Biogenesis of miRNAs.....	11
2. Bone marrow transplant protocol.....	37
3. Heatmap of miRNAs in aortic lesions.....	46
4. PLS-DA Principal component analysis of lesional miRNAs of LDL receptor knockout (LDLR-KO) mice maintained on normal chow or Western diet for 12 weeks.....	50
5. Variable Importance in Projection (VIP) scores of top 25 miRNAs that discriminate LDL receptor knockout (LDLR-KO) mice maintained on normal chow from those maintained on Western diet for 12 weeks.....	51
6. Volcano plots of differentially expressed miRNAs in atherosclerotic lesions of normal chow and Western diet-fed LDLR-KO mice.....	52
7. Volcano plots of comparative miRNA expression profiles of macrophages/inflammation in the aorta of normal chow and Western diet-fed LDLR-KO mice.....	55
8. Volcano plots of comparative miRNA expression profiles of macrophages/apoptosis in the aorta of normal chow and Western diet-fed LDLR-KO mice.....	57
9. Volcano plots and VIP scores of comparative miRNA expression	

profiles of macrophage /inflammation/apoptosis in the aorta of normal chow and Western diet-fed LDLR-KO mice.....	59
10. Effect of Western Diet on the expression of miR-21 in atherogenic mice.....	64
11. Expression of miR-21 by atherogenic stimuli in BMDM.....	66
12. Foam cell formation in miR-21 deficient BMDM.....	69
13. Gating strategy used to identify bone marrow cells by flow cytometry.....	71
14. Characterization of miR-21-KO mice.....	73
15. Formation of different blood and immune cells from hematopoietic progenitor cell.....	73
16. Gating strategy to identify circulating immune cells by flow cytometry.....	77
17. Expression of miR-21 in the chimeric mice.....	80
18. Plasma lipids in chimeric mice.....	83
19. Effect of miR-21 deficiency on lesion formation in the aortic valve.....	85
20. Lesion cellularity of miR-21 deficient chimeric mice.....	87
21. Effect of miR-21 deficiency on the polarization of macrophages to M1 phenotype.....	100
22. Effect of miR-21 deficiency on the polarization of macrophages to M2 phenotype.....	101
23. Cytokines and chemokine levels in LPS-stimulated miR-21-KO macrophages.....	109
24. Formation of IL-6 in LPS-stimulated miR-21-KO macrophages.....	110
25. Abundance of IL-1 β in atherosclerotic lesions of miR-21-KO chimeric LDLR-KO mice.....	112
26. Abundance of IL-12 in atherosclerotic lesions of miR-21-KO chimeric LDLR-KO mice.....	113
27. Effect of miR-21 deficiency on the activation of NF- κ B.....	115

28. Effect of miR-21 deficiency on the phosphorylation of p38 MAP Kinase.....	117
29. Effect of miR-21 deficiency on the ERK activation.....	118
30. Effect of miR-21 deficiency on its target proteins.....	120
31. MiR-21 deficiency increases macrophage apoptosis.....	123
32. MiR-21 protects macrophages from staurosporine-induced apoptosis.....	125
33. MiR-21 protects macrophages from HNE-induced apoptosis.....	127
34. Effect of miR-21 on the activation of caspase-3 and caspase-7 in BMDM.....	128
35. Effect of miR-21 deficiency on the activation of extrinsic and intrinsic pathways of apoptosis in BMDM.....	129
36. Effects of miR-21 deficiency on the abundance of PTEN and PDCD4.....	131
37. Apoptosis in the aortic valves of miR-21-KO chimeric LDLR-KO mice.....	133
38. Abundance of activated caspase-3 in atherosclerotic lesions of miR-21-KO chimeric LDLR-KO mice.....	134
39. Abundance of activated caspase-9 in atherosclerotic lesions of miR-21-KO chimeric LDLR-KO mice.....	135
40. Effect of miR-21 deficiency on lesional necrosis.....	137

LIST OF TABLES

TABLE	PAGE
1. Expression of miRNA in atherosclerotic plaques.....	14
2. Effect of genetic manipulation and pharmacological interventions of miRNA on atherogenesis.....	17
3. Atherogenic properties of miRNAs expressed in macrophages.....	24
4. miRNAs upregulated in aortic lesions of WD-fed LDLR-KO mice.....	41
5. miRNAs downregulated in the aortic lesions of WD-fed LDLR-KO mice.....	44
6. Novel miRNAs identified in the aortic lesions of LDLR-KO mice.....	47
7. miRNAs expressed in macrophages and associated with inflammation and apoptosis.....	60
8. Complete blood count of WT and miR-21-KO mice.....	74
9. Circulating immune cells in WT and miR-21-KO mice.....	77
10. Parameters measured in the plasma of chimeric mice after 12 weeks of WD.....	82

CHAPTER 1
GENERAL INTRODUCTION
ROLE OF MICRORNAs IN ATHEROSCLEROSIS

1.1 Cardiovascular Disease: Cardiovascular disease (CVD) is the leading cause of morbidity and mortality, and accounts for 17.3 million deaths per year. This number is expected to increase to more than 23.6 million by 2030 [1]. In the United States, CVD accounts for 31.3% of all deaths; and 1 in 3 American adults has one or more type of CVD, or increased risk factors for CVD [1]. More than 2150 Americans die of CVD each day- an average of 1 death every 40 seconds. The estimated direct cost for the management of CVD will increase from \$273 billion to \$818 billion between 2010 and 2030 [2].

1.1.1 Atherosclerosis: Atherosclerosis is the underlying cause of most CVD and accounts for 70% of all cardiovascular deaths [3]. Atherosclerosis is a multi-factorial, complex, and chronic inflammatory disease of the arterial wall. It is initiated by endothelial activation in response to excessive accumulation of lipoproteins within the vessel wall, leading to the migration of circulatory monocytes into sub-endothelial space and their differentiation into macrophages. Macrophages take up oxidized lipids in the sub-endothelial space and transform into foam cells. These foam cells secrete pro-inflammatory cytokines that facilitate lipoprotein retention and enhance lesion

inflammation and atherogenesis [4-6]. Most often, lesions are covered and stabilized by a fibrous cap, which is formed by vascular smooth muscle cells (VSMCs) [7]. Progression of this lesion into a vulnerable plaque is characterized by increased macrophage apoptosis, large necrotic cores, focal thinning of the fibrous cap, and high level of inflammatory cytokines which can further propagate or destabilize the lesions.

1.1.1.a. Diseases progression:

(i) Normal artery: The normal artery wall is comprised of three well-defined layers: the intima; media; and adventitia. These three layers are separated by two layers of elastin. Internal elastic lamina separates intima from media, and external elastic lamina separates media from the adventitia [8]. Intima is the innermost layer of the vessel wall and is lined by a single adjacent layer of endothelial cells (ECs) that lies on a basement membrane of extracellular matrix, which is bordered by the internal elastic lamina. The intimal ECs are joined together by junctional complexes which allow straight communication between cells. The endothelial cells form a dynamic barrier between the blood and the arterial wall and have functions in leukocyte trafficking, thrombosis, and vascular tone [8].

The medial layer predominantly comprises of VSMCs. There can be one or several layers of VSMCs, depending on the size of the artery [8]. Cells are held together by an extracellular matrix encompassed mainly of elastic fibers, proteoglycans, and collagen. The extracellular matrix within the arterial wall is produced mainly by the VSMCs [8]. These VSMCs express different contractile proteins such as α -smooth muscle actin. Thus, the main function of the media layer is contraction and regulation of blood flow [9]. The outermost layer of the artery is the adventitia. It is typically comprised mostly of fibroblasts and connective tissues, and therefore provides mechanical support and

stability to the blood vessels. The adventitia also accommodates a number of leukocyte populations to fight possible infection [10].

(ii) Early atherosclerotic lesion: Atherosclerotic lesions occur predominantly at sites where the blood flow is turbulent and does not cause as much shear stress as elsewhere, notably, in arterial branch points, bifurcations, and curvatures [11, 12]. The first step of the development of atherosclerosis is sub-endothelial accumulation of apolipoprotein B-containing lipoproteins [13]. In the intima lipoproteins are associated with the proteoglycans of the extracellular matrix, which restrains them from returning to the bloodstream. In the sub-endothelial space these lipoproteins are devoid of plasma antioxidants, and therefore are susceptible to oxidation [14]. These modified lipids activate the overlying ECs and result in an increased expression of adhesion molecules on ECs surface. Also, these modified lipids contribute to lipoprotein aggregation and additionally promote lipoprotein retention [5].

Following increased expression of adhesion molecules on ECs surface, monocytes become tethered and roll on endothelial cells via the interaction of monocyte P-selectin glycoprotein ligand-1 (PSGL-1) with endothelial selectins [15]. Further adhesion of monocytes with ECs is achieved by endothelial vascular cell adhesion molecule 1 (VCAM-1) and intercellular adhesion molecule 1 (ICAM-1). Finally, this firm adhesion of monocytes allows their entry into the sub-endothelial space [16]. In the intima, monocytes differentiate into macrophages, which take up modified lipoproteins and transform into foam cells [17]. Macrophages internalize modified lipids through scavenger receptors, such as the scavenger receptor A (SRA) and CD36, resulting in accumulation of cholesteryl esters in cytoplasmic droplets [6]. The accumulation of lipid-containing foam cells within the intima leads to the formation of fatty streaks. These fatty streaks can begin early in life from childhood and can remain unchanged or even

regress. Some fatty streaks however develop into advanced atherosclerotic plaques [18].

(iii) Advanced atherosclerotic lesions: The progression from the relatively simple fatty streak to the more complex lesion is characterized by increased inflammation. Macrophages are the principal mediators of this development [6]. Foam cells secrete pro-inflammatory cytokines (such as $\text{TNF}\alpha$, $\text{IL-1}\beta$, IL-6 etc.) and enhance lesion inflammation and atherogenesis [4, 5]. Also, these established lesions are characterized by proliferation and migration of VSMCs from the media layer to the intima [19]. VSMCs undergo a transformation from a contractile phenotype to a proliferative/synthetic phenotype, then release various types of proteinases that degrade the extracellular matrix (ECM) [20]. Migration of the VSMCs leads to formation of the fibrous cap that has an essential role in maintaining the mechanical stability of the lesion [19]. The cap is also composed of collagen bundles and elastic fibers. In humans, the majority of atherosclerotic lesions go unnoticed because of the formation of the fibrous cap that covers and stabilizes these lesions [19]. However, when the formation of the fibrous cap is thick enough to obstruct blood flow through a vessel, minor chest pain or angina is often felt [21].

(iv) Vulnerable lesions and plaque rupture: Progression of atherosclerotic plaques to vulnerable plaques is accompanied by a high content of inflammatory cells, large necrotic core, and a thin fibrous cap which is more prone to rupture. In advanced atherosclerotic lesions, inflammation continues to be unresolved as a result of increased infiltration of inflammatory cells, which in turn secrete pro-inflammatory cytokines, proteases, coagulation factors, and vasoactive molecules. These molecules degrade the collagen in the cap and inhibit formation of a stable fibrous cap, therefore destabilizing the plaque [22]. The composition of the plaque is thought to determine the risk of

rupture. Lesions with thick fibrous caps are considered stable; yet continuous failure to clear foam cell macrophages and resolve vascular inflammation beneath such caps progressively leads to weakening of the protective cap. Moreover, VSMCs in advanced stages undergo apoptosis which results in reduced matrix synthesis and weakens the fibrous cap [23]. Another key factor in lesion vulnerability is the necrotic core which arises from a combination of lesional macrophage apoptosis and defective clearance of these dead cells (efferocytosis) [24]. Also, the necrotic core applies physical pressure on the fibrous cap and leads to further VSMCs apoptosis [25]. Physical disruption of the fibrous cap allows plaque rupture and exposes their highly thrombogenic material to interact with blood, which can trigger coagulation and atherothrombosis, the most common cause for myocardial infarction and stroke [5, 26].

1.2. Macrophage inflammation and apoptosis in atherosclerotic plaques:

Macrophages play an important role in all stages of lesion progression and are the main component of atherosclerotic plaques [27]. They contribute largely to plaque inflammation and apoptosis, which are key processes in the development, progression, and instability of atherosclerotic lesions [28].

1.2.1 Inflammation: Macrophage-mediated inflammation plays a vital role in atherogenesis. RNA isolated from lesional macrophages by laser capture microdissection and immunohistochemistry show increased inflammation in human and animal plaques [29].

Mechanistic studies have identified several inflammatory signaling pathways which regulate vascular inflammation. Mullick *et. al.* addressed the role of toll-like receptor (TLR) signaling in lesional macrophages and demonstrated that high fat-fed LDLR-

deficient mice transplanted with bone marrow from TLR2 knockout mice had reduced lesion area only when the mice were challenged with a TLR2 agonist [30]. A TLR heterodimer of TLR4/TLR6, along with a CD36 ligand has been recognized as a common molecular mechanism by which oxidized lipids stimulate sterile inflammation and activate NF- κ B [31]. Lutgene *et al.* addressed the role of the CD40–CD40 ligand (CD40L) signaling axis, which plays a crucial part in immunological pathways, and they determined that CD40L-stimulated macrophages display NF- κ B activation [32]. Interestingly, fat-fed LDLR knockout mice transplanted with bone marrow from CD40 knockout mice had decreased lesion area and inflammation [32].

NF- κ B is a crucial regulator of inflammation [6] which controls the transcription of many genes with well-known roles in atherogenesis, such as chemokines, cytokines, and adhesion molecules [33]. Activation of NF- κ B has been demonstrated in human atherosclerotic plaques, in macrophages, smooth muscle cells, and ECs [34]. Nevertheless, Kanters *et al.* reported an increase in atherosclerotic lesions in LDL receptor– deficient mice when the classical NF- κ B –activating kinase, IKK2, was selectively ablated in macrophages [35]. Others have suggested a pro-atherogenic role of NF- κ B in macrophages [31, 32].

Monocytes can differentiate into two major types of macrophages: those that promote inflammation, referred to as classically activated (M1) macrophages; and M2 macrophages, which are anti-inflammatory and promote resolution of inflammation [36]. M1 macrophages, which are differentiated from Ly6C^{high} monocytes, are classically activated by lipopolysaccharide (LPS) in the presence of IFN γ , leading to the production of IL-2, IL-23, IL-6, IL-1, and TNF- α . On the contrary, activated M2 macrophages, which

are differentiated from Ly6C^{low} monocytes, differentiate in the presence of IL-4, IL-13, IL-10, or vitamin D3, produce a large amount of IL-10, and express scavenger receptors, mannose receptors, and arginase [37]. There is evidence that the imbalance in the ratio of M1 to M2 macrophages has different roles in different stages of atherosclerosis [38]. Studies in a murine model of atherosclerosis revealed that M2 macrophages are predominant in early lesions, while lesion progression correlates with the dominance of M1 phenotype [39]. Differential distribution of polarized macrophages within human atherosclerotic lesions links M1 activation to rupture-prone plaque areas [40].

1.2.2. Apoptosis: Macrophage apoptosis plays a vital role in lesion progression because it facilitates necrotic core formation and the conversion of a benign lesion to a vulnerable plaque [28]. The necrotic core arises from a combination of macrophage apoptosis and defective clearance of these dead cells (efferocytosis) [24]. Macrophage cell death also occurs in early atherosclerotic lesions, however efferocytosis removes apoptotic cells. This leads to reduced lesion cellularity, inflammation, and plaque progression rather than an increase in plaque necrosis [41].

Apoptosis is achieved by a group of intracellular cysteine proteases, namely caspases [42]. Caspase activation can be mediated by well-characterized extrinsic and/or intrinsic pathways. The extrinsic pathway is induced by death ligands, such as FasL, binding to cell surface receptors (e.g. Fas receptor) leading to the activation of caspase-8. The intrinsic pathway is activated after mitochondrial inter-membrane space proteins such as cytochrome C are released into the cytosol where they activate caspase-9. Activated caspase-8 and caspase-9 subsequently cleave and activate several downstream caspases, including caspase-3 and caspase-7, which then cleave intracellular substrates, resulting in apoptosis. The extrinsic apoptotic signal is amplified by the

intrinsic pathway via the cleavage of Bid by caspase-8. The truncated Bid, tBid, moves from the cytosol to the mitochondria and causes the release of apoptogenic factors from the mitochondria. The apoptotic cell also prepares itself for phagocytosis by actively flipping phosphatidylserine [42].

Several studies have identified macrophage apoptosis in and surrounding the necrotic core. In these cells signs of apoptosis have been detected by nuclear condensation, DNA fragmentation, and activated caspases [43, 44]. Also, some lesional macrophages displayed morphological features of necrosis, characterized by swollen organelles and disrupted cell membranes. Due to defective clearance of apoptotic cells in atherosclerotic lesions, it is likely that some of these necrotic macrophages originate from apoptotic cells [45]. Free cholesterol (FC) loading has been suggested to activate caspase-8-mediated apoptosis which could be blocked by an anti-Fas ligand antibody [46]. Additionally, FC accumulation in macrophages resulted in a decrease in the mitochondrial transmembrane potential, followed by release of cytochrome C and execution of the intrinsic pathway through caspase-9 activation [47]. In this model, intrinsic pathway activation is not blocked by inhibition of the extrinsic pathway, indicating that a Fas-mitochondria cross-talk pathway is not involved [47].

Several mechanisms are postulated to be responsible for macrophage apoptosis in atherogenesis, including growth factor deprivation, oxidative stress, death receptor activation by ligands that exist in advanced atheroma, and prolonged activation of endoplasmic reticulum (ER) stress pathways [48]. However, the role of these pathways in the etiology of lesion progression and stability is not clearly understood.

1.3. MicroRNA:

1.3.1. History: MicroRNAs (miRNAs) are short non-coding strands of RNA that regulate thousands of genes in most physiological and pathological conditions [49]. The first miRNAs, *lin-4* and *let-7*, were described by Lee *et. al.* in *Caenorhabditis elegans* [50]. These miRNAs were found to be expressed temporally and regulate developmental transitions in *Caenorhabditis elegans*. Since then, there has been a substantial increase in miRNA studies reflecting the interest in how these RNAs regulate protein expression and cell function. So far over 2500 mature miRNAs have been detected in humans and several of them have been shown to regulate an array of cellular processes.

1.3.2. Genomic location and biogenesis: miRNAs mainly map to an intergenic region as single or clustered genes or an intragenic region within coding or non-coding transcribed units [51, 52]. Intragenic miRNAs expression is mostly regulated by the promoter of host genes, resulting in similar expression patterns for miRNA and mRNA [53]. Intergenic miRNAs have also been shown to be expressed independently from host genes [54]. The intergenic miRNAs have their own promoters and have the features commonly associated with RNA polymerase II-mediated transcription. Clustered miRNAs have one promoter and are co-regulated and transcribed as a long primary miRNA (pri-microRNA) [53].

In eukaryotes, most miRNAs are transcribed by RNA polymerase II into long transcripts called primary miRNAs (pri-miRNAs) [55] which are several kilo bases long, capped, spliced, and polyadenylated. A few miRNAs are transcribed by RNA pol III, *e.g.*, miR-515-1, miR-517a, and miR-517c [56]. In this pri-microRNA, intra-strand regions of complementarity result in the formation of an imperfect hairpin loop (pri-miRNA). The functional miRNA sequence is present on the arm of this loop [51]. Pri-miRNAs are

recognized by a microprocessor which is comprised of the class II Ribonuclease III enzyme, Drosha, and Di George Syndrome critical region 8 (DGCR8), a double stranded RNA binding protein [57]. The DGCR8 binds the double-stranded RNA, and the RNase III enzyme Drosha cleaves the double-stranded stem about 11 bp from the base of the stem, leaving a two-nucleotide overhang at the 3' end (**Fig. 1**). The formed 70-100 bp long RNA molecule is called pre-microRNA [53, 58, 59]. After microprocessor cropping, pre-miRNAs are then exported into the cytoplasm by Exportin5/RanGTP [60]. Exportin5 is a nuclear transporter that exports pre-miRNAs in a complex with RanGTP. The entire complex then migrates to the cytoplasm, where the release of pre-miRNA occurs in response to the hydrolysis of RanGTP to RanGDP [61]. In the cytoplasm, the pre-miRNA is further cleaved by the class I Ribonuclease III, Dicer, to form imperfect duplexes. The PAZ domain of Dicer recognizes the 3' overhang of pri-miRNA and the dicer catalytic subunit, RNase III, cleaves the stem loop into the mature miRNA [62]. The processed miRNA is composed of double-stranded RNA of a 22 bp miRNA duplex [63]. Generally, the strand with the least stable 3' end base pairing functions as the guide strand while the other strand, frequently noted miR*, is degraded. However, both the canonical guide strand and the star strand of several miRNAs have been proven to be functional.

1.3.3. Mechanisms: To achieve gene silencing, the guide strand is loaded into the large enzyme complex RNA-induced silencing complex (RISC), then the miRNA seed sequence binds target mRNA 3' Untranslated regions (UTRs) [49]. The RISC's major functional unit is Argonaute (Ago2) which is a versatile enzyme involved in RNA-induced silencing. Perfect complementarity between the miRNA and the mRNA results in mRNA strand cleavage. However, the mechanism of gene silencing employed by miRNAs revolves around translational repression when miRNA targets are not based on perfect base pairing [49, 64]. Binding sites vary in their affinities based on sequence

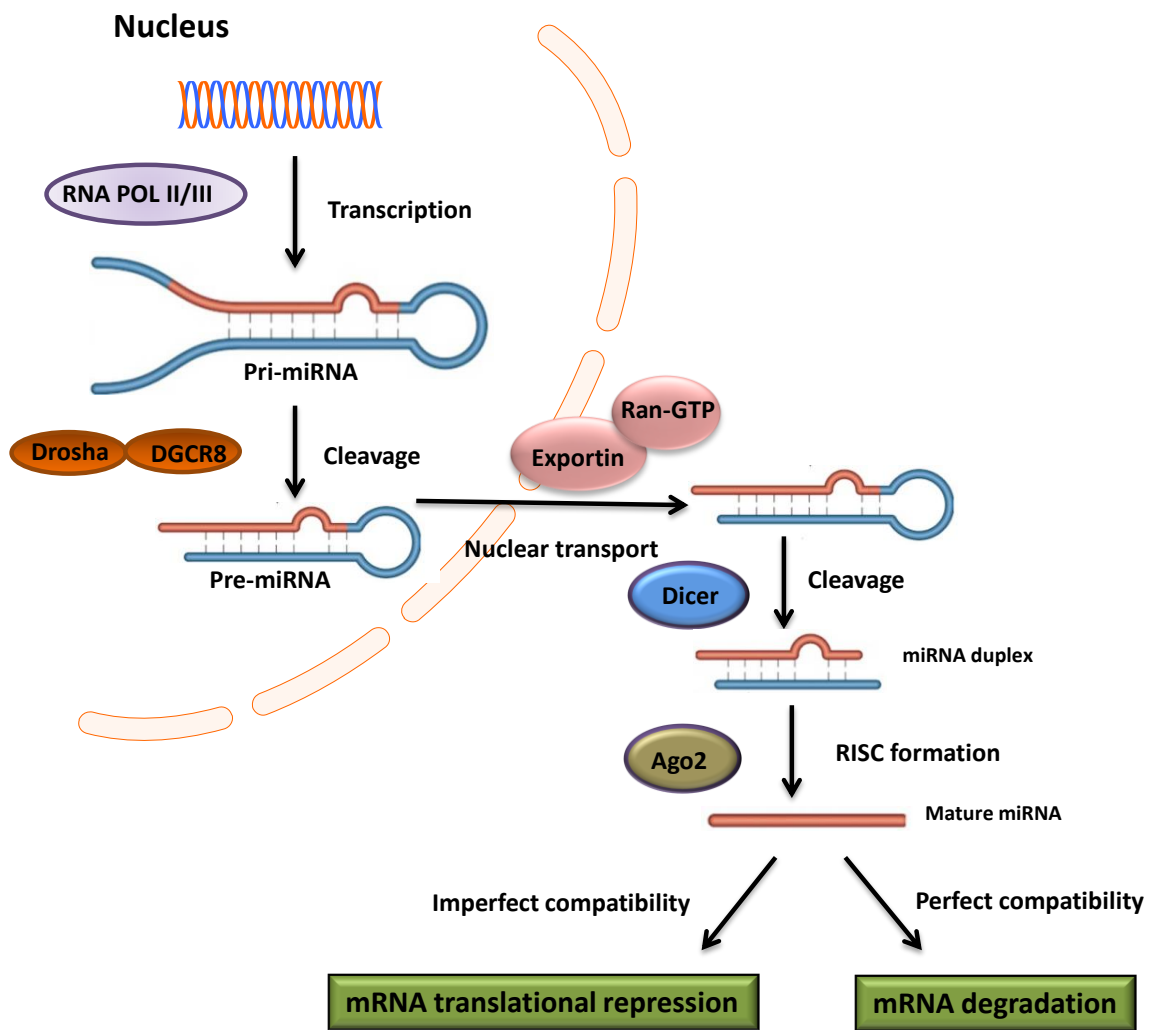


Figure 1. *Biogenesis of microRNAs.*

complementarity, in addition to the presence of an adenosine within the mRNA UTR in line with the first nucleotide of the miRNA.

Target prediction programs use the seed sequences to predict the mRNA targets for miRNAs, but the existence of a seed region binding sequence in mRNA does not ensure miRNA binding, and the predicted targets have to be experimentally validated. Furthermore, due to the short seed region, single miRNAs may bind hundreds of mRNAs, while individual mRNAs can be targeted by several miRNAs which explains the diverse roles of miRNAs in the fine-tuning of a wide range of biological processes [65]. Different levels of complementarity between the miRNA and mRNA can lead to various kinds of impacts on gene expression. Expression patterns of miRs have been reported to be altered in various disease states, including cancer and inflammatory diseases [66].

1.3.4. MicroRNAs and atherosclerosis: Results from numerous studies have demonstrated a crucial role for miRs in regulating various atherogenic processes including lipoprotein metabolism, endothelial integrity, macrophage activation, and vascular smooth muscle cell (VSMC) proliferation. **Table 1** shows the differential expression of miRNAs in atherosclerotic lesions. In atherosclerotic plaques, expression of miRNAs is modulated by different stimuli. The differentially regulated miRs then regulate various signaling pathways by modulating their target genes. A series of genetic manipulation or pharmacological intervention approaches have been applied to regulate the expression of atherogenic miRNA (**Table 2**) and their target genes. Described below are some of the miRs involved in atherogenesis.

1.3.5. Role of microRNAs in lipoprotein metabolism: miRNAs have been shown to have substantial impact on lipid metabolism. The epicenter of lipoprotein metabolism resides in the liver, which has been the focus of many miRNAs. miR-122 is the most abundant miRNA in the liver [67] and was the first miRNA shown to affect lipid homeostasis [68-73]. Antagomir inhibition of endogenous miR-122 in mice results in significant reduction of plasma cholesterol [71]. Moreover, cholesterol synthesis genes, which are not predicted targets of miR-122, were also down-regulated [71]. Results from a separate study, which used antisense oligonucleotide (ASO)-mediated inhibition of miR-122, showed 30% reduction in plasma level of total cholesterol and 40% decrease in plasma triglycerides [69]. Mice treated with miR-122 ASO exhibited increased hepatic fatty acid oxidation, a decrease in hepatic fatty acid, and activation of AMP-activated kinase (AMPK), as well as down-regulation of genes involved in cholesterol biosynthesis such as HMG-CoA reductase [69]. Interestingly, Emlen *et al.*, demonstrated a predominant increase in the low density lipoprotein (LDL) fraction in non-human primates following miR-122 inhibition by locked-nucleic acid-modified oligonucleotide (LNA-antimiR) [68]. miR-122 germ line and liver-specific knockout (LKO) mice displayed a 30% reduction in the total cholesterol [70, 73]. Interestingly, microarray analysis of hepatic gene expression in LKO mice revealed that the only statistically significantly enriched motifs corresponded to sites that match the miR-122 seed sequence [70]. These results indicate that the altered expression of a significant fraction of dys-regulated transcripts in LKO livers is attributable to direct targeting by miR-122 [70]. Moreover, genes involved in lipid metabolism were highly represented in the liver of LKO mice. Notably, among the upregulated genes were two key enzymes, *Acp1* and *Mogat1*, which catalyze triglyceride biosynthesis [70]. miR-122 deficient mice also exhibit reduction in the expression of microsomal triglyceride protein (MTTP) [73].

Table 1: Expression of miRNA in atherosclerotic plaques.

microRNA	Species	Organ/Cell	Methods of characterization	Reference
Up-regulated miRNAs				
Let-7f	Human	Sclerotic intima	Microarray, qRT-PCR	[74]
MiR-21	Human, Rat	Aortic, carotid, femoral arteries/Sclerotic intima	Microarray, qRT-PCR	[74-76]
miR-26b	Human	Carotid artery	Microarray, qRT-PCR	[77]
miR-27b	Human	Sclerotic intima	qRT-PCR	[74]
miR-30e	Human	Carotid artery	Microarray, qRT-PCR	[77]
miR-33	Human	Carotid artery	Microarray, qRT-PCR	[78]
miR-34a	Human	Aortic, carotid, femoral arteries	Microarray, qRT-PCR	[76]
miR-100	Human	Carotid artery	qRT-PCR	[79]
miR-125a	Human	Carotid artery	Microarray, qRT-PCR	[77]
miR-127	Human	Carotid artery	qRT-PCR	[79]
miR-130	Human	Sclerotic intima	qRT-PCR	[74]
miR-133b	Human	Carotid artery	qRT-PCR	[79]
miR-146	Rat	Carotid artery	Microarray, qRT-PCR	[75]
miR-146a	Human	Aortic, carotid, femoral arteries	Microarray, qRT-PCR	[76]
miR-146b	Human	Aortic, carotid, femoral arteries	Microarray, qRT-PCR	[76]

miR-147	Human, Mice	Carotid artery	qRT-PCR	[80]
miR-155	Human, Mice	Macrophage	Microarray, qRT-PCR	[76, 80]
miR-210	Human	Aortic, carotid, femoral arteries/Sclerotic intima	Microarray, qRT-PCR	[74, 76]
miR-214	Rat	Carotid artery	Microarray, qRT-PCR, NB	[75]
miR-223	Human, Rat, Mice	Aorta, carotid artery	qRT-PCR	[81]
miR-352	Rat	Carotid artery	Microarray, qRT-PCR, NB	[75]
Down-regulated miRNAs				
miR-24	Human	Coronary artery	In situ hybridization*	[82]
miR-105	Human	Carotid artery	Microarray, qRT-PCR	[77]
miR-125a	Rat	Carotid artery	Microarray, qRT-PCR, NB	[75]
miR-125b	Rat	Carotid artery	Microarray, qRT-PCR, NB	[75]
miR-126	Human	Aortic, carotid, femoral arteries	Microarray, qRT-PCR	[76]
miR143	Rat	Carotid artery	Microarray, qRT-PCR	[75]
miR-181b	Mice	Aortic intima	qRT-PCR	[83]
miR-221	Human	Sclerotic intima	qRT-PCR	[74]
miR-222	Human	Sclerotic intima	qRT-PCR	[74]
miR-347	Rat	Carotid artery	Microarray, NB	[75]
miR-365	Rat	Carotid artery	Microarray, NB	[75]

miR-520	Human	Carotid artery	Microarray, qRT-PCR	[77]
Up-regulated/down-regulated miRNAs				
miR-133a	Human, Rat	Carotid artery	Microarray, qRT-PCR	[75, 79]
miR-145	Human, Rat	Carotid artery	Microarray, qRT-PCR, NB	[75, 79]

Table 2: Effect of genetic manipulation and pharmacological interventions of miRNA on atherogenesis.

microRNA	Mice	Manipulation	References
Pro-atherogenic			
miR-19b	ApoE-KO	Precursor and inhibitor	[84]
miR-33	ApoE-KO or LDLR-KO	Double knockout mice/ BMT/ Inhibitor	[78, 85-88]
miR-92a	ApoE-KO	Inhibitor	[89]
miR-126 3p	miR-126 WT or KO	Inhibitor	[90]
miR-143/145 (cluster)	LDLR-KO	Double knockout	[91]
miR-144-3p	ApoE-KO	mimics	[92]
miR-145	ApoE-KO	Inhibitor	[93]
miR-302a	LDLR-KO	Inhibitor	[94]
miR-342-5p	ApoE-KO	antagomir	[95]
miR-712	ApoE-KO	Inhibitor	[96]
Anti-atherogenic			
miR-24	ApoE-KO	Overexpression and inhibition	[82]
miR-30c	ApoE-KO	Overexpression and inhibition	[97]
miR-126 5p	ApoE-KO	Double knockout	[98]
miR-146a	ApoE-KO/ LDLR-KO/ FVB/NJ	mimics	[99, 100]
miR-181b	ApoE-KO	mimics	[83]
miR-223	ApoE-KO	Inhibitor and genetic deletion	[81]
miR-467b	ApoE-KO	antagomir	[101]
miR-663	C57BL/6N	Overexpression	[102]
miR-467b	ApoE-KO	antagomir	[101]
miR-663	C57BL/6N	Overexpression	[102]

miR-467b	ApoE-KO	antagomir	[101]
miR-663	C57BL/6N	Overexpression	[102]
Pro/anti-atherogenic			
miR-155	ApoE-KO or LDLR-KO	Double knockout mice/ BMT/ Inhibitor/ mimics/ Genetic deletion	[80, 103- 107]

Cholesterol efflux capacity is essential for maintaining cholesterol homeostasis and is a strong predictor of atherosclerosis in humans. miR-33 was identified as a key post-transcriptional regulator of cellular cholesterol homeostasis by three independent studies [108-110]. Humans have two copies of miR-33, miR-33a, and miR-33b, which are positioned within intronic sequences of the genes encoding the SREBP2 and SREBP1 transcription factors. Rodents, on the other hand, only have one form of SREBP and miR-33 [111]. miR-33a is co-transcribed along with *Srebf-2* in both hepatocytes and macrophages and the expression of *miR-33a* and *Srebf-2* is comparable across many tissues [108, 109]. miR-33 has been shown to regulate high density lipoprotein (HDL) level post transcriptionally by regulating ATP-binding cassette A1 (ABCA1), which is responsible for the movement of free cholesterol out of the cell, and ABCG1 (which mobilizes cellular free cholesterol to more lipidated HDL particles) in liver and in macrophages. Targeting of ABCA1 and ABCG1 by miR-33 results in reduced cholesterol efflux to high-density lipoprotein (HDL) [108-110]. Studies in non-human primates showed that antisense oligonucleotides targeting miR-33a/b are effective in increasing HDL cholesterol and lowering VLDL-associated triglycerides by inducing ABCA1 expression [112, 113]. In addition to cholesterol transport, these miRNAs were demonstrated to regulate key genes involved in fatty acid metabolism and insulin signaling [114].

A recent study by Meiler *et. al.* demonstrated that miR-302a suppressed ABCA1, while anti-miR-302a treatment attenuated atherosclerosis progression in LDL receptor deficient mice [94]. miR-10b also directly suppressed ABCA1 and ABCG1, and negatively regulated cholesterol efflux from murine and human lipid-loaded macrophages [115]. Similarly, miR-27 [116], miR-144 [117, 118], miR-145 [91, 119], miR-223 [120], and miR-758 [121] target ABCA1 and post-transcriptionally regulate

cellular cholesterol efflux to apolipoprotein A-I. The final step of reverse cholesterol synthesis (RCT) is uptake of the HDL cholesterol by the liver, which is mediated by scavenger receptors. It has been proven that miR-96, miR-185, and miR-223 repress hepatic scavenger receptor B-I, delivering an additional essential mechanism to regulate HDL cholesterol transport [120, 122].

1.3.6. MicroRNAs and endothelial function: The early phase of atherosclerotic disease is characterized by the activation of endothelial cells (ECs), which is induced by both biochemical and biomechanical stimuli. Endothelial activation and inflammation is characterized by expression of adhesion molecules, such as VCAM-1, ICAM-1, and E-selectin. Numerous miRNAs have been shown to play a role in the regulation of the inflammatory response in ECs. Recent studies highlighted an important role for miR-181b as a suppressor of endothelial inflammatory responses by targeting importin- α 3, a protein required for nuclear translocation of NF- κ B and therefore inhibiting NF- κ B-responsive genes, VCAM-1 and E-selectin [123]. Systemic delivery of miR-181b reduces NF- κ B activity and atherosclerotic lesion formation in the aortic arch of ApoE-deficient mice [83]. Similarly miR-31 and miR-17-3p control EC inflammation by controlling the expression of adhesion molecules VCAM-1, ICAM-1, and E-selectin [124]. Also miR-155 and miR-221/222 have been shown to protect the endothelium by inhibiting the angiotensin II-induced inflammatory response in ECs in an Ets-1-dependent manner [125]. However, the role of miR-155 in EC function remains controversial because it has also been found to impair endothelium-dependent vasorelaxation by directly targeting endothelial nitric oxide synthase (eNOS) mRNA [126]. miR-146a and miR-146b have also been shown to inhibit endothelial activation by promoting eNOS expression via the RNA-binding protein HuR; and by suppressing the induction of adhesion molecules

through targeting TRAF6 and IRAK1/ 2 [127]. Let-7g has been suggested to exert anti-inflammatory effects on ECs through targeting transforming growth factor (TGF)- β pathway [128]. miR-126, expressed predominantly in ECs is reported to prevent atherosclerosis by inhibiting VCAM-1 expression in ECs [129, 130]. A recent study demonstrated that inhibition of miR-126-5p increased lesion formation in ApoE-KO mice [98].

Accumulating evidence indicates that alteration of flow conditions regulate miRNAs expression in ECs [131]. It was shown that shear stress is capable of inducing endothelial miR-21, which causes up-regulation of endothelial nitric oxide synthase and reduces endothelial cell apoptosis [132]. However, Zhou *et. al.* demonstrated pro-atherogenic function of miR-21 in ECs by targeting peroxisome proliferator-activated receptor α (PPAR- α), hence enhancing the expression of VCAM-1 and MCP-1 [133]. Disturbed flow also downregulates miR-126-5p and exacerbates lesion formation through upregulation of delta-like 1 homolog (Dlk1), a negative regulator of EC proliferation [98]. Other shear stress-regulated miRNAs are miR-1275, -638 and -663 which are upregulated in human umbilical vein endothelial cells (HUVECs). On the contrary, miR-320a, -b -c,- 151-3p, -195, -139-5p, and -27b are down regulated by shear stress [134].

1.3.7. Role of miRNAs in regulating macrophage functions: miRs have been suggested to play a pivotal role in regulating macrophage functions. **Table 3** illustrates the atherogenic properties of miRs expressed in macrophages. These include foam cell formation, inflammation, and apoptosis. Described below are the mechanisms by which some of the macrophage miRs affect atherogenic processes.

Ingestion of lipoproteins by macrophages causes foam cell formation, an early pathogenic event in atherosclerotic plaque development. Microarray analysis on oxidized LDL (oxLDL)-activated human primary monocytes showed the upregulation of 5 miRNAs: miR-125a-5p, miR-9, miR-146a, miR146b-5p and miR-155 [135]. Inhibition of miR-125a-5p increased lipid uptake in oxLDL-stimulated macrophages, possibly via its target Oxysterol binding protein-related Protein 9 (ORP9), which is involved in lipid metabolism and membrane transport [135]. Another study showed that the expression of miR-146a diminished in oxLDL-stimulated THP-1 macrophages via TLR4 upregulation [136]. A recent study by Li *et. al.* demonstrated that systemic delivery of miR-146a mimetic prevents macrophage activation and atherosclerosis in *ApoE^{-/-}Ldlr^{-/-}* and *Ldlr^{-/-}* mice [99]. Similar to miR-146a, miR-147 also limits the macrophage inflammatory response following TLR stimulation in a negative feed-back manner [137]. TLR4 stimulation induces NF- κ B and STAT1 binding to the miR-147 promoter [137]. Inhibition of TLR-induced miR-147 reduces the secretion of inflammatory cytokines from macrophages [137].

One of the most studied miRNAs in macrophages is miR-155. miR-155 is specifically expressed in atherosclerotic plaques and pro-inflammatory macrophages [80]. In vitro studies looking at the effect of miR-155 showed conflicting results. Several studies demonstrated an anti-inflammatory role of miR-155 [138-140]. Huang *et. al.* observed that miR-155 was involved in negative feedback regulation of oxLDL-induced inflammation via the down regulation of lectin-like oxidized LDL receptor 1 (LOX-1), CD36 and CD68, thereby resulting in reduced lipid uptake [139]. Another study showed that miR-155 repressed the expression of adhesion molecules (VCAM-1 and ICAM-1) and chemokines via targeting *secretogranin II* (SCG2), a key AP-1 regulatory protein and a direct angiogenic cytokine [138]. Likewise, miR-155, markedly up-regulated by

oxLDL stimulation, has been suggested to affect the secretion of cytokines (TNF α , IL-6, and IL-8 etc) by attenuating MyD88-mediated NF- κ B activation in atherosclerosis [139]. On the contrary, miR-155 has been reported to mediate the pro-inflammatory effects in monocytes/macrophages by suppressing B-cell CLL/lymphoma 6 (Bcl6) which can antagonize the NF- κ B pathway. Deficiency of miR-155 in oxLDL-stimulated macrophages *in vitro*, as well as in lesional macrophages, diminished the expression of the chemokine (chemokine C–C motif ligand2, CCL2) [80], suggesting a pro-atherogenic role for miR-155. Consistent with these findings, *in vivo* studies have shown that ApoE^{-/-} mice with bone marrow cells deficient in miR-155 exhibit reduced macrophage inflammatory responses, enhanced macrophage cholesterol efflux, and reduced lesion size [80]. Furthermore, the same research group demonstrated that silencing of Bcl6 in mice harboring miR-155^{-/-} macrophages enhances plaque formation and CCL2 expression [80]. By contrast, in LDL receptor knockout (LDLR-KO) mice, bone marrow miR-155 deficiency enhanced atherosclerosis by generating a more pro-inflammatory macrophage phenotype [103].

Accumulating evidence also demonstrated an important role for miRNAs in regulating macrophage polarization. miR-124 has an essential role in inhibiting macrophage activation and polarizes macrophages towards an anti-inflammatory M2 phenotype via targeting the transcription factor C/EBP- α [169]. miR-223-null macrophages displayed an increase in M1 and decrease in M2 biomarkers, indicating a suppressive effect of this miRNA on macrophage pro-inflammatory capacity, in part, by targeting the protein Pknx1 [170]. Similarly, miR-125a-5p diminished M1 phenotype expression induced by lipopolysaccharide (LPS), but promoted the expression of M2 markers in response to IL-4 [153].

Table 3: *Atherogenic properties of miRs expressed in macrophages.*

microRNA	Foam Cell Formation	Inflammation	Apoptosis	Reference
Let-7f	N	Y	N	[141]
miR-19b	Y	Y	N	[84, 142]
miR-21	Y	Y	Y	[143-145]
miR-24	N	Y	N	[146]
miR-26b	N	Y	N	[147]
miR-27b	Y	Y	N	[116, 148]
miR-30 c	N	N	Y	[149]
miR-33	Y	Y	N	[78, 88]
miR-34a	N	Y	N	[150, 151]
miR-92a	N	Y	N	[152]
miR-125a	Y	Y	N	[135, 153]
miR-125b	N	Y	Y	[154-156]
miR-127	N	Y	N	[157]
miR-143/145 Cluster	N	Y	N	[158]
miR-143	N	Y	N	[159]
miR-144-3p	N	Y	N	[92]
miR-145	N	Y	N	[158]
miR-146a	Y	Y	N	[99, 136]
miR-146b	N	Y	N	[160]
miR-147	N	Y	N	[137]
miR-155	Y	Y	Y	[139, 161]
miR-181b	N	Y	N	[162]
miR-210	N	Y	N	[163]
miR-214	N	Y	N	[164]
miR-221	N	Y	N	[165]
miR-222	N	Y	N	[166]
miR-223	Y	Y	Y	[167, 168]
miR-302a	Y	N	N	[94]
miR-342-5p	N	Y	N	[95]
miR-467b	Y	Y	N	[101]

On the contrary, miR-155 has been reported to target C/EBP α or β ? to induce M1 phenotype [171].

To the best of my knowledge only one study has been performed thus far which directly tested the contribution of miRNAs in macrophage apoptosis in atherosclerotic lesions. In this study Wei *et. al.* showed that miR-155 deficiency diminished the progression of atherogenesis by decreasing the necrotic core and deposition of apoptotic cell debris in the plaque [105].

1.3.8. Role of microRNAs in regulating VSMCs: miRs have also been recognized as important modulators of vascular smooth muscle cell (VSMC) phenotype switching and their proliferation. During the formation of an atherosclerotic plaque, some VSMCs go through a phenotypic change from a contractile to a secreting phenotype. The secreting VSMCs produce extracellular matrix proteins and metalloproteinases. miRNAs are phenotypic regulators of VSMCs. In general, miR-221[172], miR-24 [173], miR-31 [174], miR-146a [175], miR-208 [176], and miR-26a [177] have been associated with the synthetic phenotype of VSMCs mainly functioning in the platelet-derived growth factor signaling and cell cycle. On the other hand, miR-1 [178], miR-133 [179], miR-21, miR-143, miR-145 [180], miR-100 [181], and let-7d [182] expression have been related to contractile VSMCs, where they have been linked with the inhibition of cell proliferation, migration, and promotion of contractility.

MiR-21 stimulates VSMCs proliferation by targeting phosphatase and tensin homolog (PTEN) and B-cell CLL/lymphoma 2 (Bcl-2) [75]. Interestingly, antisense mediated depletion of miR-21 significantly reduces neointima formation in balloon-injured rat carotid arteries [75]. Moreover, upregulated miR-21 expression inhibits reactive oxygen

species-induced SMC apoptosis and death [183] in a programmed cell death 4(PDCD4) - dependent manner [183]. Li *et. al.* demonstrated that miR-21 promotes VSMC proliferation, invasion, and migration through targeting activator protein-1 (AP-1) [184]. miR-146a can promote VSMC proliferation and neointimal hyperplasia by decreasing Krüppel-like factor 4 (KLF4) expression [175].

1.4. MicroRNA-21: miR-21 is evolutionarily conserved across different vertebrate species, and is encoded by a single gene located on the short arm of human chromosome 17 within the intronic region of the protein coding gene *TMEM49*. Despite the fact that miR-21 and *TMEM49* are overlapping genes in the same direction of transcription, pri-miR-21 is independently transcribed from a conserved promoter that is located within the intron of the overlapping protein-coding gene [185]. miR-21 is one of the most studied miRNAs because it modulates a plethora of biological processes. miR-21 is extensively studied in cancer because it is consistently upregulated in nearly all types of solid [186] and hematological tumors [187-189]. It is involved in various immunological and developmental processes [144, 190, 191]. miR-21 has also been implicated in the manifestation of several aspects of CVD including restenosis, myocardial ischemia, and heart failure [192]. Expression of miR-21 is highly regulated by multiple transcription factors including AP-1[185], NF-κB [193], and STAT3 [194] which directly bind the miR-21 promoter and alters its expression. There are more than 1000 predicted target genes of miR-21.

1.4.1. miR-21 and inflammation: Several studies indicate that miR-21 plays a key role in regulating proteins that orchestrate the inflammatory process, and it is thought to be involved in the transition between the pro- and anti-inflammatory phases of the immune response [144, 190, 195]. It has been shown that miR-21 plays an important role during

hematopoiesis, and its expression increases as different cell types such as neutrophils [196], bone marrow-derived mast-cells [197], and various lineages of activated T-cells [198, 199] mature to an “active” state. Kashashima *et. al.* demonstrated that treatment of monocytes with 12-O-tetradecanoylphorbol-13-acetate (TPA) to differentiate monocytes toward macrophages increased miR-21 expression significantly [200]. Subsequent studies revealed significant up-regulation of miR-21 in cells treated with all-trans retinoic acid to generate neutrophils [196], GM-CSF/IL-4 to generate immature dendritic cells (DCs) [201, 202], and LPS to generate activated macrophages [144, 203], as well as LPS-mediated B-cell activation [204]. Moreover parallel with miR-21 induction in various immune cell types, *in vivo* studies of diseased tissue often display increased expression of miR-21 relative to healthy control tissue. This has been shown in different models of allergic airway inflammation [203, 205], psoriasis, atopic eczema [206], and osteoarthritis [207]--many of which are characterized by infiltration of immunocytes. Increased miR-21 expression was associated with increased IL-10 induction via targeting PDCD4, and increased TNF α formation by targeting PTEN, which collectively resulted in the resolution of inflammation [198, 199, 208, 209].

Beyond its direct effects on macrophages, miR-21 was shown as marker of activated T-cells [198, 199, 208, 209]. Interestingly, T-cells transfected with miR-21 acquire a more Th2 phenotype [210]. Stagakis *et. al.* demonstrated that miR-21 regulates T-cell activation and polarization via targeting PDCD4 [211].

Analysis of miR-21 predicted target genes through target-pathway analysis indicated the following two signaling pathways that are significantly regulated by miR-21: (a) Janus kinase (JAK) and signal transducer and activators of transcription (STAT); and (b) cytokine–cytokine receptor interaction [212]. Together, these pathways are the core of

the cytokine response system. Dysregulation of cytokine signaling is known to be a main cause of inflammation [213, 214]. Moreover, miR-21 has also been reported to inhibit toll-like receptor 2 (TLR-2) agonist-induced lung inflammation in mice [215], exhibiting its anti-inflammatory role.

1.4.2. miR-21 and apoptosis: The biological roles of miR-21 are extensively studied in cancer because it is consistently overexpressed in nearly all types of solid tumors-- including breast, pancreas, lung, gastric, prostate, colon, head and neck, and esophageal cancers [186]. It is also upregulated in hematological malignancies such as leukemia [187], lymphoma [188], and multiple myeloma [189]. Therefore, miR-21 can be classed as an oncomir. Experimental data from numerous transgenic and/or deficient mouse models of miR-21 show that miR-21 exerts its oncogenic function mainly through the inhibition of cellular apoptosis [216, 217]. Moreover, knockdown of miR-21 increases apoptotic cell death *in vitro* [218] and in murine models of cancer [219]. Therefore, miR-21 has an established role as an anti-apoptotic factor which suppresses the expression of a large number of genes that participate (directly or indirectly) in the (extrinsic or intrinsic) apoptotic pathway to promote tumorigenesis [220].

Anti-apoptotic effects of miR-21 have also been described in CVD. Chen *et. al.* demonstrated that miR-21 inhibitors increased H₂O₂-induced cardiac myocyte death and apoptosis, while pre-miR-21 had the opposite effect. The authors showed that miR-21 exerts an anti-apoptotic function in cardiac myocytes through targeting PDCD4 [221]. Interestingly, in acute myocardial infarction (AMI), miR-21 was identified as a protective miRNA in ischemia-induced cell apoptosis via targeting PDCD4, and local viral delivery of miR-21 reduced the infarct size [222]. Sayed *et. al.* reported that miR-21 exert its anti-apoptotic function in cardiac myocytes in an AKT/FasL (a key initiator of the extrinsic

apoptotic pathway) dependent manner. In this study the authors demonstrated that miR-21 decreases in cardiac myocytes in response to hypoxia, which was associated with enhanced expression of PTEN and FasL protein [223]. In endothelial cells it was shown that shear stress is capable of inducing endothelial miR-21, which causes up-regulation of endothelial nitric oxide synthase and reduces endothelial cell apoptosis [132]. In VSMC several studies identified anti-apoptotic and proliferative effect of miR-21 on VSMCs *in vitro* and in rat carotid arteries *in vivo* through targeting (PTEN) [75] and programmed cell death 4 (PDCD4) [183].

Recently the role of miR-21 in immune cell apoptosis has received great interest. A study by Ruan *et. al.* demonstrated that in activated T-cells, miR-21 expression was upregulated, resulting in reduction of T-cell apoptosis via targeting Tipe2. Conversely overexpression of Tipe2 in T-cells augmented their susceptibility to activation-induced apoptosis [208]. In a recent study (Shang *et. al.*) inhibition of miR-21 expression was shown to augment glucose-induced caspase-3 activation and apoptosis in macrophages in a PDCD4 dependent manner, suggesting an anti-apoptotic role of miR-21. [145].

1.5. PROJECT OBJECTIVE: A thorough review of literature suggested although several miRs have been implicated in atherogenesis, a big gap in understanding persists in identifying which miRs are expressed/induced in macrophages, and which ones regulate atherogenic processes such as foam cell formation, inflammation and apoptosis, both *in vitro* and in atherosclerotic lesions. Experiments should be conducted to elucidate the underlying mechanisms associated with these processes. Based on the available literature and my pilot studies, I hypothesized that *miR-21 prevents atherogenesis by inhibiting NF- κ B mediated macrophage inflammation and apoptosis.* To test this hypothesis the following two aims were formulated:

1. **Examine the effects of myeloid cell-specific deficiency of miR-21 on atherogenesis.** Examine how atherogenic and inflammatory stimuli affect the expression of miR-21 in cultured macrophages and in the aortic lesions of Western diet-fed LDLR-KO mice. Investigate the atherogenicity of miR-21 by transplanting the myeloid cells from miR-21-KO and WT mice into LDLR -KO mice, and analyze the lesion size and composition in the recipient mice fed Western diet for 12 weeks.
2. **Elucidate the mechanisms by which miR-21 affects atherogenic functions of macrophages.** Investigate the effect of deficiency of miR-21 in macrophages on foam cell formation, macrophage polarization, cytokine formation, and apoptosis. Examine the role of NF- κ B and MAP kinases in inflammatory signaling and contribution of intrinsic and extrinsic pathways of apoptosis by measuring the activation of caspases.

CHAPTER 2

EXPRESSION OF MICRORNA-21 IN RESPONSE TO ATHEROGENIC AND INFLAMMATORY STIMULI, AND CONTRIBUTION OF MICRORNA-21 IN ATHEROGENESIS

2.0 INTRODUCTION

Atherosclerosis, the underlying cause of most cardiovascular disease, is a chronic inflammatory disease that arises from maladaptive inflammatory responses to sub-endothelial lipoproteins. A central aspect of these responses is a failure to clear sub-intimal LDL, which results in the accumulation of cholesterol-laden macrophages or foam cells. These foam cells continue to establish a chronic inflammatory response by secreting pro-inflammatory mediators such as chemokines, cytokines, and matrix-degrading proteases [6]. The significance of macrophages in atherogenesis is emphasized by the observation that macrophage-deficient mice are resistant to atherosclerotic lesion formation [224]. Progression of atherogenesis is characterized by the apoptosis of these macrophages in the lipid core. Contribution of macrophage apoptosis is a complex phenomenon. In early stages of the lesions, macrophage efferocytosis eradicates apoptotic cells and prevents lesion progression, whereas in advanced lesions, efferocytosis is not sufficient to clear the apoptotic cells which leads to the formation of necrotic cores instability of lesions [225].

MicroRNAs (miRs) are highly conserved short non-coding RNAs which regulate a variety of physiological and pathological functions. These ~22 nucleotide long single-stranded RNA fragments can facilitate the degradation of mRNA targets and/or inhibit mRNA translation. The first miRNA, discovered in *C. elegans*, was found to be a regulator of development [50, 51], however, subsequent studies have revealed a crucial role of miRNAs in all major cellular processes.

miRs have been implicated in all processes and phases of atherosclerosis [226]. They are involved in: the regulation of cholesterol homeostasis, endothelial activation and leukocyte recruitment, vascular inflammation, macrophage apoptosis and necrosis, smooth muscle cell proliferation, and thinning of the fibrous cap [226-228]. Since macrophages play a critical role in lesion inflammation and atherogenesis, I measured the expression of miRs which regulate both macrophage inflammation and apoptosis in atherosclerotic plaques of LDL receptor-null mice. My systematic, thorough, and rigorous screening of miRs expressed in atherosclerotic lesions showed that miR-21, implicated in inflammation and apoptosis, is expressed in atherosclerotic lesions, and its expression is induced by atherogenic and inflammatory stimuli in cultured macrophages. This chapter describes the role of miR-21 in atherogenesis.

EXPERIMENTAL PROCEDURES

2.1 Animal studies:

2.1.1. Animal housing and husbandry: Wild type C57BL/6 (WT) mice and LDL receptor-knockout (LDLR-KO; B6.129S7-*Ldlr*^{tm1Her/J}) mice on C57BL/6 background were obtained from the Jackson Laboratory, Bar Harbor, ME. miR-21-KO mice were kindly provided by Dr. Yong Li. Since these mice were on a mixed background [229], they were bred with C57BL/6 mice by congenic breeding for 9 generations to obtain miR-21-KO

mice on a C57-KO background. The mice were housed and bred under pathogen-free conditions in a barrier facility at the University of Louisville vivarium under controlled temperature and 12 h light/12 h dark cycle, following the guidelines of the *Association for the Accreditation of Laboratory Animal Care*. Prior to the indicated protocols, all the mice were maintained on a normal chow (NC; PicoLab Rodent Chow 20 containing 4.5 % fat by weight and 0.02 % cholesterol). Studies were performed under protocols approved by the University of Louisville Institutional Animal Care and Use Committee.

2.1.2. Animal treatment: Eight week old C57BL/6 and LDLR-KO mice were placed on either a NC or Western Diet (WD; Teklad TD 88137 containing 21.2% fat and 4.5% cholesterol) for 12 weeks. Water and diet were provided *ad libitum* and body weights were measured on a weekly basis for the duration of the study. At 20 weeks of age mice were anesthetized with pentobarbital, and blood was withdrawn by cardiac puncture using EDTA as an anti-coagulant. The vasculature was perfused with phosphate buffer saline (PBS), and entire aorta from the heart, extending to the iliac arteries and including the sub-clavian right and left common carotid arteries, was removed and washed with PBS, followed by immediate immersing in RNALater solution from Ambion (Austin, TX, USA) to stabilize the RNA. Peri-adventetial tissue was removed under the dissecting microscope. Aortas were snap-frozen in liquid nitrogen followed by pulverization and homogenization of aortic tissues. Total RNA was then isolated using a miRCUR RNA isolation kit from Exiqon (Woburn, MA, USA).

2.1.3. MicroRNA expression array: Expression of miRNAs in the aorta of NC (n=6) or WD- fed LDLR-KO mice (n=6) was measured by miRNA array at Exiqon. The quality of the total RNA was confirmed by an Agilent 2100 Bioanalyzer profile. RNA (400ng) was labeled with fluorescent Hy3™ and Hy5™, using the miRCURY LNA™ microRNA Hi-

Power Labeling Kit, Hy3TM/Hy5TM (Exiqon, Denmark). The Hy3TM-labeled samples and a Hy5TM-labeled reference RNA sample were mixed pair-wise and hybridized to the miRCURY LNATM microRNA Array 7th Gen (Exiqon, Denmark), which contains capture probes targeting all microRNAs for human, mouse, or rat registered in the miRBASE 18.0. The hybridization was performed according to the miRCURY LNATM microRNA Array Instruction manual using a Tecan HS4800TM hybridization station (Tecan, Austria). After hybridization the microarray slides were scanned and stored in an ozone-free environment (ozone level below 2.0 ppb) in order to prevent potential bleaching of the fluorescent dyes. The miRCURY LNATM microRNA Array slides were scanned using the Agilent G2565BA Microarray Scanner System (Agilent Technologies, Inc., USA), and the image analysis was carried out using the ImaGeneR 9 (miRCURY LNATM microRNA Array Analysis Software, Exiqon, Denmark). The quantified signals were background-corrected and normalized using the global Lowess (Locally Weighted Scatterplot Smoothing) regression algorithm.

We detected 503 miRNAs in the NC and WD fed LDLR-KO mice. The data were log-transformed and normalized using auto scaling (mean-centered and divided by the standard deviation of each variable). This step was performed to transform the expression values so that the distribution is more Gaussian. Univariate analysis methods were used to compare the two groups. Fold Change (FC) analysis and the t-test was used to create the volcano plots.

2.1.3. Isolation of bone marrow cells and generation of bone marrow derived macrophages: To isolate bone marrow cells, tibias and femurs of C57/BL6, miR-21-KO, and LDLR-KO mice were aseptically removed and flushed with 5ml of PBS containing 2% FBS. Cells were passed through a cell strainer (100 μ m, BD Falcon) and centrifuged

at 500xg for 5min. The pellets were re-suspended in RPMI-1640 medium supplemented with 5% FBS and 10ng/ml macrophage-colony stimulating factor (M-CSF, a macrophage growth factor required for the differentiation of mononuclear progenitor cells into macrophages) from R & D System (Minneapolis, MN, USA). Cells were plated in a 10 cm-dish and incubated at 37°C for 16h. The non-adherent bone marrow cells were then cultured in RPMI-1640 containing 5% FBS, 10ng/ml M-CSF, and L-929 conditioning media. The cells were seeded in a 6-well, ultra-low attachment plate from Corning (Corning, NY, USA) and cultured at 37°C for 7 days to allow for differentiation into primary macrophages. Total RNA was isolated using the miRCUR RNA isolation kit from Exiqon (Woburn, MA, USA).

2.1.4 Phenotyping of blood cells by flow cytometry: One hundred micro liter blood was mixed with 1.0ml red blood cell lysis buffer and incubated for 10 minutes at room temperature. Cells were centrifuged at 500xg for 5min and rinsed twice with 2% FBS in PBS. The Fc receptor (FcR) was blocked for 10min at 4°C to prevent non-specific antibody binding with FcR Blocking Reagent (Miltenyi Biotec, San Diego, CA, USA). Cells were incubated with a panel of fluorescent conjugated antibodies for 30min at 4°C. After washing, samples were analyzed using the BD LSR II. Experiment files were exported and further analyzed using the FlowJo analysis software. Antibodies used were: FITC-NK1.1, PE-Ly6c, PerCP-e710-CD8a, PE-Cy7-CD62L, APC-CD19, Alexa 700-Gr-1, APC-e780-CD3e, e605 NC BD-CD11b, and e650 NC-CD4. Bone marrow cells were detected by using the following antibodies: APC-CD45, ALEXA 700-CD34, APCe 780-CD117(c-kit), FITC-SCA, PE-CD16/32 FcγR, and e450-lin. All antibodies were obtained from BD Biosciences (San Jose, CA, USA) or eBioscience (San Diego, CA, USA).

2.1.5. Phenotyping of bone marrow cells by flow cytometry: To isolate bone marrow cells, tibias and femurs of C57/BL6 and miR-21-KO mice were aseptically removed and flushed with 5 ml of PBS containing 2% FBS. Cells were passed through a cell strainer (100µm, BD Falcon) and centrifuged at 500xg for 5 min. The Fc receptor was blocked as described above. Cells were incubated with desired antibodies for 30 min at 4°C as described above.

2.1.5. Bone marrow transplant: Bone marrow transplant experiments were performed as previously described [230]. Briefly, 6 week old LDLR-KO mice were acclimated to the animal facility for one week before being subjected to an ablative dose of whole body irradiation. (at a dosage of 950cGy by way of a cesium source for 10 minutes), to ablate the endogenous bone marrow cells. After 24h, all irradiated mice were injected with 1×10^7 bone marrow cells isolated from tibias and femurs of WT or miR-21-KO mice. After 5 weeks of recovery, recipient mice were characterized for hematopoietic recovery and chimerism by q-RT-PCR measurement of miR-21 expression in white blood cells. Mice were then fed WD for 12 weeks. Subsequently, mice were euthanized to collect blood and tissues for biochemical and pathological analyses (**Fig 2**).

2.1.6. Atherosclerotic lesion analyses: For the analysis of lesion formation in the aortic sinus, the tissue was frozen in OCT reagent and serial cryosections of 8µm-thickness were taken from the origin of the aortic valve leaflets throughout the aortic sinus as described [231, 232]. Mean lesion area was calculated from the analysis of digital images obtained from 9-12 serial sections from each mouse, using Image J software. Oil red O staining was used to detect the lipid deposition in these sections while Sirius Red staining was used to visualize collagen. Digital images were acquired using Spot Advanced camera and analyzed by Image J software by a blinded observer.

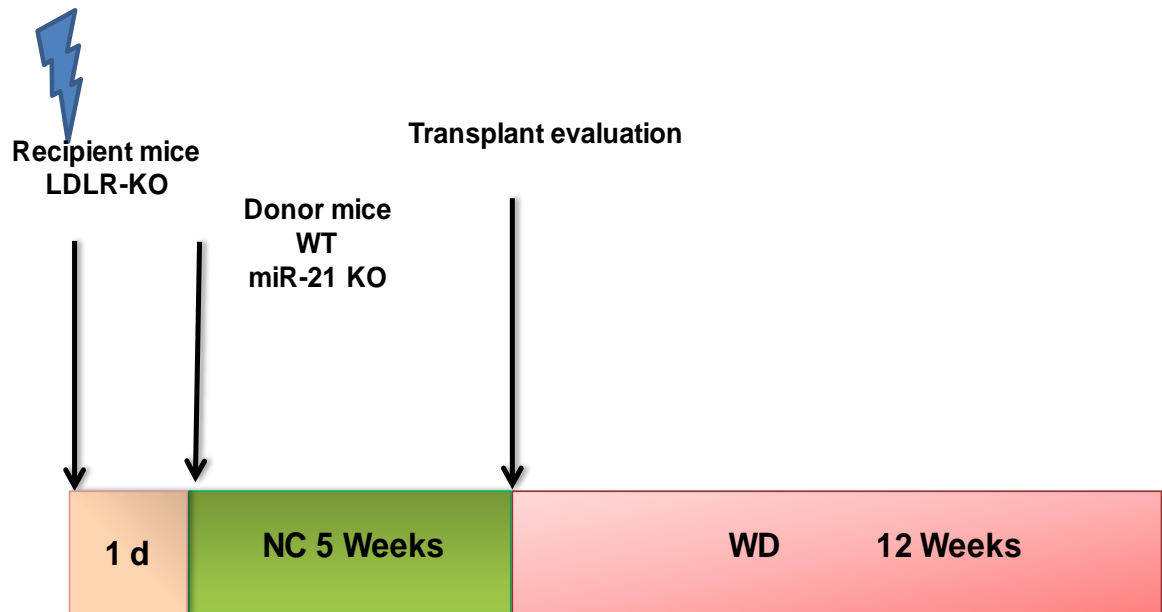


Figure 2. Bone marrow transplant protocol. Bone marrow cells isolated from the hind limbs of miR-21-KO mice and WT mice under sterile conditions were reconstituted in sterile PBS, and 1×10^7 cells were transplanted in lethally-irradiated LDLR-KO mice via retro-orbital injection. Five weeks after reconstitution, mice were checked for chimerism and then placed on Western diet (WD; 42% fat) for 12 weeks.

2.1.7. Immunohistochemical analyses:

a) Fluorescent labeling of antibodies: Anti- α -smooth muscle actin was linked with DyLight®488, and anti-CD3 antibody was labeled with Texas Red using a fast conjugation kit from Abcam (Cambridge, MA, USA) as per the manufacturer's instructions. Briefly, 100-200 μ g of the antibody was incubated with the modifier and Cy5/DyLight®488/Texas Red conjugate reagents for 15 minutes in the dark at room temperature, followed by the addition of the quencher reagent. The conjugated (fluorescent) antibodies were stored at 4°C until used.

b) Immuno-staining: Air-dried cryostat sections were fixed in cold acetone for 30 minutes or 4% paraformaldehyde in PBS (phosphate buffered saline) for 20 minutes, followed by permeabilization with 0.1% Triton-X100 for 10 minutes. The sections were stained with appropriate fluorescent primary antibodies; macrophages were stained with RPE or Alexa 647-conjugated rat anti-mouse CD68 (Serotec, Raleigh, NC; 1:50, overnight at 4° C); smooth muscle cells were identified with DyLight®488-conjugated monoclonal anti- α -smooth muscle cell actin, clone A4 (Sigma Chemicals, St. Louis, MO; 1:250, overnight at 4° C); T-lymphocytes were stained with Texas Red conjugated rabbit polyclonal anti-CD3 antibody (Abcam, Cambridge, MA; 1:50, overnight at 4° C).

2.1.9. Biochemical Analysis:

Blood Glucose: Mice were fasted for 12 h and blood was collected from the tail vein. Blood glucose was measured using a glucometer.

Complete blood cell count: Complete cell blood count (CBC) was measured on a Hemavet 1700 flexible veterinary multi-species hematology system (Drew Scientific, Miami Lakes, FL, USA).

Plasma cholesterol: Plasma cholesterol was measured enzymatically with a commercially available kit from Wako (Richmond, VA, USA) as described [231-233].

PATHSCREEN: Measurement of plasma albumin, total protein, ALT, AST, CK, LDH and creatinine level was done by COBAS MIRA Plus Automated Chemistry Analyzer 5600 (Roche, Indianapolis, IN, USA), using commercial kits from Wako Chemicals Inc. (Richmond, VA, USA) as described [234].

2.2 In Vitro Analyses:

2.2.1. Cell culture: Immortalized bone marrow-derived macrophage cell lines (BMDM) were established by infecting the bone marrow of C57BL/6 mice with the murine recombinant J2 retrovirus containing the *v-myc* and *v-raf* oncogenes as previously described [235]. Cells were cultured in RPMI-1640 medium supplemented with 5% Fetal Bovine Serum (FBS), 1% HEPES, and 0.1% gentamicin (Sigma Aldrich, St. Louis, MO, USA). Cells were maintained in a humidified atmosphere of air and 5% CO₂ at 37°C.

2.2.2. Expression of miR-21: To examine the effect of atherogenic and inflammatory stimuli on the expression of miR-21, BMDM from C57BL/6 mice were seeded in 12 well plates incubated in RPMI-1640 medium containing 0.5 % FBS for 18h. Cells were then incubated with LDL (50µg/mL), acetylated-LDL (50µg/mL), oxidized-LDL (50µg/mL), and lipopolysaccharide (LPS; 100ng/mL) for 24h in RPMI-1640 medium and expression of miR-21 was measured by Real Time Quantitative PCR.

2.2.3. Real Time-PCR: RNA concentrations and purity were determined using the NanoDrop 2000 (Thermo Scientific, Hudson, NH). All samples fulfilled the quality criteria (A260/280 ratio between 1.8 and 2.1). Total RNA was reverse-transcribed to cDNA using Taqman microRNA RT kit from Life Technologies (Foster City, CA, USA). miR-21

expression was measured using Taqman miRNA and Taqman Universal PCR Master Mix from Life Technologies (Foster City, CA, USA). Data were normalized to a housekeeping gene snoRNA20.

RESULTS

Expression profile of miRs in the aortic lesions: To investigate the contributions of miRs in atherosclerosis the expression of miRs in atherosclerotic lesions was first examined. Eight week old LDLR-KO mice were maintained either on NC or WD for 12 weeks, and expression of miRs in the aortae was measured by miRNA microarray. As shown in **Tables 4** and **5**, we detected a total of 503 miRs in the aortae, out of which 100 miRNAs were significantly upregulated (**Table 4**; $P < 0.05$) and 50 miRNAs were downregulated (**Table 5**; $P < 0.05$) in WD fed mice. Differential expression of the top 100 miRs is illustrated in the heat map (**Fig. 3**). Eleven out of 50 downregulated and 22 out of 100 upregulated miRs identified in my study are novel miRs, which have not been described in the literature. Moreover, I also observed that several miRs differentially expressed in aortic lesions that have not been studied in the context of inflammation and apoptosis, which are hallmarks of the process of atherogenesis (**Table 6**).

To find a predictive model that describes the direction of maximum covariance between variables and the class membership, we applied *Partial Least Squares – Discriminant*.

Table 4: *MicroRNAs upregulated in aortic lesions of WD-fed LDLR-KO mice.*

MicroRNA	Fold Change (FC)	log2(FC)	P value
mmu-miR-3473a	1.9539	0.96632	9.55E-12
mmu-miR-690	1.8193	0.86338	8.35E-10
mmu-miR-3473b	1.7682	0.82227	2.14E-10
mmu-miR-669m-3p	1.7317	0.79221	1.99E-08
mmu-miR-3082-5p	1.7175	0.78031	1.12E-08
mmu-miR-544-5p	1.684	0.75193	1.71E-06
mmu-miR-466i-5p	1.6357	0.70994	4.79E-09
mmu-miR-669b-3p	1.6258	0.70111	8.37E-10
mmu-miR-1192	1.6055	0.68298	1.27E-07
mmu-miR-669a-3-3p	1.5882	0.66739	1.06E-08
mmu-miR-199a-5p	1.5697	0.65048	1.97E-08
mmu-miR-302c-3p	1.5688	0.64968	1.84E-06
mmu-miR-466f-3p	1.542	0.62481	1.28E-08
mmu-miR-669f-3p	1.5406	0.62351	6.97E-11
mmu-miR-467g	1.537	0.62016	6.01E-08
mmu-miR-7b-3p	1.537	0.62014	0.00036158
mmu-miR-1298-5p	1.5349	0.61814	2.31E-06
mmu-miR-669c-3p	1.5336	0.61691	2.90E-09
mmu-miR-29b-3p	1.5299	0.61342	9.53E-07
mmu-miR-468-3p	1.5299	0.6134	5.05E-10
mmu-miR-669p-3p	1.5292	0.61277	4.56E-09
mmu-miR-7a-2-3p	1.5267	0.61038	4.33E-06
mmu-miR-143-5p	1.5088	0.5934	1.47E-05
mmu-miR-466q	1.5067	0.59138	1.99E-07
mmu-miR-466(a,b,c,e,p)-3p	1.5058	0.59058	1.65E-08
mmu-miR-214-3p	1.5057	0.59047	3.20E-05
mmu-miR-140-5p	1.4927	0.57791	1.82E-06
mmu-miR-466d-3p	1.478	0.56364	8.58E-07
mmu-miR-467e-3p	1.4761	0.56178	3.56E-07
mmu-miR-466a-5p/mmu-miR-466p-5p	1.4714	0.55722	1.53E-08
mmu-miR-199b-5p	1.468	0.5539	7.22E-08
mmu-miR-27a-3p	1.4658	0.55168	3.08E-08
mmu-miR-32-3p	1.4649	0.55079	3.12E-07
mmu-miR-669a-3p/mmu-miR-669o-3p	1.4575	0.54346	2.23E-08

mmu-miR-466d-5p	1.4501	0.53614	5.39E-08
mmu-miR-5622-5p	1.4438	0.52989	9.88E-09
mmu-miR-669k-5p	1.4432	0.52929	1.94E-08
mmu-miR-1899	1.4278	0.51382	7.36E-07
mmu-miR-29c-3p	1.4229	0.50879	5.84E-07
mmu-miR-574-5p	1.4183	0.50411	1.61E-06
mmu-miR-24-1-5p	1.4168	0.50262	1.46E-07
mmu-miR-467f	1.4164	0.50221	1.23E-08
mmu-miR-30b-5p	1.4134	0.49921	1.21E-06
mmu-miR-466i-3p	1.4103	0.49601	7.72E-07
mmu-miR-466f	1.4088	0.49443	2.33E-08
mmu-miR-219b-5p	1.4063	0.4919	3.75E-05
mmu-miR-21a-5p	1.4045	0.49009	2.86E-06
mmu-miR-467a-3p	1.4027	0.48821	1.40E-07
mmu-miR-3097-5p	1.4	0.4854	4.46E-05
mmu-miR-212-3p	1.3994	0.48486	5.17E-07
mmu-miR-669l-3p	1.3987	0.48405	6.78E-07
mmu-miR-466c-5p	1.3982	0.48355	1.53E-09
mmu-miR-23b-3p	1.3973	0.48262	9.17E-07
mmu-miR-24-3p	1.3944	0.47964	3.23E-08
mmu-miR-27b-3p	1.3923	0.47747	6.76E-07
mmu-miR-499-3p	1.389	0.47407	0.00031691
mmu-miR-467c-3p	1.389	0.47404	2.16E-05
mmu-miR-669e-3p	1.3884	0.4734	2.38E-06
mmu-miR-140-3p	1.3836	0.46847	2.11E-06
mmu-miR-34c-3p	1.3719	0.45622	0.00073564
mmu-miR-467b-3p	1.3708	0.45503	9.24E-06
mmu-miR-24-2-5p	1.3686	0.45274	3.18E-09
mmu-miR-574-3p	1.3665	0.45049	2.86E-08
mmu-miR-145a-5p/mmumir-145b	1.3577	0.4412	0.0001327
mmu-miR-669d-5p	1.3535	0.43672	1.42E-08
mmu-miR-466b-5p/mmumir-466o-5p	1.3531	0.43627	1.82E-08
mmu-miR-466e-5p	1.346	0.42871	3.29E-05
mmu-miR-669d-2-3p	1.3395	0.42173	4.23E-05
mmu-miR-669h-3p	1.334	0.41578	0.00019577
mmu-miR-669f-5p	1.3331	0.41478	5.37E-06
mmu-miR-669d-2-3p/mmumir-669d-3p	1.3315	0.41302	8.52E-08
mmu-miR-1929-5p	1.3196	0.40014	0.00090059

mmu-miR-669l-5p	1.3142	0.39415	2.25E-06
mmu-miR-5119	1.3109	0.39058	4.50E-06
mmu-miR-467d-3p	1.3082	0.38755	0.00084184
mmu-miR-466a-5p	1.306	0.38515	3.02E-08
mmu-miR-196a-1-3p	1.3054	0.38448	0.00010696
mmu-miR-31-5p	1.303	0.38183	0.0017204
mmu-miR-297a-3p/mmumir-297b-3p/mmumir-297c-3p	1.302	0.38076	1.32E-07
mmu-miR-1187	1.3018	0.38055	5.14E-07
mmu-miR-3078-3p	1.3013	0.37997	0.00019798
mmu-miR-466m-3p	1.2999	0.37841	0.0023432
mmu-miR-1907	1.2997	0.3782	0.0010376
mmu-miR-130a-3p	1.2989	0.37729	4.60E-05
mmu-miR-713	1.2927	0.37033	0.00020919
mmu-miR-669e-5p	1.2913	0.36885	1.03E-05
mmu-miR-30c-5p	1.2893	0.36656	1.02E-06
mmu-miR-669i	1.2861	0.36305	0.00064834
mmu-miR-210-3p	1.2779	0.35374	5.61E-06
mmu-miR-881-5p	1.2748	0.35024	0.00048273
mmu-miR-143-3p	1.2647	0.3388	2.07E-07
mmu-miR-490-3p	1.2619	0.33557	0.00084483
mmu-miR-466a-3p/mmumir-466e-3p	1.2602	0.33362	0.00010367
mmu-miR-466f-5p	1.2593	0.33264	1.10E-05
mmu-miR-301a-3p	1.2577	0.33078	0.00019132
mmu-miR-669o-5p	1.2543	0.32688	0.00086269
mmu-miR-697	1.2515	0.32368	0.0013927
mmu-miR-145a-3p	1.2504	0.32241	6.23E-05

Table 5: *MicroRNAs downregulated in the aortic lesions of WD-fed LDLR-KO mice.*

MicroRNA	Fold Change (FC)	log2(FC)	P value
mmu-miR-592-3p	0.29732	-1.7499	6.31E-12
mmu-miR-551b-5p	0.47888	-1.0623	1.13E-07
mmu-miR-677-3p	0.51159	-0.96694	1.01E-11
mmu-miR-142a-3p	0.52117	-0.94017	1.34E-06
mmu-miR-142a-5p	0.53128	-0.91246	2.61E-06
mmu-miR-3102-5p	0.59296	-0.754	2.46E-05
mmu-miR-346-3p	0.59622	-0.74608	2.85E-09
mmu-miR-2861	0.59976	-0.73755	3.04E-09
mmu-miR-762	0.61598	-0.69905	5.28E-07
mmu-miR-1971	0.62061	-0.68823	1.95E-10
mmu-miR-3572-3p	0.62092	-0.68752	3.43E-07
mmu-miR-3474	0.62338	-0.68182	4.48E-07
mmu-miR-425-3p	0.64964	-0.62228	6.11E-05
mmu-miR-541-3p	0.65363	-0.61346	5.85E-10
mmu-miR-1947-3p	0.66676	-0.58476	2.07E-08
mmu-miR-378a-3p/mmumir-378b/mmumir-378c	0.66929	-0.5793	3.16E-11
mmu-miR-2137	0.6807	-0.5549	6.19E-08
mmu-miR-3090-5p	0.6894	-0.53659	2.74E-08
mmu-miR-503-5p	0.69298	-0.52911	1.07E-06
mmu-miR-205-5p	0.69343	-0.52818	2.49E-05
mmu-miR-542-3p	0.7036	-0.50717	0.00021434
mmu-miR-21a-3p	0.71707	-0.47982	1.92E-05
mmu-miR-92a-3p	0.72133	-0.47127	0.0027195
mmu-miR-378a-3p	0.72223	-0.46946	6.22E-08
mmu-miR-3103-3p	0.72377	-0.46639	2.40E-07
mmu-miR-1934-5p	0.73189	-0.45031	2.65E-06
mmu-miR-1843b-3p	0.7332	-0.44772	8.86E-08
mmu-miR-20a-5p	0.74702	-0.42078	3.85E-06
mmu-miR-322-5p	0.748	-0.41889	4.96E-07
mmu-miR-744-5p	0.74913	-0.41671	4.47E-10
mmu-miR-763	0.75243	-0.41037	5.66E-08
mmu-miR-126a-3p	0.75506	-0.40533	3.99E-05
mmu-miR-139-5p	0.75764	-0.40042	6.51E-07
mmu-miR-20b-5p	0.75819	-0.39936	2.57E-05
mmu-miR-708-5p	0.76574	-0.38507	2.07E-05
mmu-miR-155-5p	0.76916	-0.37864	0.006224

mmu-miR-146a-5p	0.76926	-0.37846	7.05E-07
mmu-let-7a-2-3p	0.77013	-0.37682	2.57E-06
mmu-miR-351-5p	0.77232	-0.37273	4.32E-05
mmu-miR-185-3p	0.77682	-0.36435	0.00032576
mg hv-miR-M1-8-5p	0.78053	-0.35747	1.55E-07
mmu-miR-770-3p	0.78481	-0.34959	1.42E-05
mmu-miR-499-5p	0.78967	-0.34067	0.00049803
mmu-miR-1941-3p	0.78999	-0.34009	1.95E-07

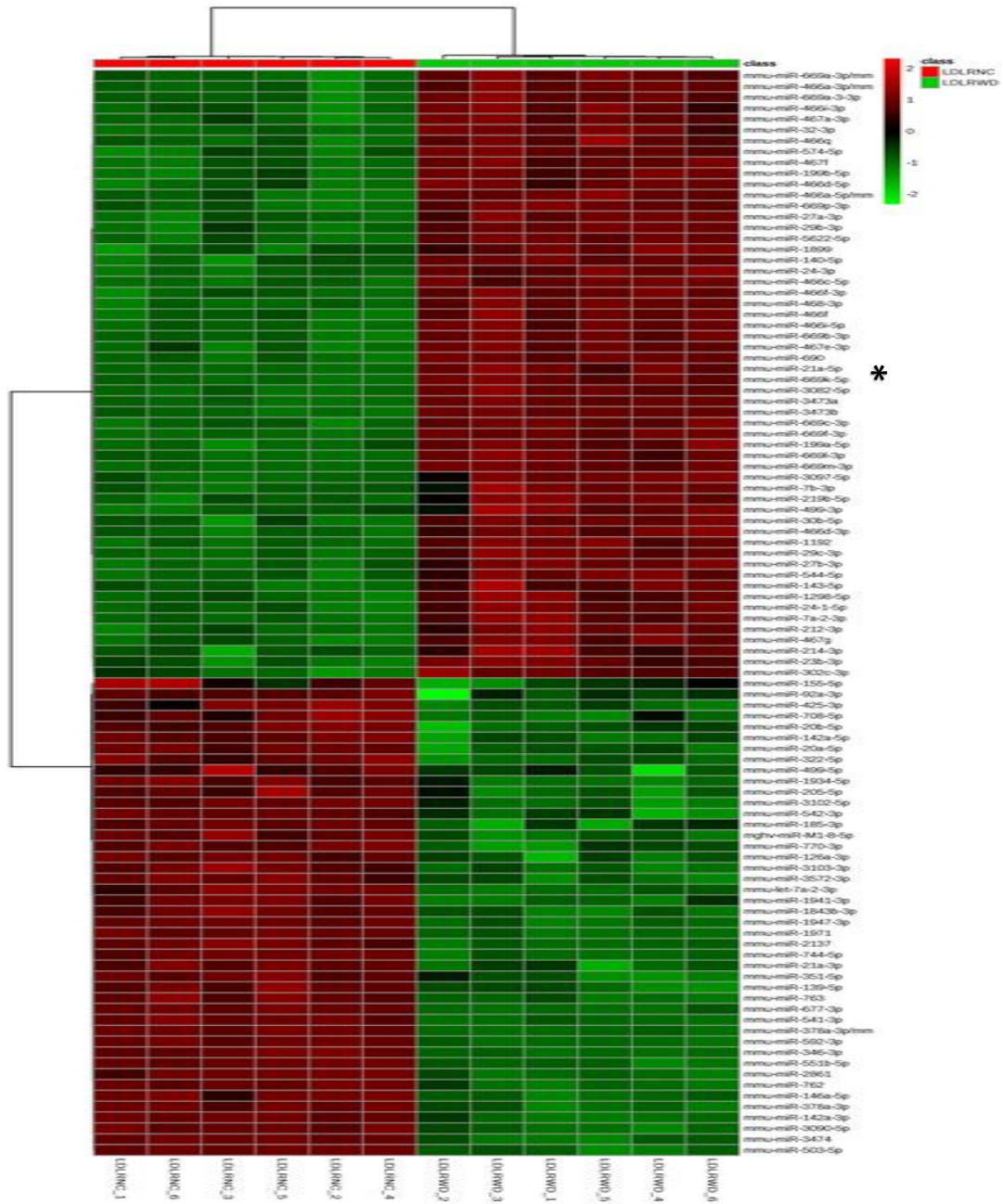


Figure 3. Heatmap of miRNAs in aortic lesions. Hierarchical clustering heatmap and dendrogram analyses of the 100 most significantly changed miRNAs in 8 week old LDLR-KO mice maintained on normal chow or Western diet for 12 weeks. Six mice per group were used for analyses.

Table 6: Novel miRNAs identified in the aortic lesions of LDLR-KO mice.

Novel miRNAs expressed in aortic lesions	miRNAs not studied in inflammation	miRNAs not studied in apoptosis
Up-regulated		
mmu-miR-3473a	mmu-miR-544-5p	mmu-miR-466i-5p
mmu-miR-690	mmu-miR-669b-3p	mmu-miR-669b-3p
mmu-miR-3473b	mmu-miR-1192	mmu-miR-1192
mmu-miR-669m-3p	mmu-miR-669a-3-3p	mmu-miR-669a-3-3p
mmu-miR-3082-5p	mmu-miR-466f-3p	mmu-miR-466f-3p
mmu-miR-669p-3p	mmu-miR-669f-3p	mmu-miR-467g
mmu-miR-466q	mmu-miR-467g	mmu-miR-669c-3p
mmu-miR-5622-5p	mmu-miR-669c-3p	mmu-miR-1298-5p
mmu-miR-669k-5p	mmu-miR-1298-5p	mmu-miR-467e-3p
mmu-miR-1899	mmu-miR-468-3p	mmu-miR-466d-3p
mmu-miR-467f	mmu-miR-7b-3p	mmu-miR-466d-5p
mmu-miR-669l-3p	mmu-miR-466(a,b,c,e,p)-3p	mmu-miR-466i-3p
mmu-miR-3097-5p	mmu-miR-467e-3p	mmu-miR-466c-5p
mmu-miR-669e-3p	mmu-miR-466d-3p	mmu-miR-467b-3p
mmu-miR-467c-3p	mmu-miR-466(a,p)-5p	mmu-miR-466(b,o)-5p
mmu-miR-669d-5p	mmu-miR-669(a,o)-3p	mmu-miR-466e-5p
mmu-miR-669d-2-3p	mmu-miR-466d-5p	
mmu-miR-669h-3p	mmu-miR-466i-3p	
mmu-miR-1929-5p	mmu-miR-466f	
mmu-miR-669l-5p	mmu-miR-467a-3p	
mmu-miR-5119	mmu-miR-466c-5p	
mmu-miR-3078-3p	mmu-miR-466(b,o)-5p	
	mmu-miR-466e-5p	
	mmu-miR-669f-5p	
	mmu-miR-466a-5p	
	mmu-miR-1187	
	mmu-miR-297(a,b,c)-3p	
Down-regulated		
mghv-miR-M1-6-5p	mmu-miR-770-3p	mmu-miR-21a-3p
mmu-miR-1941-3p	mmu-miR-378a-3p	mmu-miR-3090-5p
mghv-miR-M1-8-5p	mmu-miR-21a-3p	mmu-miR-2137
mmu-miR-763	mmu-miR-503-5p	mmu-miR-1971
mmu-miR-1843b-3p	mmu-miR-3090-5p	mmu-miR-142a-5p
mmu-miR-1934-5p	mmu-miR-2137	mmu-miR-142a-3p
mmu-miR-3103-3p	mmu-miR-541-3p	mmu-miR-677-3p

mmu-miR-1947-3p	mmu-miR-1971	
mmu-miR-3474	mmu-miR-2861	
mmu-miR-3572-3p	mmu-miR-142a-5p	
mmu-miR-3102-5p	mmu-miR-677-3p	
	mmu-miR-551b-5p	

Analysis (PLS-DA). This method is similar to *Principal Component Analysis* (PCA) with the advantage that it also provides the Variable Importance in Projection (VIP) scores. This provides information on how the two groups are classified. As shown in **Fig. 4**, the PLS-DA scores plot between the first and second component, clearly separating the expression pattern of miRs in non-atherogenic (NC) vs atherogenic (WD) aortae. **Fig. 5** shows the VIP scores of the top 25 miRs which distinguish the two experimental groups. Differential expression pattern of miRs in the aortic lesions (WD) is illustrated in the volcano plot (**Fig. 6**).

A Pub Med search showed that out of 150 differentially expressed miRs in the aortic lesions, 4 miRs are associated with foam cells, 60 miRs are linked with inflammation, and 80 miRs are implicated in apoptosis. It has also been shown that 14 down-regulated and 34 upregulated miRs in the aortic lesions are expressed in macrophages (**Fig. 7**). Thirteen out of 23 down regulated and 30 out of 37 up-regulated inflammatory miRs (**Fig. 8**) are associated with macrophage inflammation; and 13 out of 28 downregulated and 29 out of 52 upregulated miRs are related to apoptosis and macrophages.

Since inflammation and apoptosis are critical features of lesion stability and nature, and macrophages are the major constituents of atherosclerotic plaques, I next examined which of the miRs expressed in macrophages are associated with both inflammation and apoptosis. As shown in **Fig. 9** and **Table 7**, 39 miRs expressed in macrophages are associated with both inflammation and apoptosis. VIP scores of the hierarchy show that miR-21 is among the top 5 miRs which drive the separation of the expression pattern of differentially expressed miRs. Since miR-21 is associated with inflammation and apoptosis in a variety of pathological conditions, subsequent studies focused on examining the contribution of this miR in atherogenesis.

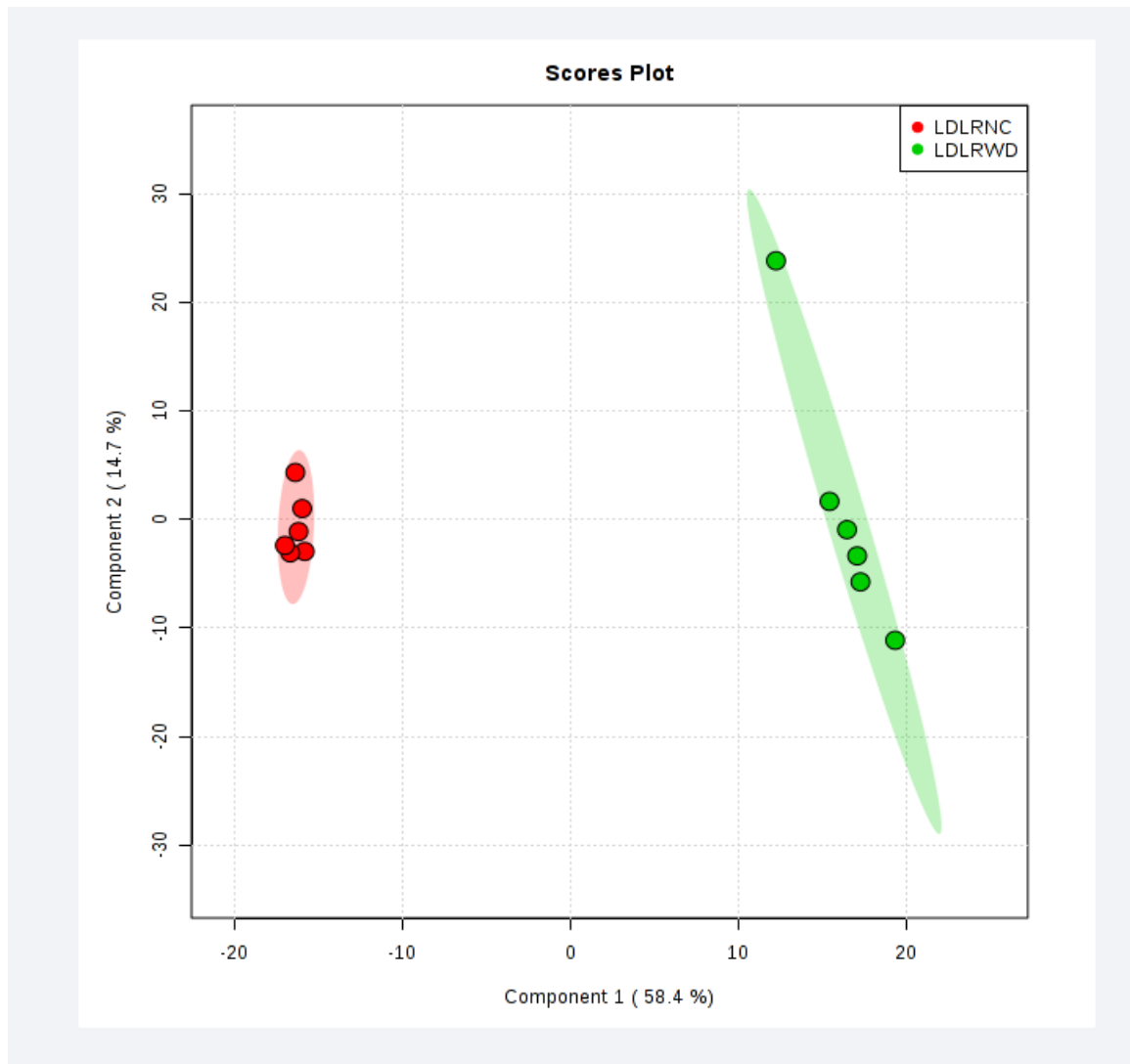


Figure 4. PLS-DA Principal component analysis of lesional miRNAs of LDL receptor knockout (LDLR-KO) mice maintained on normal chow (red) or Western diet (green) for 12 weeks.

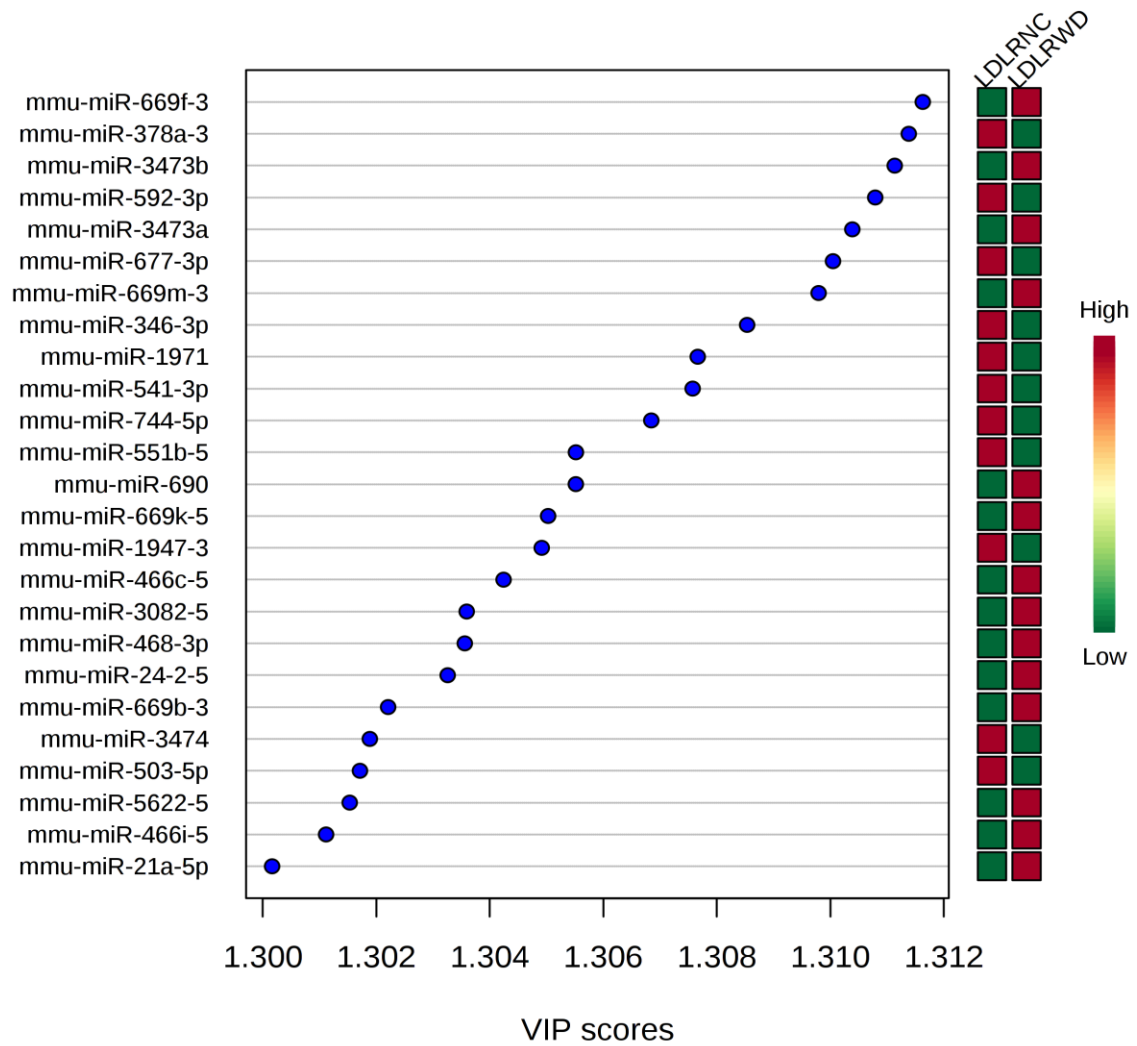


Figure 5. Variable Importance in Projection (VIP) scores of top 25 miRNAs that discriminate LDL receptor knockout (LDLR-KO) mice maintained on normal chow from those maintained on Western diet for 12 weeks.

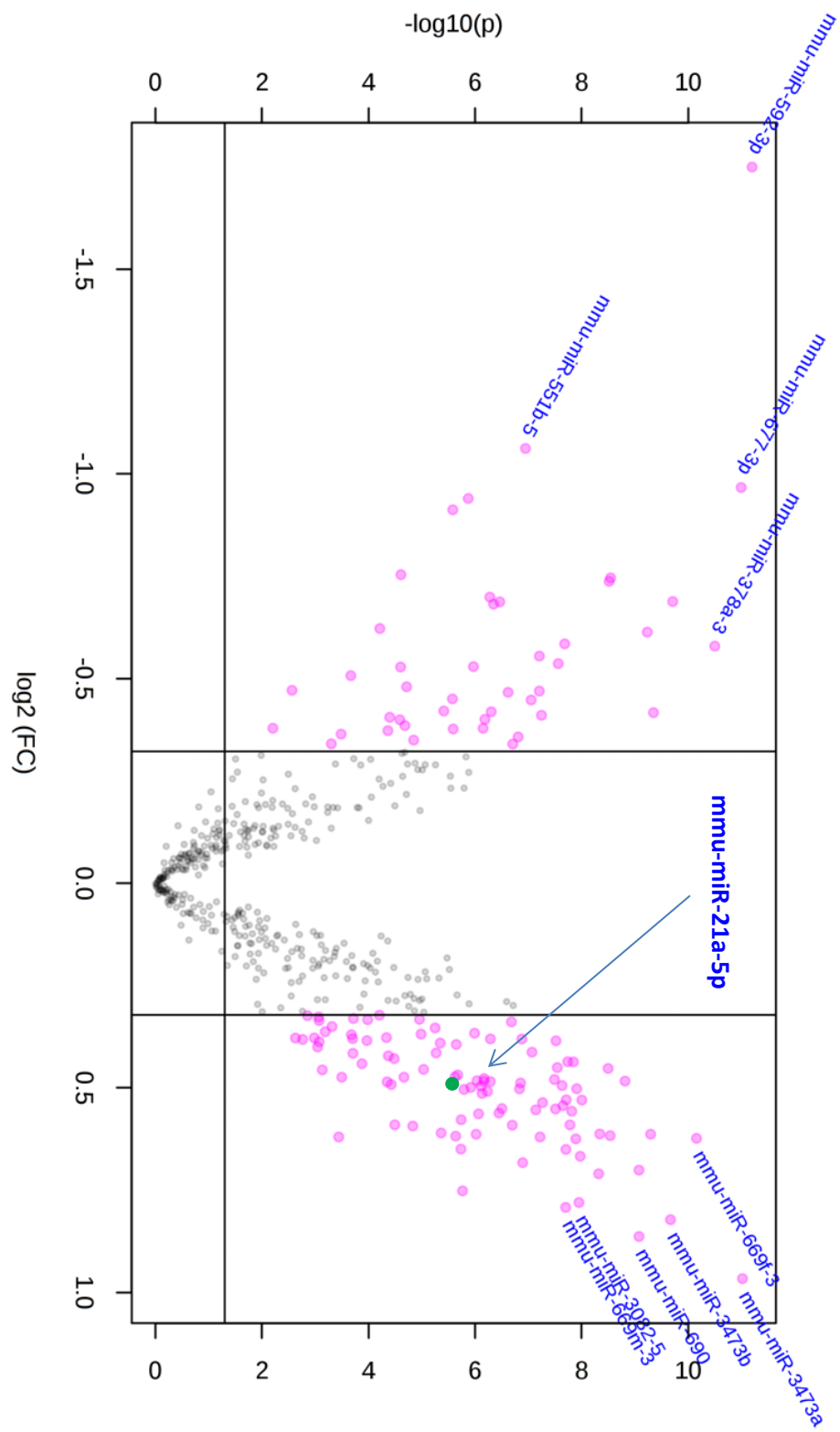


Figure 6. Volcano plots of differentially expressed miRNAs in atherosclerotic lesions of normal chow and Western diet-fed LDLR-KO mice. Fold change (FC) threshold was 1.25 (x axis) and the P value threshold was set at 0.05 (y axis). Values in pink were found to be significantly expressed.

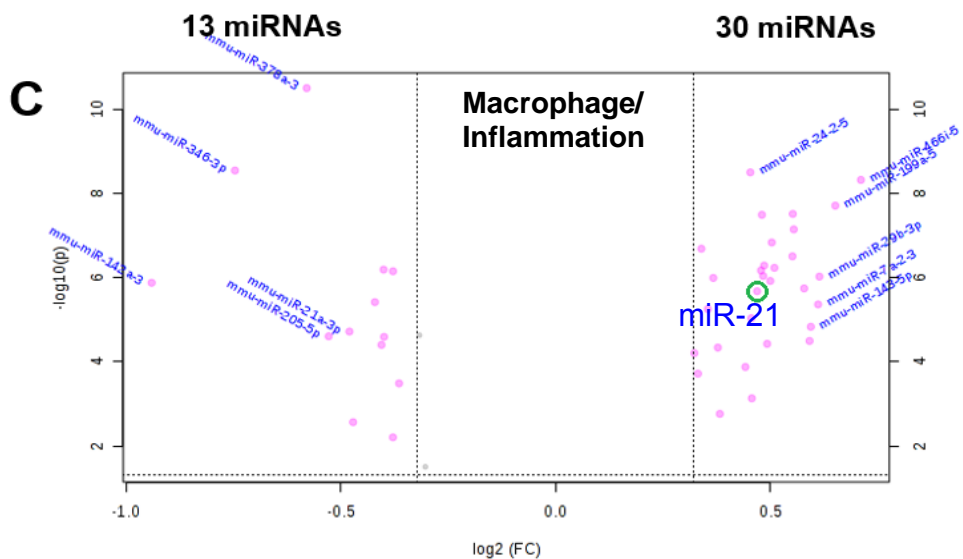
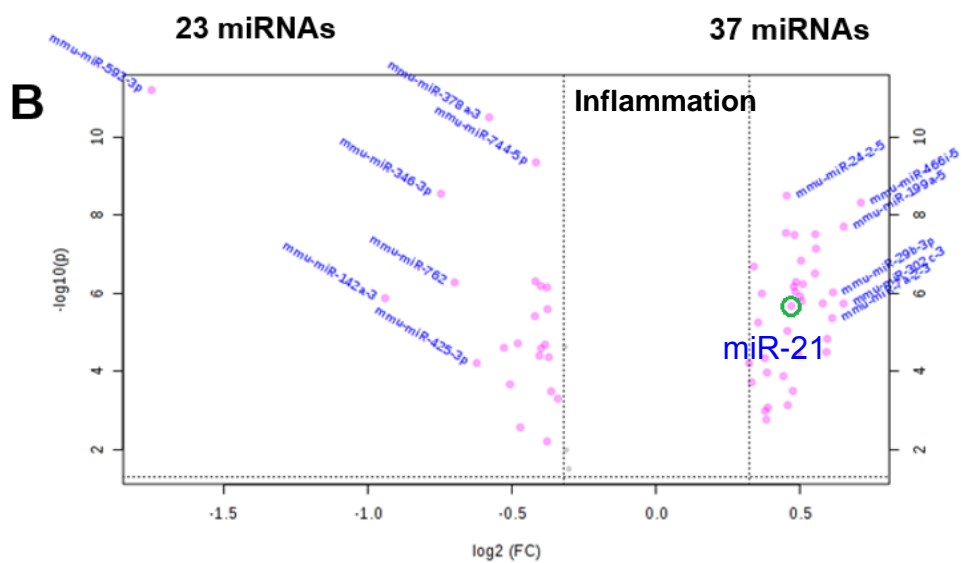
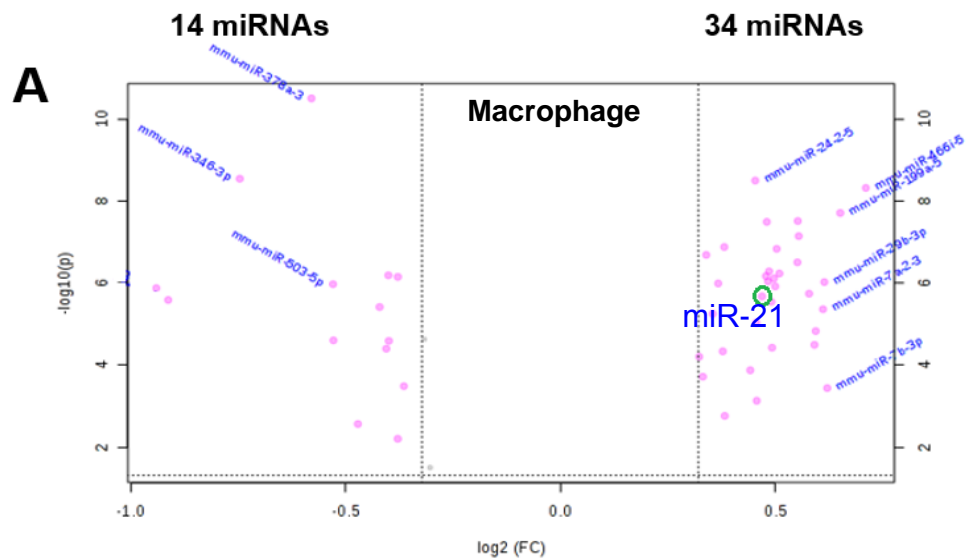


Figure 7. Volcano plots of comparative miRNA expression profiles of macrophages/inflammation in the aortae of normal chow and Western diet-fed LDLR-KO mice. Those miRNAs that increased significantly are in the right, and those that decreased significantly are in the in the left ($p < 0.05$; unpaired t-test, $n = 12$ animals: 6NC and 6WD). X-axis indicates the log transformed fold change and the Y-axis represents corresponding p-values. (A) miRNAs that are expressed in macrophage; (B) miRNAs associated with inflammation; and (C) miRNAs that are expressed in macrophages and associated with inflammation.

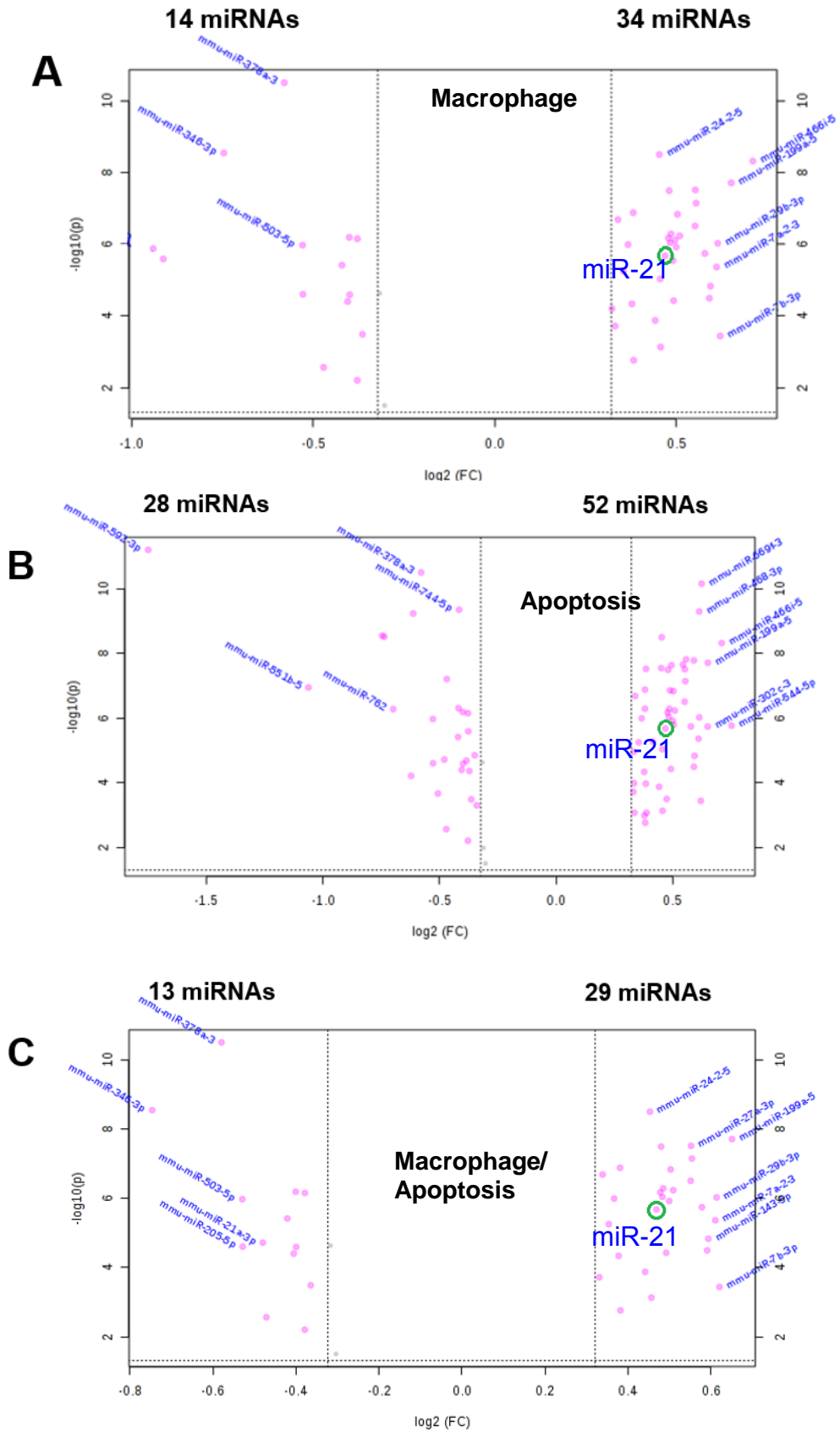


Figure 8. Volcano plots of comparative miRNA expression profiles of macrophages/apoptosis in the aortae of normal chow and Western diet-fed LDLR-KO mice. Those miRNAs that increased significantly are in the right and those that decreased significantly are in the in the left ($p < 0.05$; unpaired t-test $n = 12$ animals: 6NC and 6WD). X-axis indicates the log transformed fold change and the Y-axis represents corresponding p-values. (A) miRNAs that are expressed in macrophage; (B) miRNAs associated with apoptosis; and (C) miRNAs that are expressed in macrophage and associated with apoptosis.

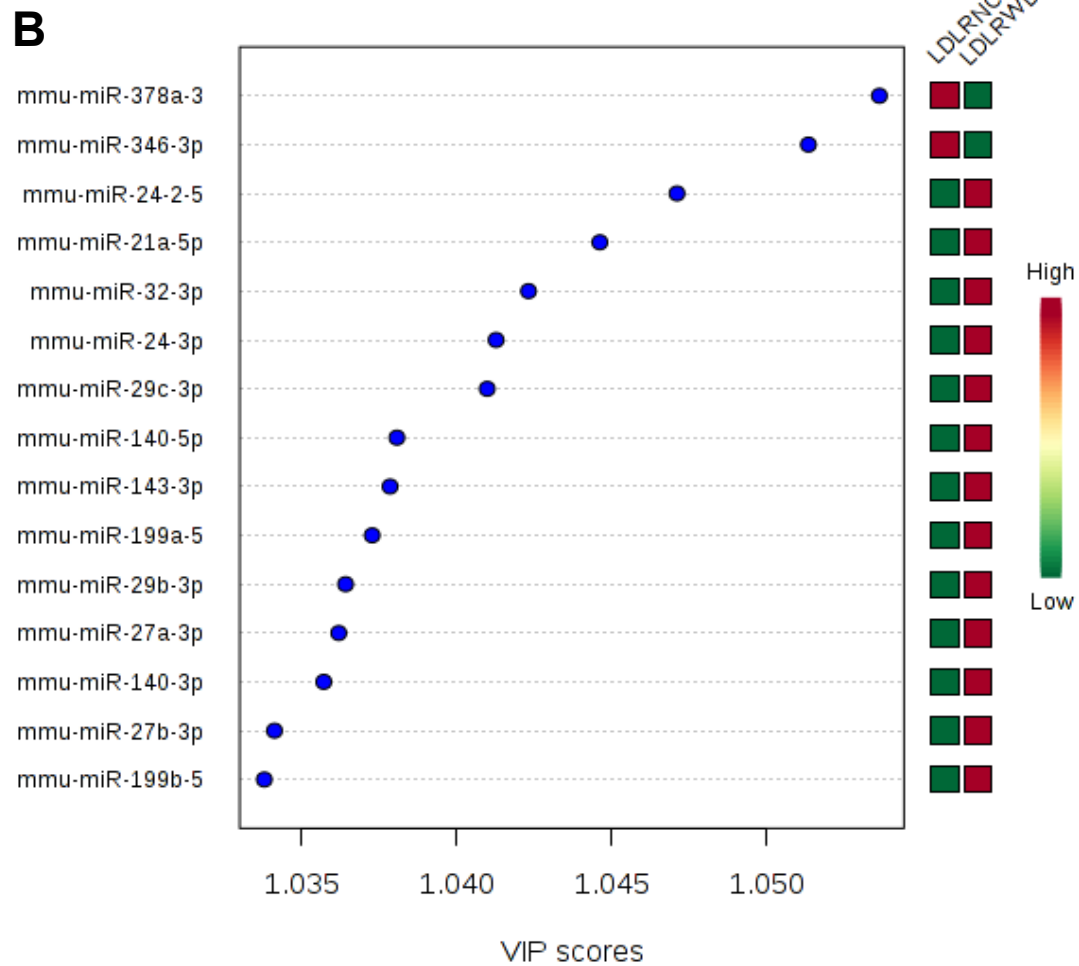
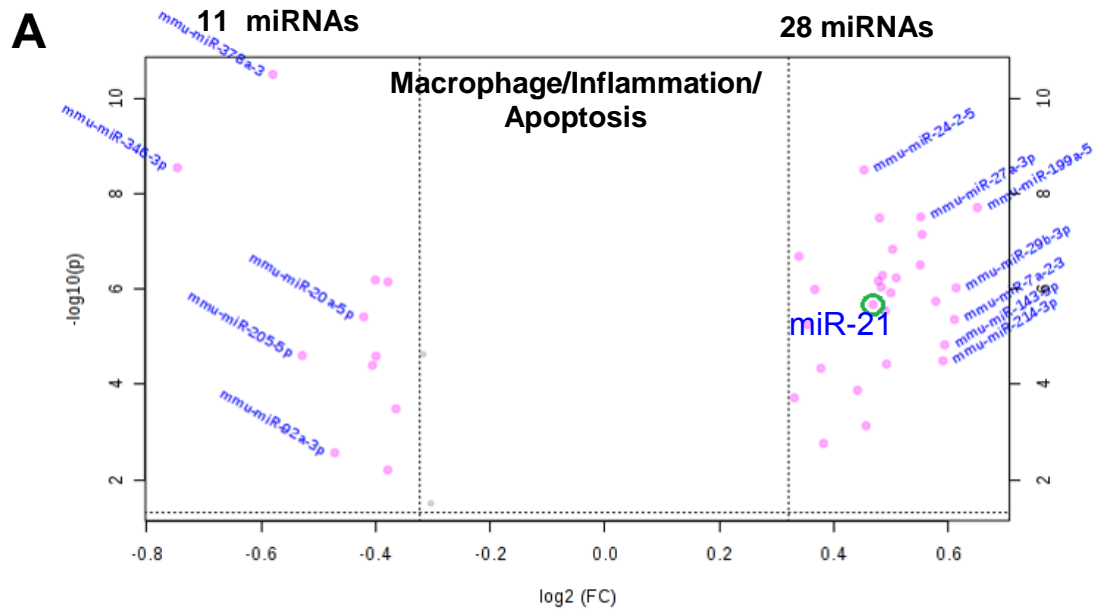


Figure 9. Volcano plots and VIP scores of comparative miRNA expression profiles of macrophage /inflammation/apoptosis in the aortae of normal chow and Western diet-fed LDLR-KO mice. (A) Volcano plots of comparative expression profile of miRNAs that are known to be expressed in macrophages and associated with inflammation and apoptosis. (B) Variable Importance in Projection (VIP) scores of top 15 miRs that discriminate LDL receptor knockout (LDLR-KO) mice maintained on Western diet (WD) from those maintained on normal chow (NC) for 12 weeks, n = 6 per group.

Table 7: Differential expression of miRNAs in macrophages and their association with inflammation and apoptosis.

mmu-MIR	VIP SCORE	Fold change (FC)	log2(FC)	P value
mmu-miR-378a-3p/mmumir-378b/mmumir-378c	1.0536	0.66929	-0.5793	3.18E-11
mmu-miR-346-3p	1.0513	0.59622	-0.74608	2.88E-09
mmu-miR-24-2-5p	1.0471	1.3686	0.45274	3.19E-09
mmu-miR-21a-5p	1.0446	1.4045	0.49009	2.87E-06
mmu-miR-32-3p	1.0423	1.4649	0.55079	3.13E-07
mmu-miR-24-3p	1.0413	1.3944	0.47964	3.25E-08
mmu-miR-29c-3p	1.041	1.4229	0.50879	5.87E-07
mmu-miR-140-5p	1.0381	1.4927	0.57791	1.81E-06
mmu-miR-143-3p	1.0379	1.2647	0.3388	2.07E-07
mmu-miR-199a-5p	1.0373	1.5697	0.65048	1.97E-08
mmu-miR-29b-3p	1.0364	1.5299	0.61342	9.48E-07
mmu-miR-27a-3p	1.0362	1.4658	0.55168	3.09E-08
mmu-miR-140-3p	1.0357	1.3836	0.46847	2.11E-06
mmu-miR-27b-3p	1.0341	1.3923	0.47747	6.78E-07
mmu-miR-199b-5p	1.0338	1.468	0.5539	7.19E-08
mmu-miR-146a-5p	1.0323	0.76926	-0.37846	7.07E-07
mmu-miR-7a-2-3p	1.0318	1.5267	0.61038	4.35E-06
mmu-miR-24-1-5p	1.0313	1.4168	0.50262	1.47E-07
mmu-miR-30b-5p	1.028	1.4134	0.49921	1.20E-06
mmu-miR-212-3p	1.026	1.3994	0.48486	5.19E-07
mmu-miR-20a-5p	1.0239	0.74702	-0.42078	3.84E-06
mmu-miR-139-5p	1.0223	0.75764	-0.40042	6.48E-07
mmu-miR-30c-5p	1.0193	1.2893	0.36656	1.02E-06
mmu-miR-143-5p	1.014	1.5088	0.5934	1.48E-05
mmu-miR-23b-3p	1.0138	1.3973	0.48262	9.17E-07
mmu-miR-126a-3p	1.0046	0.75506	-0.40533	3.97E-05
mmu-miR-219b-5p	1.0018	1.4063	0.4919	3.76E-05
mmu-miR-210-3p	0.99421	1.2779	0.35374	5.61E-06
mmu-miR-20b-5p	0.99142	0.75819	-0.39936	2.56E-05
mmu-miR-130a-3p	0.98563	1.2989	0.37729	4.60E-05
mmu-miR-185-3p	0.98258	0.77682	-0.36435	0.000325
mmu-miR-205-5p	0.97951	0.69343	-0.52818	2.49E-05
mmu-miR-214-3p	0.97328	1.5057	0.59047	3.20E-05
mmu-miR-145a-5p/mmumir-145b	0.97154	1.3577	0.4412	0.000133

mmu-miR-34c-3p	0.96066	1.3719	0.45622	0.000736
mmu-miR-301a-3p	0.94645	1.2577	0.33078	0.000192
mmu-miR-92a-3p	0.90447	0.72133	-0.47127	0.002713
mmu-miR-31-5p	0.87873	1.303	0.38183	0.001722
mmu-miR-155-5p	0.78511	0.76916	-0.37864	0.006225

Expression of miR-21 in atherosclerotic mice: Microarray analyses (**Fig. 10A**) and quantitative real time PCR analyses (**Fig. 10B**) showed that the expression of miR-21 increased by 1.4-2.4-fold in the aortae of WD fed LDLR-KO mice as compared with NC fed mice. To examine the expression of miR-21 in macrophages under atherogenic conditions, expression of miR-21 in BMDM (after 12 weeks of WD) and in peritoneal macrophages (after 20 weeks of WD) was compared with corresponding NC fed WT (C57BL/6) and LDLR-KO mice. As shown in **Fig. 10C**, WD had no effect on the expression of miR-21 in WT BMDM; however, it increased the expression of miR-21 by 1.7-fold ($P<0.05$) in LDLR-KO BMDM. Similarly, WD increased the expression of miR-21 in the peritoneal macrophages of LDLR-KO mice (**Fig. 10D**). Together, these data suggest that under atherogenic conditions, the expression of miR-21 is significantly increased in aortae and macrophages.

Expression of miR-21 in cultured macrophages by atherogenic lipoproteins: Oxidized LDL and acetylated LDL (AcLDL) are known to be taken up by the scavenger receptors on the macrophages to form foam cells. Therefore, an examination of how these lipoproteins affect the expression of miR-21 was conducted. As shown in **Fig. 11A** and **B**, incubation of BMDM with 50 μ g LDL, oxLDL and AcLDL for 24h increased the expression of miR-21 by 1.5-4 fold ($P<0.05$). Similarly, BMDM stimulated with LPS (100 ng/mL) under the identical conditions increased the expression of miR-21 by 2-fold (**Fig. 11C**). LPS also down regulated PDCD4 (**Fig. 11D**), one of the target proteins of miR-21; however, it did not affect the expression of other target proteins of miR-21 such as FABP4 and Vimentin. Collectively, these data suggest that similar to atherogenic mice, macrophage expression of miR-21 is also increased by atherogenic lipoproteins *in vitro*.

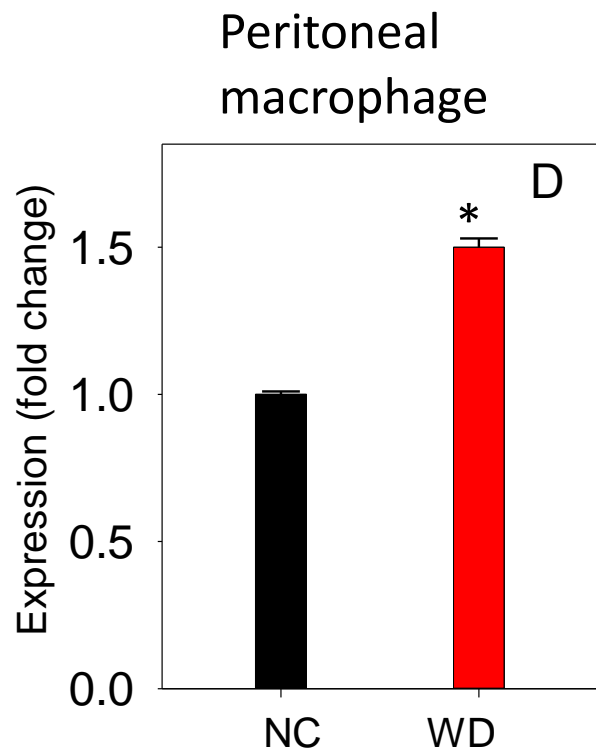
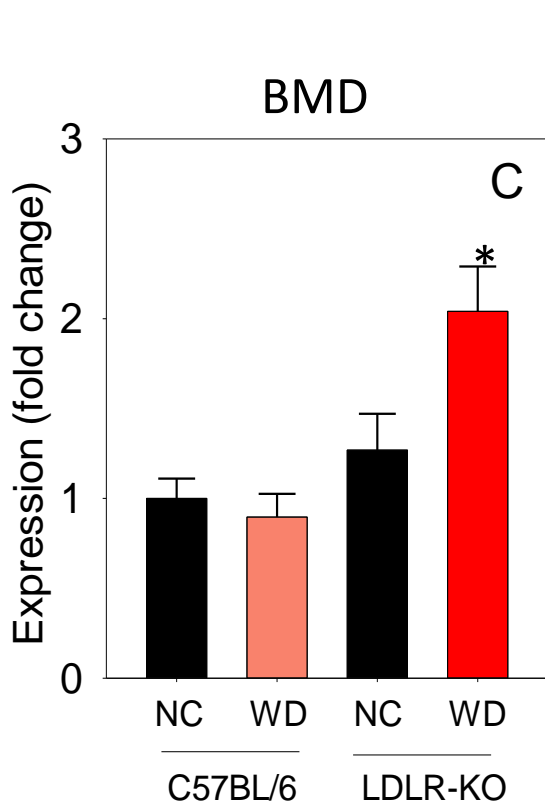
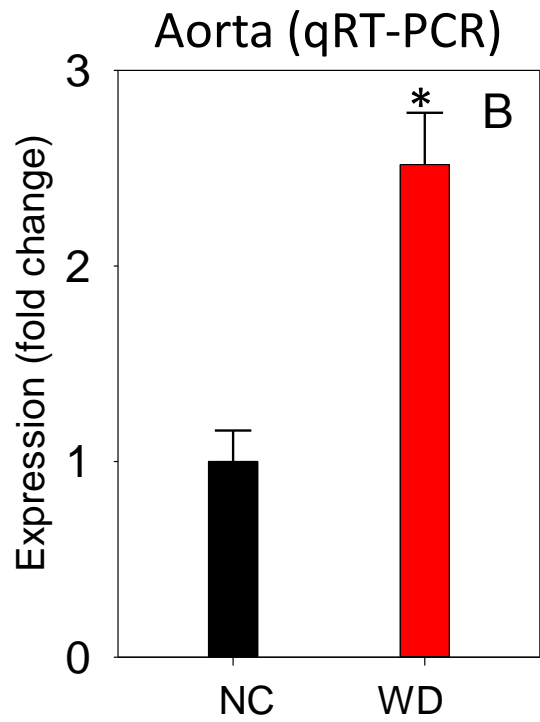
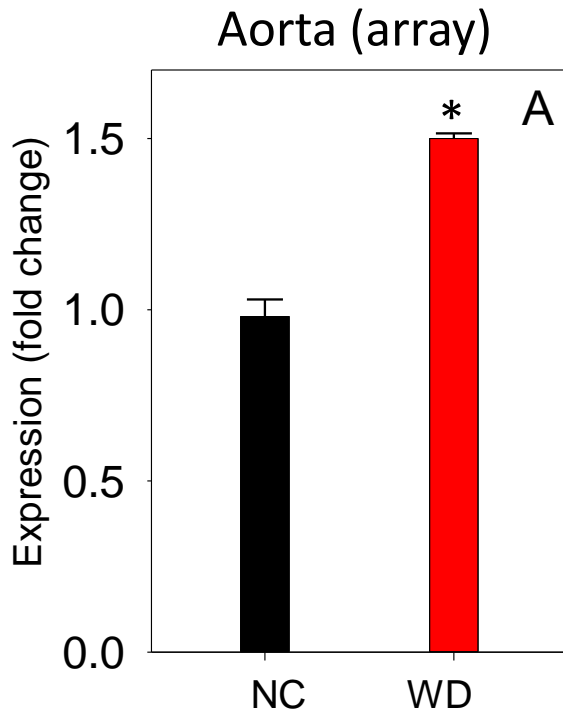


Figure 10. Effect of Western Diet on the expression of miR-21 in atherogenic mice.

LDLR-KO mice were maintained on NC or WD for 12 weeks and expression of miR-21 in the aortae was measured by (A) microRNA array (n = 6) and (B) qRT-PCR (n = 8). Panel C shows the expression of miR-21 (by qRT-PCR; n=12/group) in the bone marrow- derived macrophages (BMDM) of WT C57BL/6 and LDLR-KO mice maintained on NC or WD for 12 weeks. (D) Expression of miR-21 in peritoneal macrophages isolated from LDLR-KO mice maintained on NC or WD for 20 weeks (n = 12/group). Values are mean \pm SEM. *P < 0.05 vs NC.

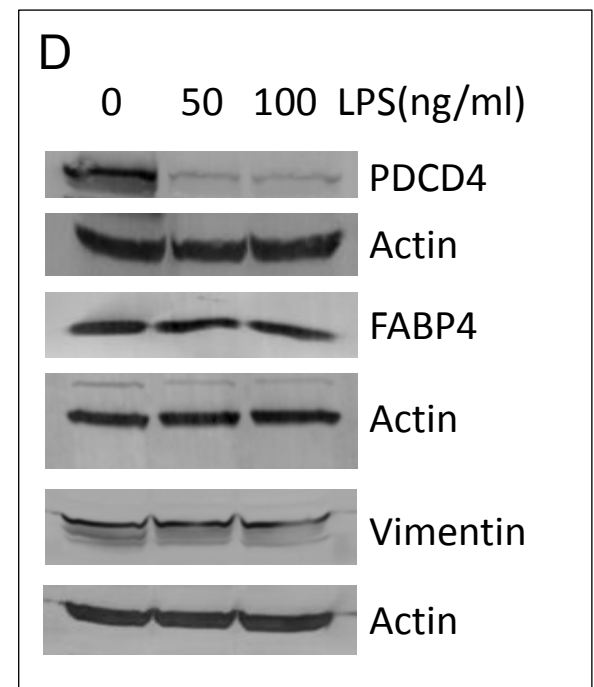
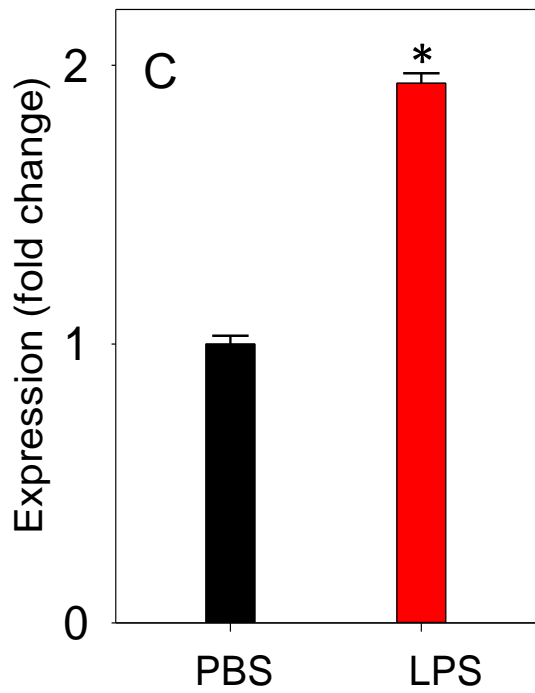
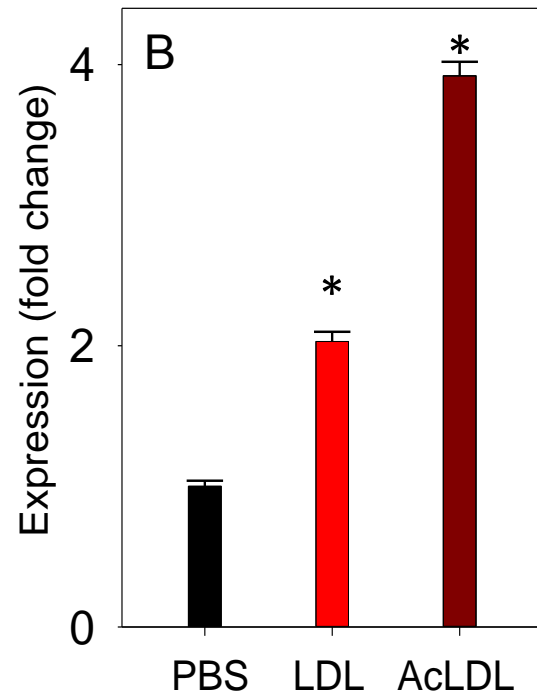
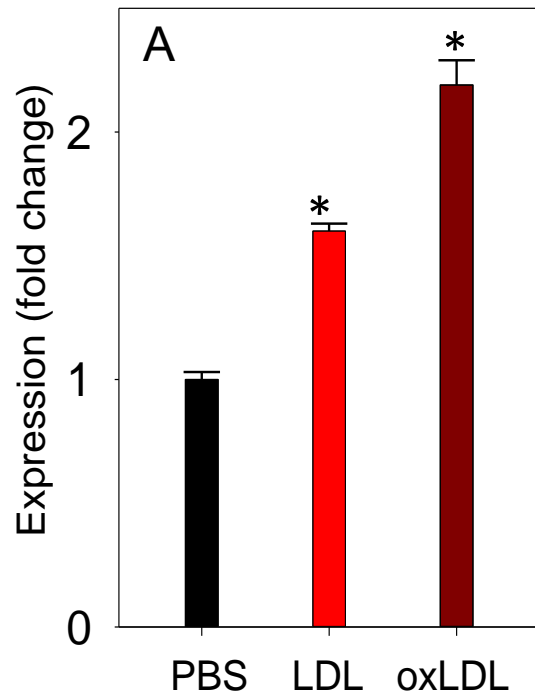


Figure 11. Expression of miR-21 by atherogenic stimuli in BMDM. BMDM were incubated with PBS (control), LDL (50 μ g), oxLDL (50 μ g) (A), AcLDL (50 μ g) (B), or LPS (100 ng/ml) (C) for 24 hours. Expression of miR-21 was measured by real time quantitative PCR. Data are expressed as mean \pm SEM. *P < 0.05 vs PBS. (D) Western blot analyses of BMDM from WT mice treated with LPS (50 ng/ml and 100 ng/ml) for 24h.

Effect of miR-21 deficiency on foam cell formation: To examine the effect of miR-21 on atherogenesis, we first examined how deficiency of miR-21 affects foam cell formation. As shown in **Fig. 12**, incubation of WT or miR-21-KO BMDM for 72h with LDL had no effect on lipid uptake. However, AcLDL increased the lipid deposition in WT macrophages, while the deficiency of miR-21 in the macrophages increased the foam cell formation by 2.3-fold ($P < 0.05$). These data are consistent with our hypothesis that miR-21 in macrophages is anti-atherogenic, and it is induced under atherogenic conditions as an adaptive response.

Characterization of MiR-21-KO mice: Next, experiments were designed to examine how the deficiency of miR-21 affects atherogenesis. Prior to performing these experiments, a rigorous characterization of the miR-21-KO mice was conducted focusing on the abundance of immune cells.

Effect of miR-21 deficiency on bone marrow cells, CBC, and immune cells: Gating strategy for the flow cytometric analyses of immune cells is depicted in **Fig. 13**. As shown in **Fig. 14**, bone marrow cells isolated from miR-21-KO and WT mice showed no difference in the number of common myeloid progenitors ($c\text{-kit}^+/Sca\text{-1}^-/CD34^+$), erythroid progenitors ($c\text{-kit}^+/Sca\text{-1}^-/CD16/32^-$), granulocyte monocyte progenitors ($c\text{-kit}^+/Sca\text{-1}^-/CD16/32^+$), hematopoietic progenitors ($c\text{-kit}^+/Sca\text{-1}^+/CD34^-$), and multipotent progenitors ($c\text{-kit}^+/Sca\text{-1}^+/CD34^-$).

As shown in **Fig. 15**, hematopoietic progenitor cells generate various blood cells. Data presented in **Table 8** showed that deficiency of miR-21 did not affect the levels of white blood cells (WBCs), red blood cells (RBCs), hemoglobin, hematocrit, mean cell volume, mean cell hemoglobin, platelets, or mean platelet volume.

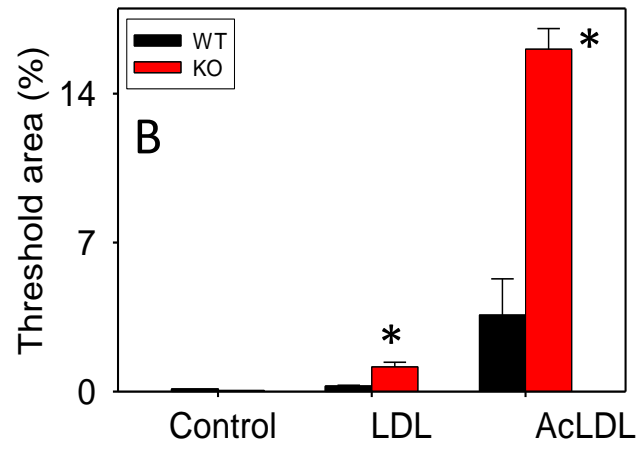
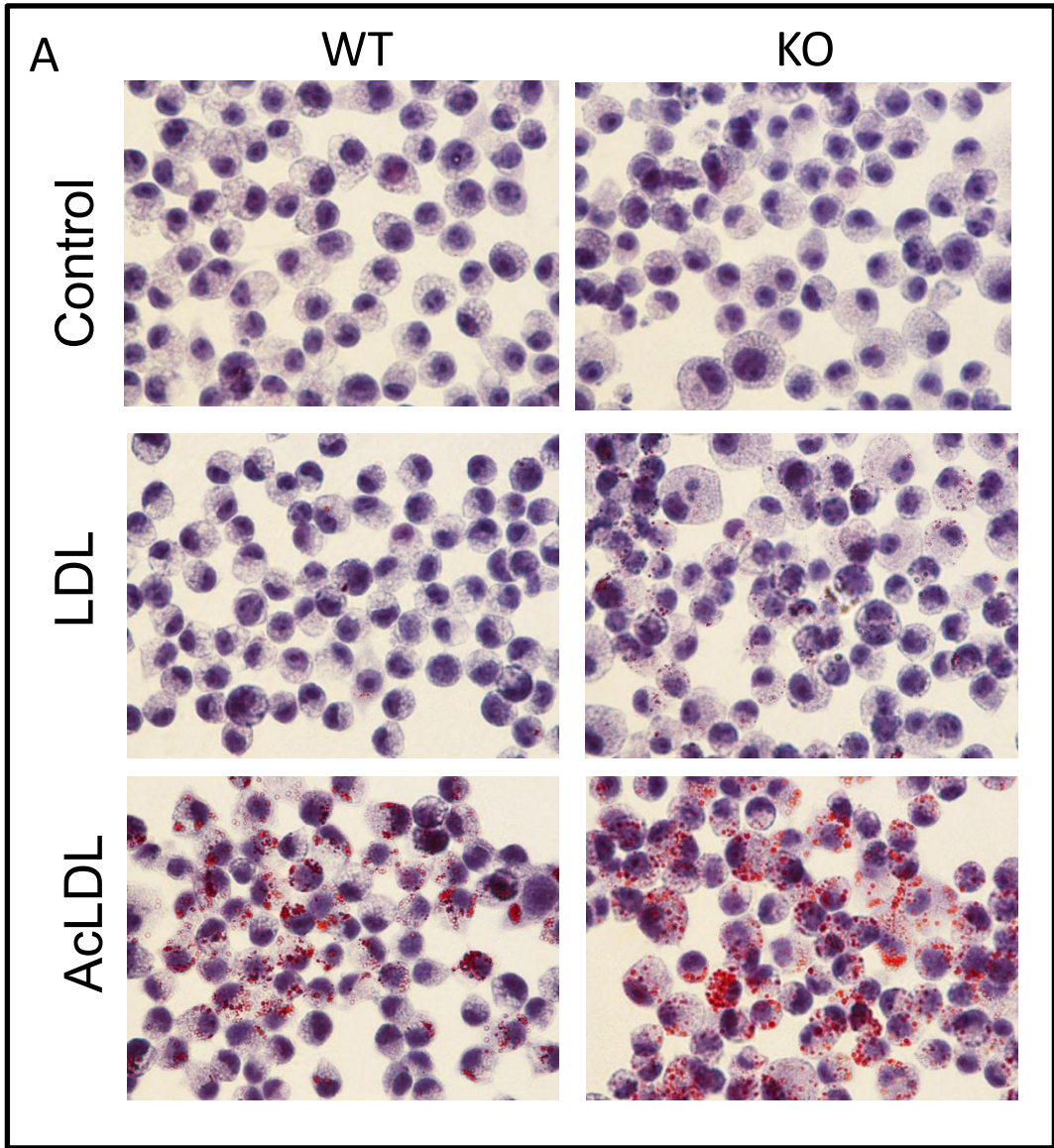


Figure 12. Foam cell formation in miR-21 deficient BMDM. WT and miR-21-KO BMDM treated with PBS (control), LDL (50 µg/ml) and AcLDL (50 µg/ml) for 72 h and foam cell formation was measured following staining with Oil red O. (A) Representative photomicrograph of lipid laden foam cells. (B) Quantitation of Oil red O staining. Three fields per slide were used for analyses. Values are mean ± SE of three independent experiments.

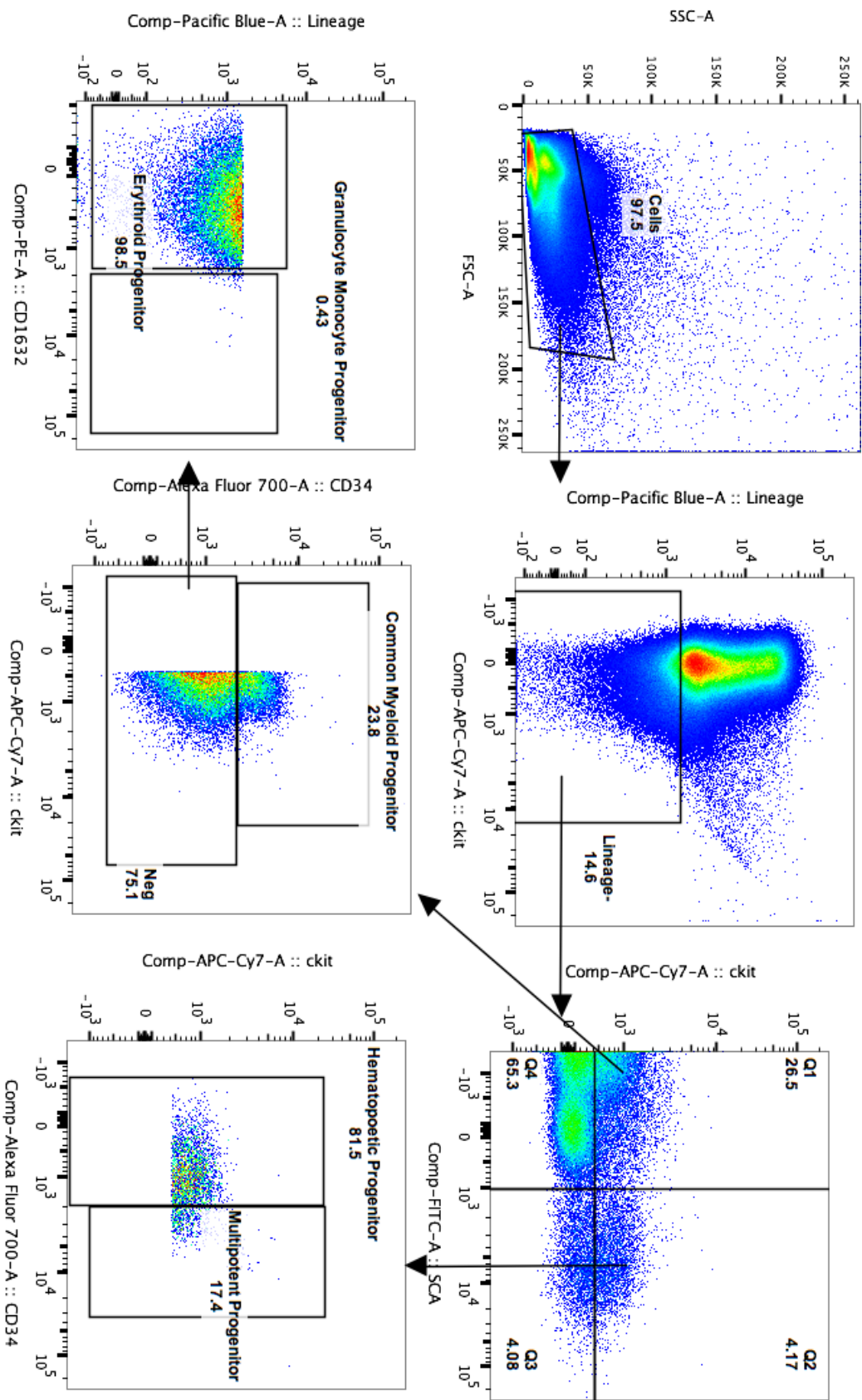


Figure 13. *Gating strategy used to identify bone marrow cells by flow cytometry.*

Cells were isolated from bone marrow of miR-21 WT and KO mice and stained with anti- CD45, CD34, CD117(c-kit), SCA, CD16/32 FcgR, and e450-lin antibodies.

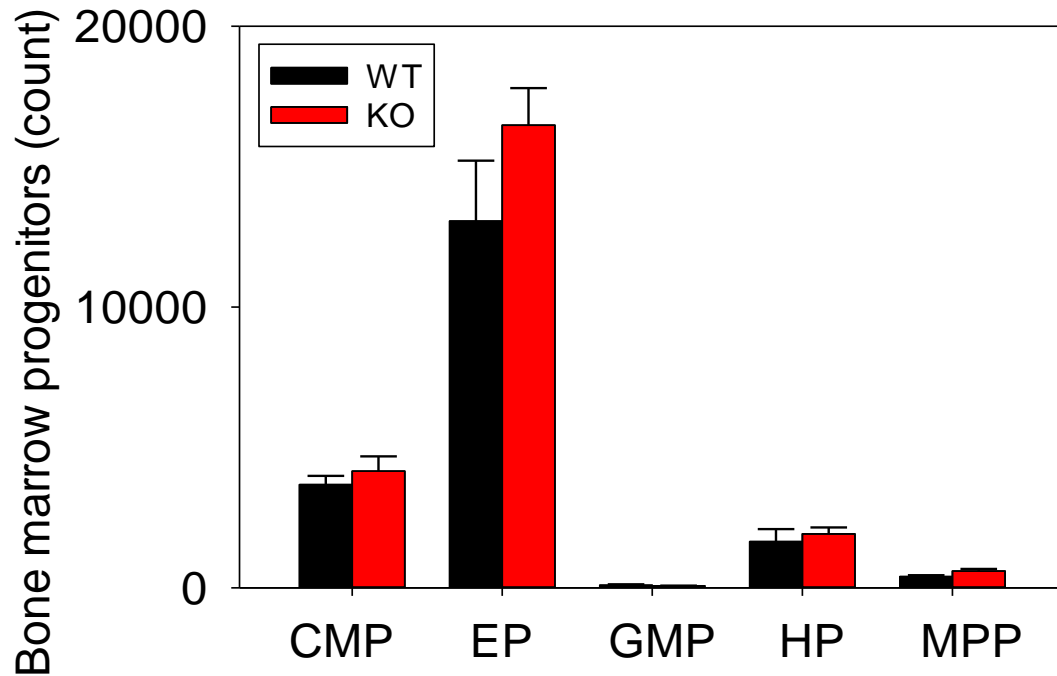


Figure 14. Characterization of *miR-21-KO* mice. Bone marrow cell differentiation was analyzed by flow cytometry. Common myeloid progenitors (CMP), erythroid progenitors (EP), granulocyte monocyte progenitors (GMP), hematopoietic progenitors (HP), and multipotent progenitors (MPP) cell counts are shown. Eight mice per group were used for analyses. Data are expressed as mean \pm SEM.

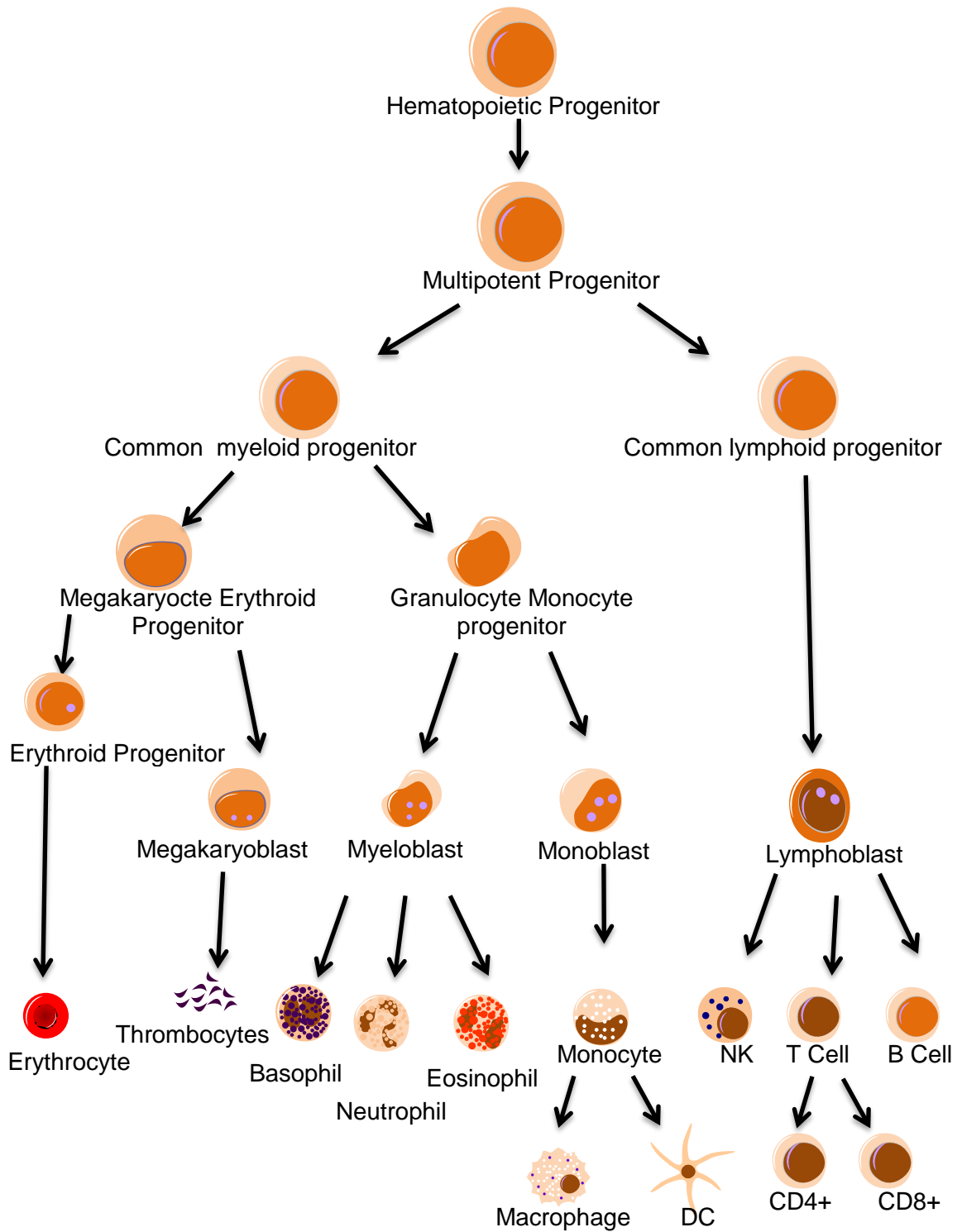


Figure 15. Formation of different blood and immune cells from hematopoietic progenitor cell.

Table 8: Complete blood count of WT and miR-21-KO mice

Parameters	WT	KO
WBC/ μ l	2652.5 \pm 230.5	2452.5 \pm 224.7
Neutrophils / μ l	603.75 \pm 80.6	806 \pm 101.26
Lymphocytes / μ l	1992.5 \pm 159.8	1542.5 \pm 159.9
Monocytes / μ l	52.5 \pm 10.6	45.0 \pm 8.24
Eosinophils / μ l	Traces	Traces
Basophils / μ l	Traces	Traces
Platelets (10^3 / μ L)	652.4 \pm 24.3	702.6 \pm 35.4
RBC (10^6 / μ L)	8.38 \pm 0.08	7.91 \pm 0.17*
Hemoglobin (g/dL)	10.70 \pm 0.18	11.18 \pm 0.21
Hematocrit (%)	38.35 \pm 0.45	36.99 \pm 0.69
Mean Cell Volume (fL)	45.76 \pm 0.16	46.80 \pm 0.54
Mean Cell Hemoglobin (pg)	12.79 \pm 0.22	14.13 \pm 0.14*
Mean Cell Hemoglobin Concentration (g/dL)	27.89 \pm 0.48	30.21 \pm 0.22*
Red Cell Distribution (%)	17.58 \pm 0.24	17.40 \pm 0.27
Mean Platelet Volume (fL)	4.10 \pm 0.06	4.15 \pm 0.05

Values are mean \pm SEM. *P<0.05 vs WT mice.

Sub-populations of WBCs – total lymphocytes, monocytes, neutrophils, eosinophils, and basophils in miR-21-KO were also comparable to WT mice. To determine whether miR-21 deficiency affects circulating immune cells, flow cytometry analyses was performed on circulating leukocytes. Gating strategy for these experiments is illustrated in **Fig. 16**. In the lymphoid lineage, we observed no difference in the abundance of B-cells, CD4⁺- or CD8⁺ - T cells, natural killer (NK) cells, granulocytes or monocytes (**Table 9**). Examination of the sub-population of monocytes showed that the levels of CD62L⁻/Ly6C⁻ (anti-inflammatory) monocytes were lower in miR-21-KO cells (**Table 9**, P< 0.05). Together, these data suggest that deficiency of miR-21 does not affect bone marrow cells or immune cells.

Effect of miR-21 deficiency on atherogenesis: After establishing that miR-21-KO mice are phenotypically normal, the effect of miR-21 deficiency in myeloid cells on atherogenesis was examined. For these experiments, bone marrow cells from miR-21-KO and WT mice were transplanted in LDLR-KO mice.

Characterization of chimeric mice: Five weeks after reconstitution of bone marrow cells, the recipient LDLR-KO mice were characterized for hematopoietic recovery and chimeric expression of miR-21 in WBCs. As shown in **Fig. 17**, the levels of miR-21 were depleted by 85% in the chimeric mice derived with miR-21-KO bone marrow than the WT bone marrow reconstituted mice. All the recipient LDLR-KO mice were then maintained on WD for 12 weeks and then euthanized to measure various biochemical and pathological parameters.

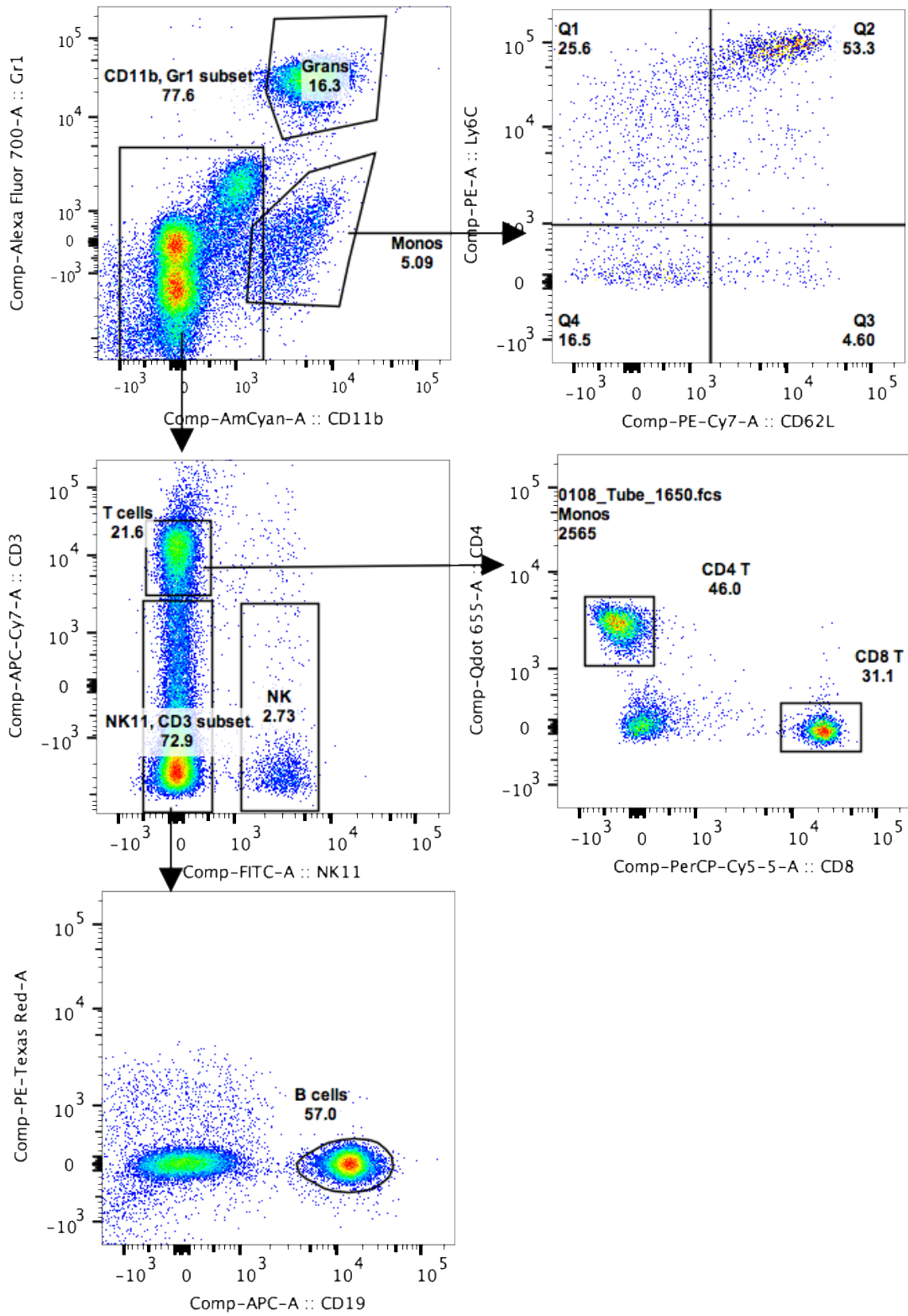


Figure 16. Gating strategy to identify circulating immune cells by flow cytometry.

RBCs were lysed, and after the exclusion of doublets and debris, immune cells were identified by CD45 staining. A sequential gating strategy was used to identify populations expressing specific markers: granulocytes (Grans) (Gr-1, CD11b), monocytes (Monos) (CD11b), monocyte sub-population (CD11b ,CD62L, Ly6c), natural killer cells (NK) (GR-1, NK1.1), CD4 T Cells (CD3e, CD4), CD8 T Cells (CD3e, CD8), and B-cells (CD19, NK1.1).

Table 9: *Circulating immune cells in WT and miR-21-KO mice.*

Parameters	WT	KO
CD4+ T-Cells/μl	75.2 \pm 14.5	56.6 \pm 10.3
CD8+ T-Cells/μl	37.6 \pm 7.4	33.1 \pm 5.7
NK /μl	27.6 \pm 2.6	24.3 \pm 2.7
B-Cells/μl	359.1 \pm 58.5	264.5 \pm 36.2
Granulocytes /μl	138.7 \pm 21.8	202.1 \pm 40.4
Monocytes /μl	73.0 \pm 12.2	46.91 \pm 7.6
Monocyte sub-population		
CD62L- /Ly6C+ (%)	15.4 \pm 1.5	18.6 \pm 1.3
CD62L+ /Ly6C+ (%)	36.7 \pm 5.0	42.2 \pm 4.5
CD62L+ /Ly6C- (%)	12.8 \pm 1.5	16.0 \pm 2.5*
CD62L-/Ly6C- (%)	35.2 \pm 5.4	23.2 \pm 2.8

Values are mean \pm SEM. *P<0.05 vs WT mice.

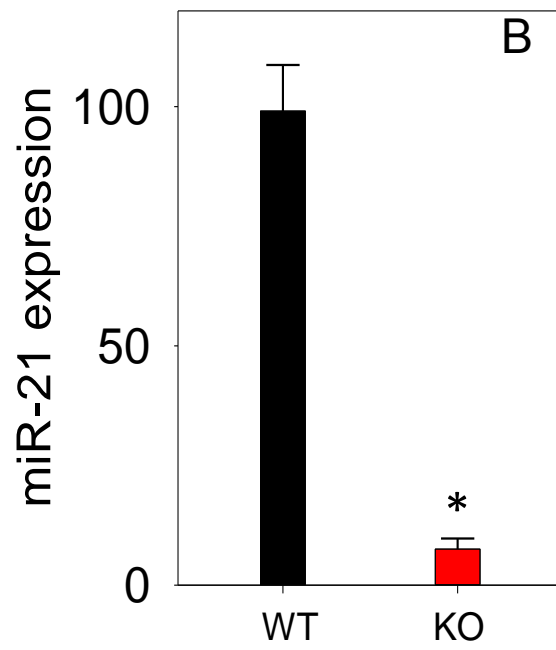
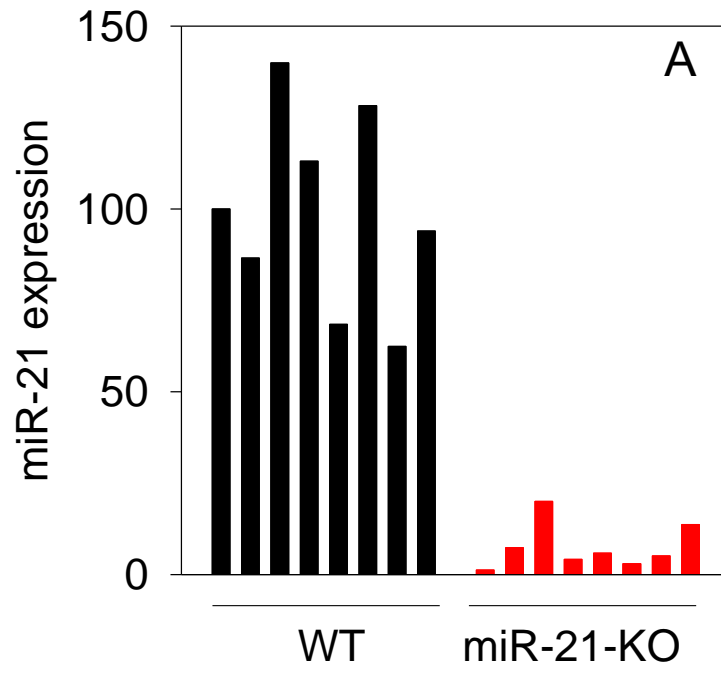


Figure 17. Expression of miR-21 in the chimeric mice. Bone marrow cells in LDLR-KO mice were lethally irradiated and then repopulated with the bone marrow cells of WT or miR-21-KO mice. Five weeks after the recovery, expression of miR-21 in the chimeric mice was measured by quantitative PCR in white blood cells. (A) Expression of miR-21 in each individual recipient mouse. (B) Group data of recipient mice. Values are mean \pm SEM. *P<0.05 vs WT mice.

Biochemical analyses: As shown in **Table 10**, myeloid cell-specific deficiency of miR-21 had no effect on body weight, blood glucose, liver enzymes, surrogate markers of injury, or renal functions. Plasma cholesterol and triglyceride levels of miR-21 chimeric mice were also comparable with controls (**Fig. 18**).

Analyses of atherosclerotic lesions: To examine the role of miR-21 in atherogenesis, lesions in the aortic valves were examined in the miR-21 chimeric and WT mice. Morphometric analysis of the lesion area in the aortic valve showed that the mean lesion area of LDLR-KO mice transplanted with miR-21 bone marrow was 1.5 fold higher than the lesion area of LDLR-KO mice transplanted with WT bone marrow (**Fig. 19**). Quantitation of lipid staining in the non-necrotic area showed that the lesions of miR-KO mice accumulate more fat than the WT mice. Staining for the macrophages and CD3+ T-cells in the non- necrotic area was comparable in the miR-21-KO chimeric mice with WT-chimeric mice (**Fig. 20A and 20B**). However, staining for the intimal smooth muscle cells was significantly lower in the miR-21-KO mice than WT mice (**Fig. 20C**). Sirius Red staining of the lesions showed that collagen staining in the miR-21-KO group was comparable with controls (**Fig. 20D**).

Table 10: *Parameters measured in the plasma of chimeric mice after 12 weeks of WD.*

Parameters	WT	KO
Blood Weight (g)	31.63±0.93	31.81±0.78
Blood Glucose (mg/dl)	248.2±13.3	233.05±6.7
Total Protein (g/dl)	7.02±0.4	10.9±1.2*
Albumin (g/dl)	2.7±0.05	3.0±0.1*
Alanine aminotransferase (U/l)	50.96±5.8	68.5±7.2
Aspartate aminotransferase (U/l)	92.3±11.4	117.8±10.1
Creatinine (mg/dl)	0.19±0.03	0.3±0.06
Creatinine kinase (U/l)	282.7±52.9	251.7±27.1
Lactate dehydrogenase (U/l)	464.6±45.8	591.3±37.1*

Values (n=15/group) are mean ± SEM. *P<0.05 vs WT mice.

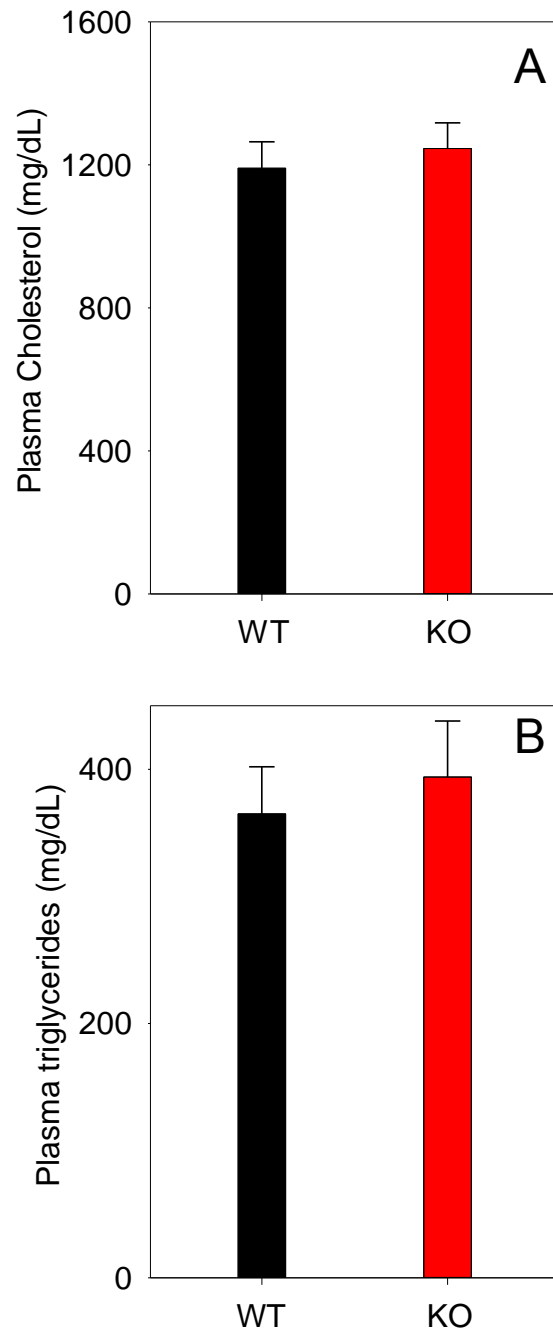


Figure 18. Plasma lipids in chimeric mice: MiR-21-KO or WT chimeric LDLR-KO mice were maintained on WD for 12 weeks (n = 15 per group) and plasma cholesterol (A) and triglycerides (B) were measured enzymatically. Values are mean \pm SEM.

WT



KO

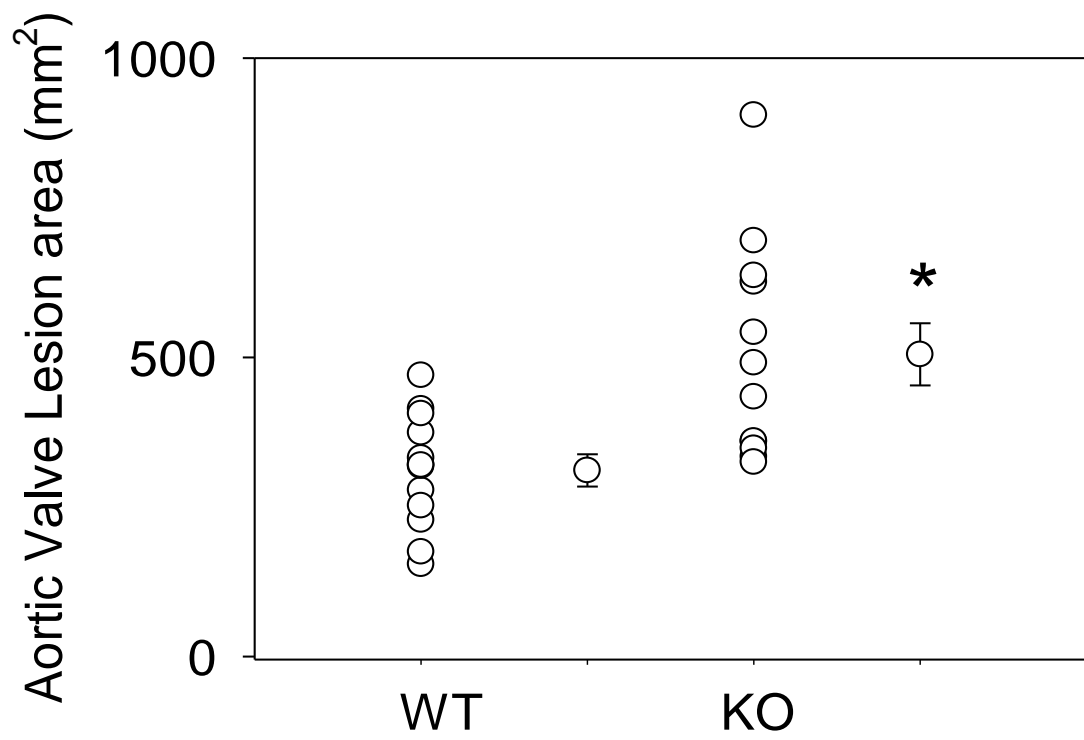
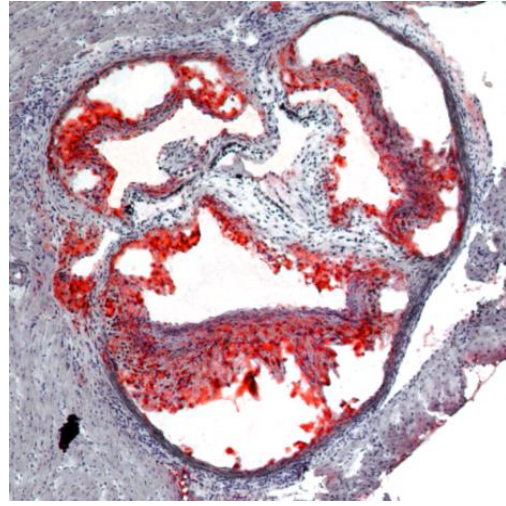


Figure 19. Effect of miR-21 deficiency on lesion formation in the aortic valve. MiR-21-KO or WT chimeric LDLR-KO mice were maintained on WD for 12 weeks (n = 15 per group), and lesions in the aortic valves were quantified. Lipids were visualized by Oil Red O staining. Upper panel are representative photomicrographs of aortic valve and Lower are the group data of lesion quantitation. Values are mean \pm SEM. *P<0.05 vs WT mice.

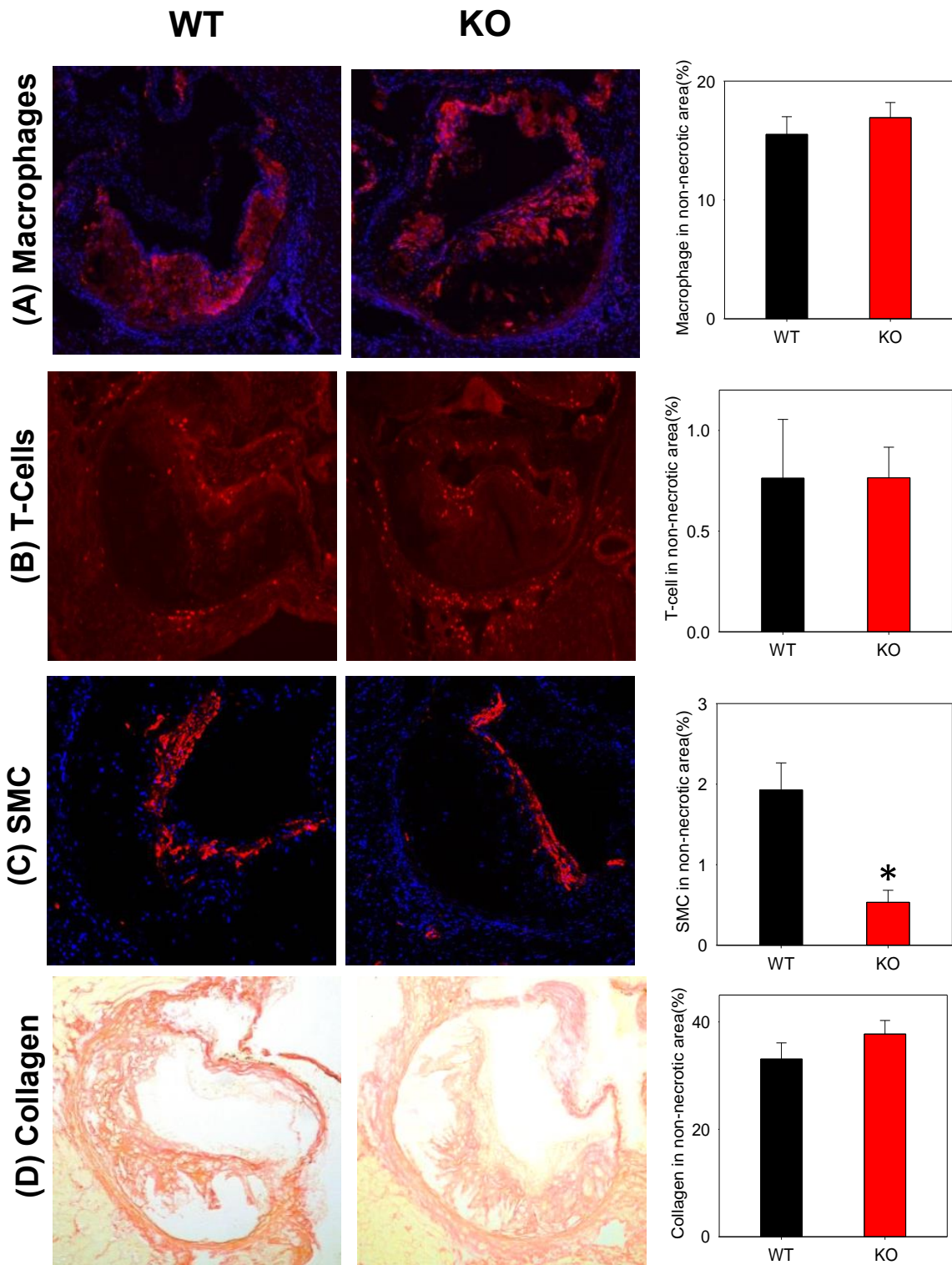


Figure 20. Lesion cellularity of miR-21 deficient chimeric mice. MiR-21-KO or WT chimeric LDLR-KO mice were maintained on WD for 12 weeks and lesions in the aortic valves were stained with A) anti- CD68 (macrophage), B) CD3 (T-cells), C) α -smooth muscle cell actin (SMC), and D) Sirius Red (collagen). Values are mean \pm SEM. *P<0.05 vs WT mice.

DISCUSSION

Major findings of the studies presented in this chapter are: a) several miRs associated with inflammation and apoptosis, including miR-21, are expressed in atherosclerotic lesions; b) expression of miR-21 is increased by atherogenic stimuli *in vivo* and *in vitro*; and c) myeloid cell-specific deficiency of miR-21 exacerbates atherogenesis in LDL receptor-KO mice. Since miR-21 has been suggested to play a vital role in inflammation and apoptosis in a variety of pathophysiological conditions, these findings support the concept that inflammation and apoptosis are the key elements of atherogenesis. The observation that myeloid cell-specific deficiency of miR-21 does not affect plasma cholesterol but increases atherogenesis indicates that it is the processes within the lesions such as inflammation and apoptosis, which drive atherogenesis in the conditions of miR-21 deficiency.

Atherosclerosis usually occurs in medium and large-sized arteries. Arterial stenosis or thrombotic occlusion of the artery leads to myocardial ischemia, stroke and renal ischemia [236]. Since atherogenesis progresses for years before displaying clinical symptoms, early detection of the disease along with therapeutic intervention can significantly diminish subsequent events, improve the quality of life, and increase the life span. Therefore, understanding the mechanisms of atherogenesis is of prime significance. In the last decade, miRs have emerged as critical modulators of various cell types and functions which govern inflammatory responses in atherogenesis. These include: endothelial activation, monocyte recruitment, foam cell formation, macrophage polarization and apoptosis, and smooth muscle cell proliferation [237].

I identified several novel miRs which are differentially expressed in the aortic lesions of LDLR-KO mice. Differential expression of several miRs, which have been studied in

various cellular and pathophysiological processes, but have not been investigated in the context of atherosclerosis, was observed in murine aortic lesions. This opens up new avenues to examine the contribution of these miRs in the etiology of atherosclerosis.

Among the other miRs differentially regulated in murine aortic lesions in my study, several miRs have been shown to be either expressed in atherosclerotic lesions or are associated with atherogenic processes such as cholesterol homeostasis, foam cell formation, vascular inflammation, and apoptosis. These include miR-17, miR-92a, miR-499, miR-155, miR-146a, miR-21, miR-29b, and miR-143. Forty eight of these differentially expressed miRs in atherosclerotic lesions are expressed/associated with macrophages.

My studies show that only 4 out of these 48 miRs (miR-155, miR-27a, miR-24 and miR-21) have been implicated in foam cell formation (as evident from Pub Med search). My data showing that the expression of miR-21 is increased *in vitro* and *in vivo* under atherogenic conditions are in agreement with the observed upregulation of miR-21 in human atherosclerotic plaques by Raitoharju E *et al* [76]. However, the contribution of miR-21 in atherosclerosis has not been directly tested. In this study, I show for the first time that the deficiency of miR-21 increases foam cells formation *in vitro*, and myeloid cell-specific deficiency of miR-21 exacerbates atherosclerosis in LDLR-KO mice. These studies are significant because they a) describe a new pathological role of miR-21, and b) provide new insight about the potential biochemical mechanisms by which miR-21 affects atherogenesis.

Complementary to my studies, it was recently reported that LPS increases the expression of miR-21 in macrophages. Additionally, inhibition of miR-21 decreases while

overexpression of miR-21 increases lipid accumulation in LPS-treated macrophages [143]. However, the role of miR-21 in LPS-induced inflammation is quite complex. In epithelial cells, miR-21 downregulates its target PTEN and thereby increases AKT phosphorylation and NF- κ B activation [238]. Contrary to these observations, miR-21 is induced by LPS to mitigate TLR4 mediated pro-inflammatory signaling by inhibiting NF- κ B [144]. Mice deficient in miR-21 target PDCD4, have elevated levels of IL-10 decreased levels of IL-6, and decreased LPS-induced mortality [239]. Inhibition of miR-21 blocks LPS-induced PDCD4 downregulation and increases NF- κ B activation and IL-6 formation, suggesting the anti-inflammatory role of miR-21. In endothelial cells miR-21 is induced by shear stress, and overexpression of miR-21 increases nitric oxide production and decreases apoptosis [132]. On the contrary, oscillatory shear stress induces miR-21 and increases the expression of atherogenic molecules MCP-1 and VCAM-1 in PPAR- α -dependent manner.

Consistent with the increased expression of miR-21 in atherosclerotic lesions in this study, induction of miR-21 has also been reported in several other inflammatory conditions such as colitis, type 2 diabetes, allergic airway inflammation, psoriasis and atopic eczema, and osteoarthritis [190]. Moreover, high expression of miR-21 was observed in experimental peritonitis, which was further increased during the resolution of inflammation [240]. This suggests that miR-21 may also act as a pro-inflammatory molecule under specific conditions.

While my data clearly demonstrates that myeloid cell-specific deficiency exacerbates an intermediate phase of atherogenesis, further studies are required to examine the contribution of myeloid/macrophage specific-miR-21 in early and advanced (complex)

lesions. Potentially, miR-21 could be deleterious early on by promoting vascular inflammation, whereas it may facilitate the resolution of inflammation. Contribution of endothelial cells and macrophage-specific miR-21 at various stages of lesions also needs to be investigated. It is conceivable that endothelial miR-21 would prevent shear stress and endothelial cell apoptosis, and prevent early atherogenesis.

My studies also show that deficiency of miR-21 decreases the abundance of intimal smooth muscle cells in atherosclerotic lesions. Inhibition of miR-21 has previously been shown to decrease smooth muscle cell proliferation and neointima formation in balloon-injured rat carotid arteries [75]. Although this study is in agreement with my data, the underlying mechanisms are potentially different because in the bone marrow transplant model, proliferation and migration of smooth muscle cells from the media to the intima is unlikely. It is possible that deficiency of miR-21 prevents the recruitment of stem cell-derived smooth muscle cells to the lesion. Alternatively, lack of miR-21 promotes smooth muscle cell apoptosis. While in early and intermediate phases of atherosclerosis, deficiency of smooth muscle cells decreases the lesion growth, decrease in smooth muscle cells in advanced lesions around the necrotic core would lead to the thinning of necrotic core and destabilization of the plaque. Further studies are required to examine how miR-21 affects smooth muscle cell abundance at different stages of lesion formation, as well as the underlying mechanisms and consequences of these processes.

In addition to miR-21, I observed an upregulation of miR-24 in murine atherosclerotic plaques. miR-24 is also expressed in human coronary artery lesions [82], where it is inversely associated with MMP-14. Expression of miR-24 is more abundant in stable plaques as compared to unstable plaques. Inhibition of miR-24 in ApoE-KO mice increased lesion size and MMP-14 expression, causing the plaques to become more

unstable. These studies support the notion that induction of miRs such as miR-21 and miR-24 in atherosclerotic lesions is a reflection of their anti-inflammatory nature.

Interestingly, my data also show that miR-155 was downregulated in atherosclerotic lesions. This is contrary to the studies of Nazai-Jahantigh *et. Al.* which showed that miR-155 was induced in atherosclerotic lesions and promoted atherosclerosis by inhibiting Bcl6 in macrophages [80]. Although, in agreement with these studies, deficiency of miR-155 in myeloid cells decreased macrophage inflammation and atherosclerosis [104]. However, deficiency of miR-155 in the bone marrow cells of LDLR-KO mice increased vascular inflammation and atherogenesis [103]. Collectively these data suggest that similar to miR-21, the role of miR-155 in vascular inflammation and atherogenesis is also very complex and appears to be atherosclerotic stage-specific. Therefore caution should be exercised in interpreting these data.

While miR-155 is one of the most studied miRNAs, less is known about the contribution of miR-27a/b in atherosclerosis. My data show that miR-27a is upregulated in the lesions of LDLR-KO mice. *In vitro* studies have shown that while miR-27a/b do not affect cellular cholesterol accumulation, they can inhibit cholesterol efflux by decreasing the expression of ATP binding cassette transporter A1 (ABCA1) and apoA-1 [116]. Several miRs such as miR-19b, miR-144-3p, and miR-302a have been reported to promote macrophage lipid accumulation *in vitro* and atherogenesis in mice, primarily by targeting ABCA1 [84, 92, 94]. However, expression of these miRs was not differentially regulated in my study. Given the varying functions and effects of different miRs in various cell types, as well as disease progression, a thorough investigation of miRNAs contribution in foam cell formation and atherogenesis is warranted.

CHAPTER 3

CONTRIBUTION OF MICRORNA-21 IN REGULATING MACROPHAGE INFLAMMATION AND APOPTOSIS *IN VITRO* AND IN MURINE ATHEROSCLEROTIC PLAQUE FORMATION

3.0. INTRODUCTION:

MiR-21 has been shown to be upregulated in atherosclerotic plaques [76]. My studies in Chapter 2 show that the expression of miR-21 is increased both under atherogenic conditions *in vitro* and in aortic lesions of LDLR-KO mice. My data in Chapter 2 also, for the first time, showed that the myeloid cell-specific deficiency of miR-21 exacerbates atherogenesis in LDLR-KO mice. However, the biochemical mechanisms by which miR-21 affects atherogenesis are not known. Since macrophage-induced generation of cytokines and apoptosis of macrophages are two critical determinants of atherosclerotic lesion formation and progression, my studies in this chapter will be focused on the role of miR-21 in regulating inflammatory signaling and apoptotic responses.

Inflammation is a hallmark of atherosclerosis [241]. It includes both innate and adaptive immunity, primarily via macrophages and T-cells, respectively. Activation of macrophages to the pro-inflammatory phenotype via TLR4 activation enhances the generation of pro-inflammatory cytokines and enhances vascular inflammation [242]. MicroRNA-155 was the first miR that was shown to be induced by TLR4 agonist LPS

during the macrophage inflammatory response [243]. Subsequently, several miRs have been suggested to modulate LPS/TLR4-induced cytokine formation in macrophages [242]. The role of miR-21 in LPS-induced inflammation has been a subject of intense investigation of late. Recently my mentor, in collaboration with others, showed that miR-21 protects from LPS-induced peritonitis [244]. However, the contribution of miR-21 in regulating TLR4 signaling in the context of atherosclerosis has not been examined. In this chapter, I will examine how miR-21 affects macrophage polarization and cytokine formation both *in vitro* and in atherosclerotic lesions, and I will delineate the role of NF- κ B and MAP Kinases in these processes.

Macrophage apoptosis is another key determinant of the progression, nature, and stability of atherosclerotic lesions. Several miRNAs, including miR-21, have been suggested to regulate cellular apoptosis. Upregulation of miR-21 in tumorigenesis has been linked to its anti-apoptotic role [216-218]. However, it is unclear whether atherogenic stimuli cause apoptosis in a miR-21-dependent manner. In this chapter I will examine the role of miR-21 in macrophage apoptosis under atherogenic conditions *in vitro* and *in vivo* and describe the mechanisms by which miR-21 affects macrophage apoptosis.

3.1. EXPERIMENTAL PROCEDURES:

3.1.1. Macrophage Polarization: BMDM were seeded in a 6-well plate at 1×10^6 cells per well. Cells were primed with IFN- γ (2,5 ng/ml) for 16h followed by incubation with LPS (10 ng/ml) to polarize them to a M1 phenotype. Incubation of BMDM with IL-4 (10 ng/ml) was used to polarize the cells to a M2 phenotype. Following treatment, cells were washed twice with PBS, and the pellets were suspended in FACS buffer (1% FBS in PBS). They were then incubated with Fc Block (BD Biosciences, San Jose, CA, USA) for

10min at 4°C before being stained with fluorescent-conjugated primary antibodies or appropriate isotype controls for 30min at 4°C. The following antibodies were used for macrophage polarization characterization: phycoerythrin (PE)-conjugated anti-F4/80 (Biolegends, San Diego, CA, USA), V 450-conjugated anti-CD80 (BD Biosciences Franklin Lakes, New Jersey, USA), A 700-conjugated anti-CD86 (BD Biosciences Franklin Lakes, New Jersey, USA), PE-Cy7-conjugated anti-CD11c (eBioscience, San Diego, CA, USA), AlexaFluor 647-conjugated anti-Mgl-1 (CD301a; AbD Serotec, Raleigh, NC, USA), and Alexa 488-conjugated anti-CD206 (AbD Serotec, Raleigh, NC, USA).

3.1.2. Measurement of cytokines: To examine the effect of miR-21 on cytokine production, WT and miR-21-KO BMDM were incubated with LPS as described above, and cytokines excreted in the cell culture medium were measured by the mouse cytokine/chemokine 32-plex array (Eotaxin, G-CSF, GM-CSF, IFN γ , IL-1 α , IL-1 β , IL-2, IL-3, IL-4, IL-5, IL-6, IL-7, IL-9, IL-10, IL-12 (p40), IL-12 (p70), IL-13, IL-15, IL-17, IP-10, KC, LIF, LIX, MCP-1, M-CSF, MIG, MIP-1 α , MIP-1 β , MIP-2, RANTES, TNF α , and VEGF; Eve Technologies Corporation, Calgary, AB, Canada). The assay sensitivities of these markers ranged from 0.1 – 33.3 pg/mL. To confirm the results of the multiplex assay, IL-6 levels were also measured by ELISA (e-Biosciences, San Diego, CA, USA).

3.1.3. Macrophage Apoptosis: To examine the effect of miR-21 on macrophage apoptosis, WT and miR-21-KO BMDM were incubated with staurosporine (STS; 500 nM) or 4-hydroxynonenal (HNE, 25 μ M) in serum-free medium for 2h followed by incubation for 4h in complete incubation medium at 37°C. Apoptosis was measured using the *Apoptosis Detection Kit* (eBioscience, San Diego, CA USA) as per the manufacturer's instructions. In this method, Annexin V-fluorescein

isothiocyanate (FITC) binds phosphatidylserine (PS) and propidium iodide (PI) or 7-aminoactinomycin D (7-AAD). Exclusion of vital cells was used to discriminate between apoptotic and necrotic cells. Briefly, after treatment, cells were washed once in PBS and then once in Annexin V binding buffer. Harvested cells were suspended in Annexin V binding buffer at a concentration of 1×10^6 cells/ml. Suspended cells were stained with 5 μ L Annexin V-FITC and incubated for 10 minutes (in the dark) at room temperature. Cells were washed with the Annexin V binding buffer and stained with PI or 7-AAD. Flow cytometry was performed using an LSR II (BD Biosciences). Data were analyzed using the Flow software (Tree Star, Ashland, OR). Data of apoptosis were confirmed by the staining for cleaved caspases by Western blotting.

3.1.4. Western blotting: Following treatments, cells were rinsed twice with PBS and lysed in a protein lysis buffer containing 25 mM HEPES, 1 mM EDTA, 1 mM EGTA, 0.1 % SDS, 1 % NP-40, and 1X protease and phosphatase inhibitors. Protein concentration was estimated in crude cell extracts using the Bradford method (Bio-Rad, Hercules, CA, USA). Approximately 10-50 μ g of crude cell extract was applied to each lane of a 4-20% Bis-Tris-HCl gel and electro blotted onto a PVDF membrane. The membrane was then blocked with 5% skim milk or 5% bovine serum albumin for 1h followed by probing with appropriate dilutions of primary antibodies overnight at 4°C. PVDF membranes were then incubated with horseradish peroxidase-conjugated secondary antibodies for 1h at room temperature. Immunoreactive bands were detected using a Typhoon scanner (SA Biosciences, Valencia, CA, USA) after exposure to ECL detection reagent. Band intensity was quantified by using ImageQuant software. Primary antibodies used were anti-PDCD4 (Cell Signaling), anti-PTEN (Cell Signaling), anti-FABP4 (Cell Signaling), anti- α -tubulin (Cell Signaling), anti- α -tubulin (Cell Signaling), anti-AKT phospho S473 (Abcam), and anti-AKT (abcam). The apoptotic pathway antibodies used were: caspase-

3 (Cell Signaling), caspase-9 (Cell Signaling), cleaved caspase-8 (Cell Signaling), and caspase-8 (Cell Signaling).

3.1.5. Western blotting for the detection of NF- κ B activation: Untreated and LPS (100 ng/ml) treated cells were harvested, and the nuclear proteins were extracted from the cells using EpiSeeker Nuclear Extraction Kit (Abcam, ab113474) as per manufacturer's instructions. Samples were electrophoresed and stained with anti- NF- κ B p65 (phospho S536) and anti-histone H1 antibodies

3.1.6. Immunohistochemical analyses: IL12, IL-1 β , cleaved-caspase-3, and cleaved-caspase-9 were detected using Cy5-conjugated rat-anti-IL-6, rat anti-IL-12, hamster anti-IL1 β (Biolegend, San Diego, CA), anti-cleaved caspase-3 and anti-cleaved caspase-9 (Cell Signaling Technology, Inc., Danvers, MA) antibodies respectively. DAPI was used to stain the nuclei.

3.1.7. TUNEL staining for apoptosis: To detect apoptotic cells in the lesions, sections of the aortic valve were fixed, permeabilized, and incubated with the TUNEL reaction mixture (In Situ Cell Death Detection Kit, Fluorescein, Roche Applied Science, Indianapolis, IN) containing TdT and fluorescein-dUTP as per manufacturer's instructions. Sections were counterstained with DAPI to identify the nuclei.

3.1.8. Lesional Necrosis: Sections of the aortic valves were stained with hematoxylin and eosin, and plaque necrosis was quantified by measuring the area acellular hematoxylin and eosin-negative areas in the intima, as described [245].

3.1.9. Statistical Analyses: Statistical Analyses were performed as described in chapter 2.

3.2.0. RESULTS:

3.2.1. Polarization of miR-21-KO macrophages: To investigate how miR-21 regulates macrophage functions, we examined the effect of miR-21 deficiency on macrophage polarization. Macrophages were either polarized to the classical M1 phenotype by (INF γ +LPS) or alternatively spliced with IL-4. In the first series of experiments, WT and miR-21-KO macrophages were primed with INF γ (2.5 ng for 16h) and then incubated with LPS (10 ng/mL) for 24h. As shown in **Fig. 21**, 24h after stimulation with INF γ +LPS, M1 markers CD11c and CD86 were significantly increased in miR-21-KO macrophages as compared with WT cells, whereas only a modest change was observed in the abundance of CD80, another M1 marker. Similarly, stimulation of cells with LPS (10 ng/ml; without priming with INF γ) for 24h also increased the abundance of CD11c and CD86 but did not change the levels of CD80 in miR-21-KO cells. The INF γ +LPS or LPS alone catalyzed induction of M1 markers CD11c and CD86 in miR-21-KO BMDM, but they disappeared after 48h of stimulation. In the second series of experiments, the effect of IL-4 was examined on M2 polarization in miR-21-KO BMDM. Twenty four hours of incubation with IL-4 levels of CD301 increased in miR-21-KO macrophages, whereas abundance of CD206 and CD209 was unchanged (**Fig. 22**). In addition, 48h of incubation of miR-21-KO cells with IL-4 significantly increased the levels of CD301 and CD206; however, only a modest increase in the level of CD209 was observed. Together, these data suggest that miR-21-KO macrophages have a unique phenotype because only specific markers of both M1 and M2 are induced in these macrophages in response to M1 and M2 stimuli.

24 h

48 h

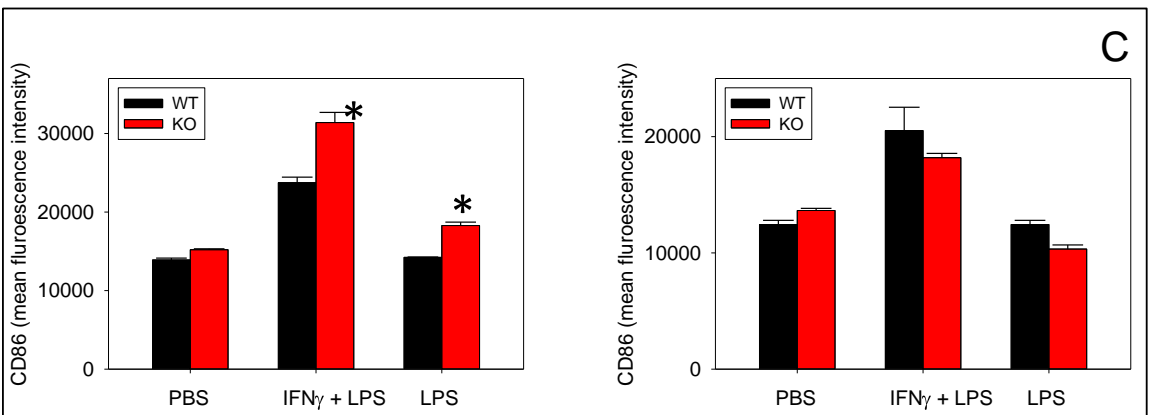
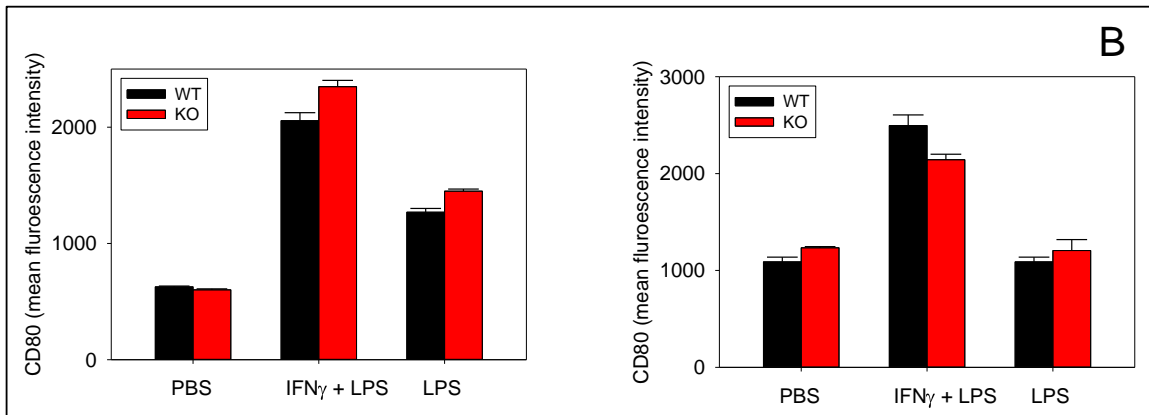
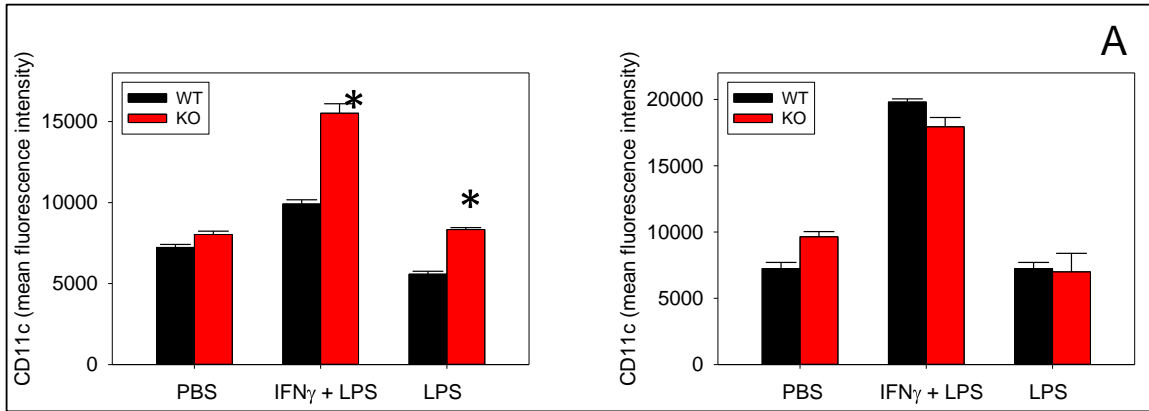


Figure 21. Effect of miR-21 deficiency on the polarization of macrophages to a M1 phenotype. MiR-21-KO and WT BMDM were primed with IFN γ (2.5 ng/ml) for 16h, followed by stimulation with LPS (10 ng/mL) for 24 or 48h; incubated with LPS (10 ng/mL) for 24 or 48h; and incubated with PBS (vehicle) for 24 or 48h. Expression of CD11c (A), CD80 (B), and CD86 (C) was measured by flow cytometry. Data (n=3/group) are mean \pm SEM. *P<0.05 vs PBS group.

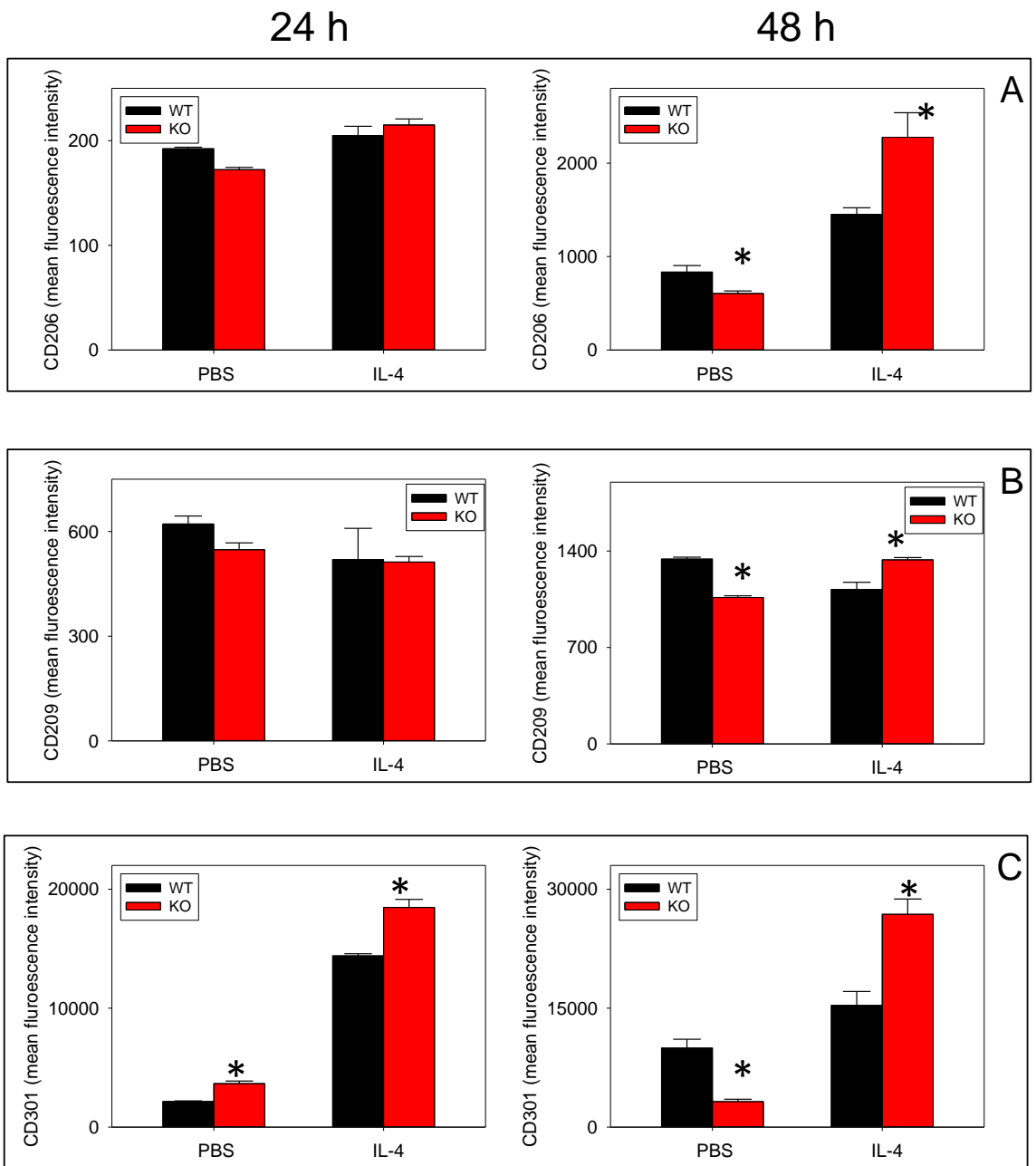
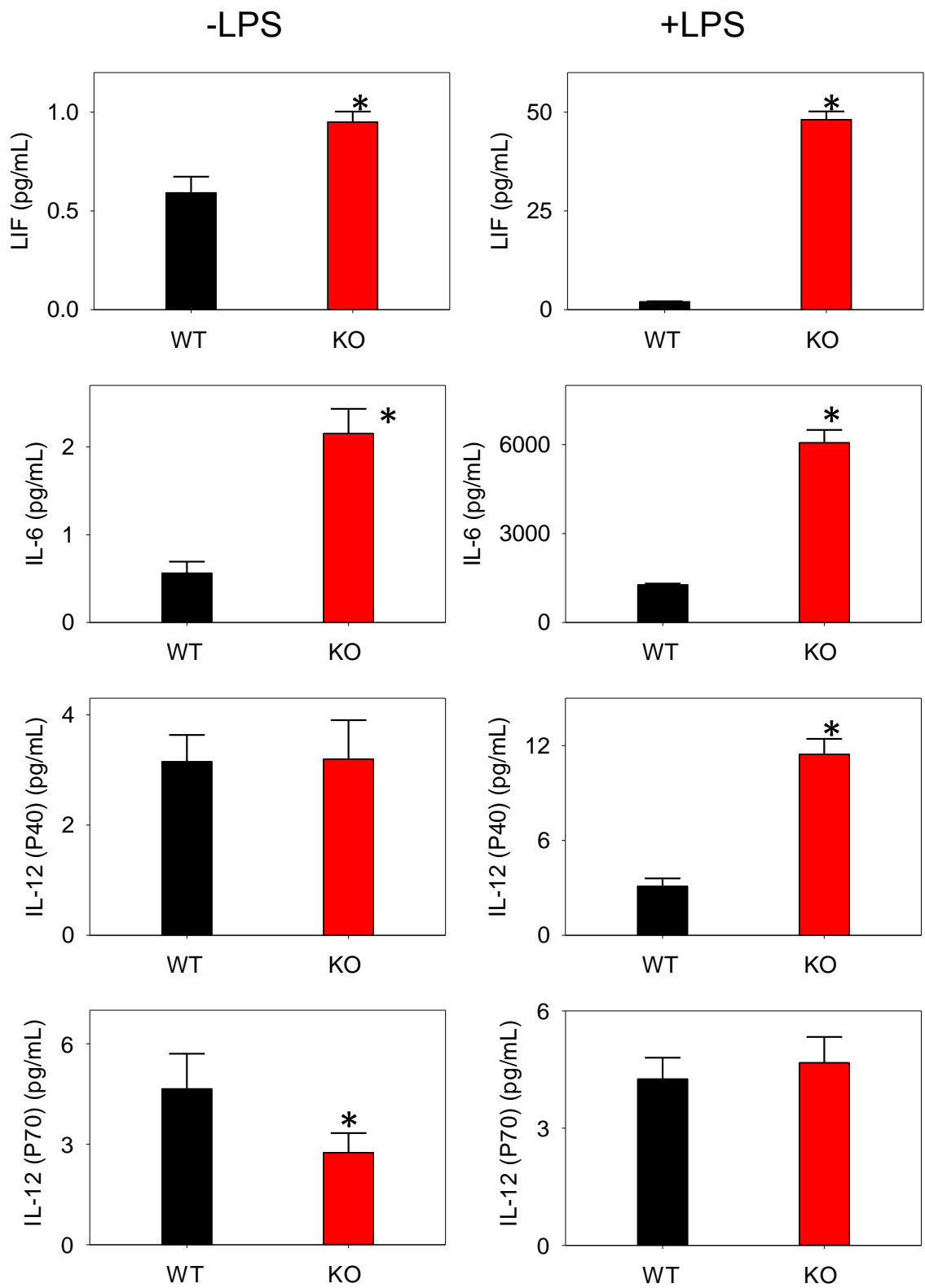
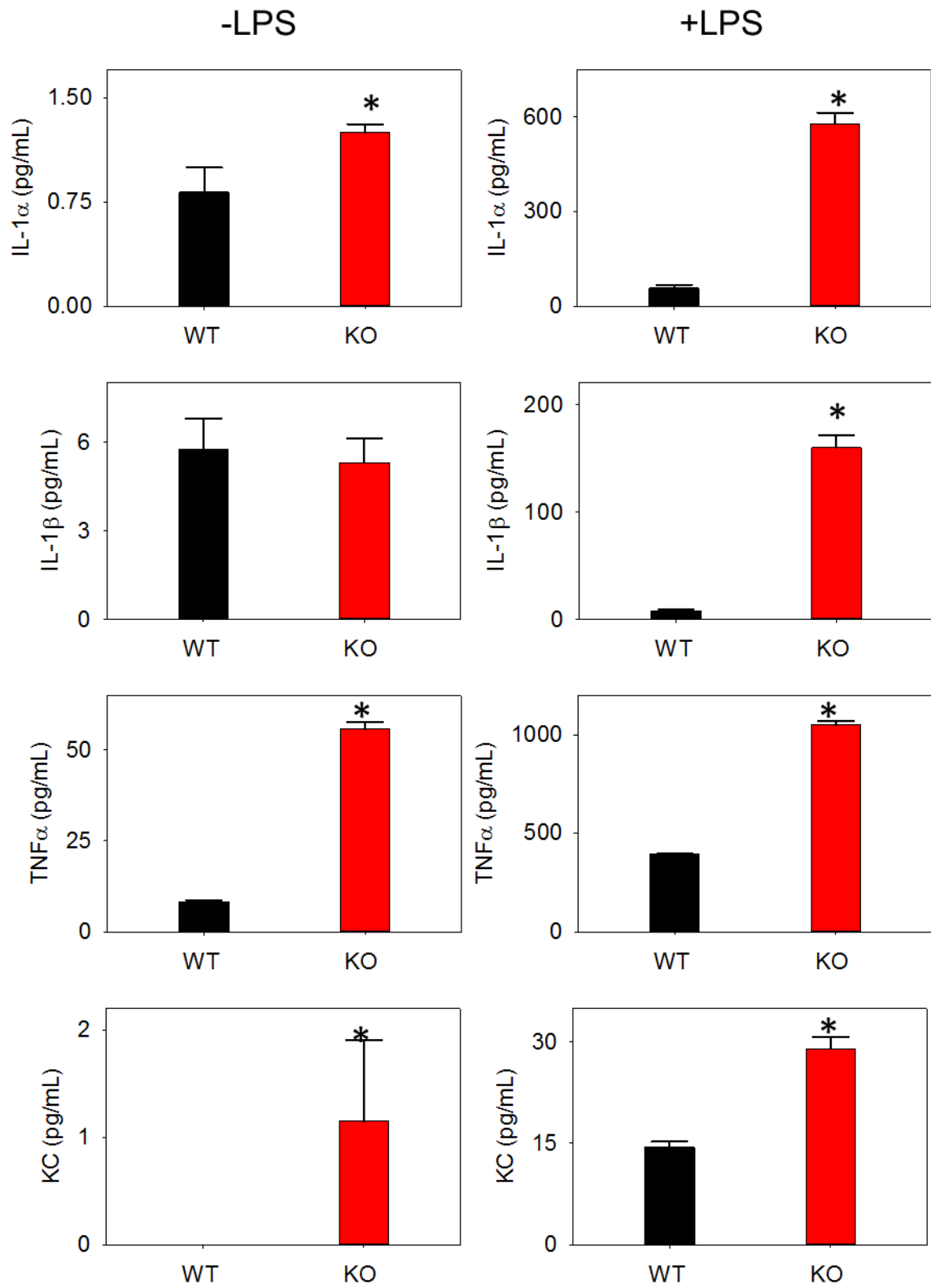


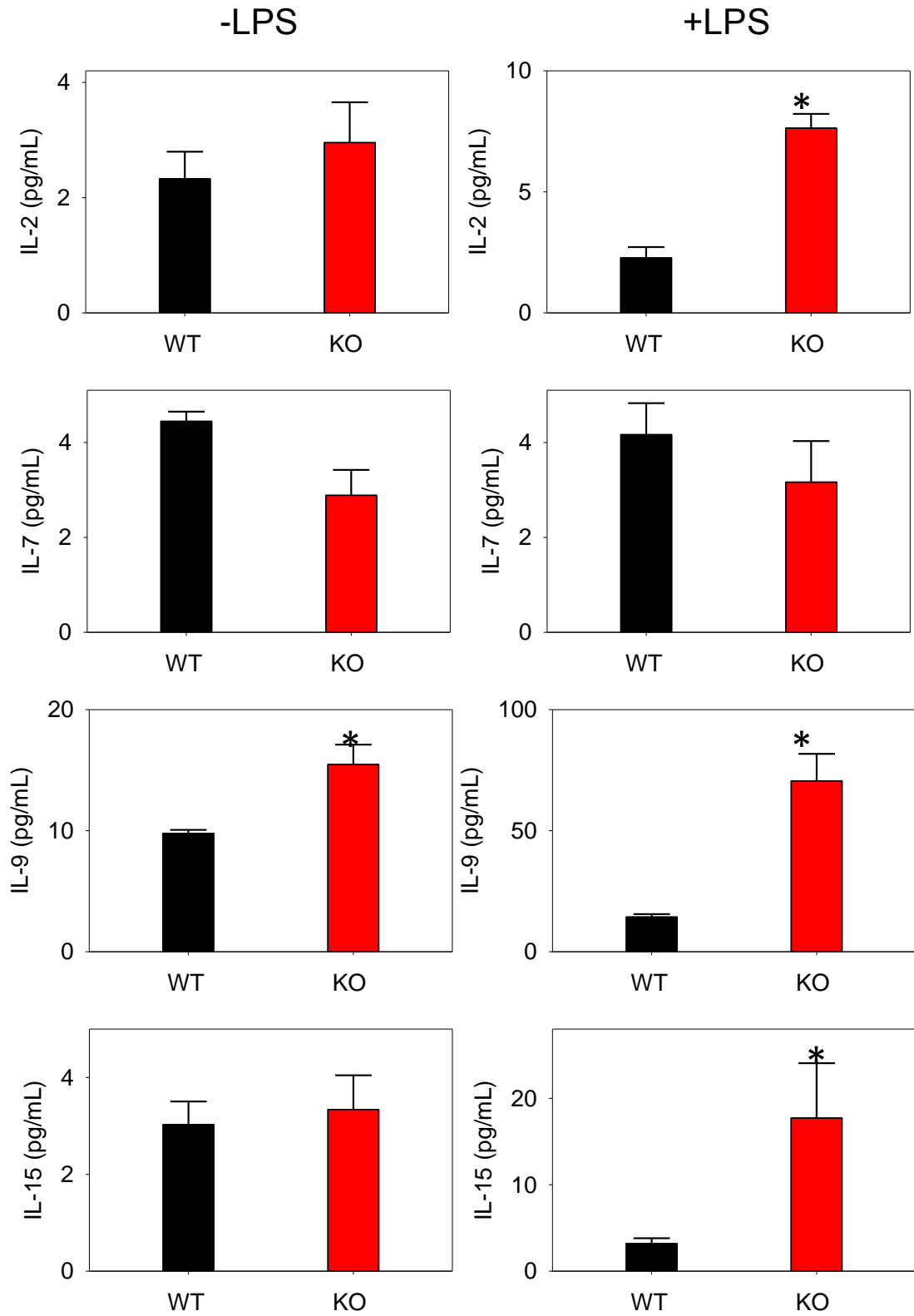
Figure 22. Effect of miR-21 deficiency on the polarization of macrophages to a M2 phenotype. MiR-21-KO and WT BMDM were incubated with IL-4 or PBS (vehicle) for 24/48h, and the expression of CD206 (A), CD209 (B), and CD301 (C) was measured by flow cytometry. Data (n=3/group) are mean \pm SEM. *P<0.05 vs PBS group.

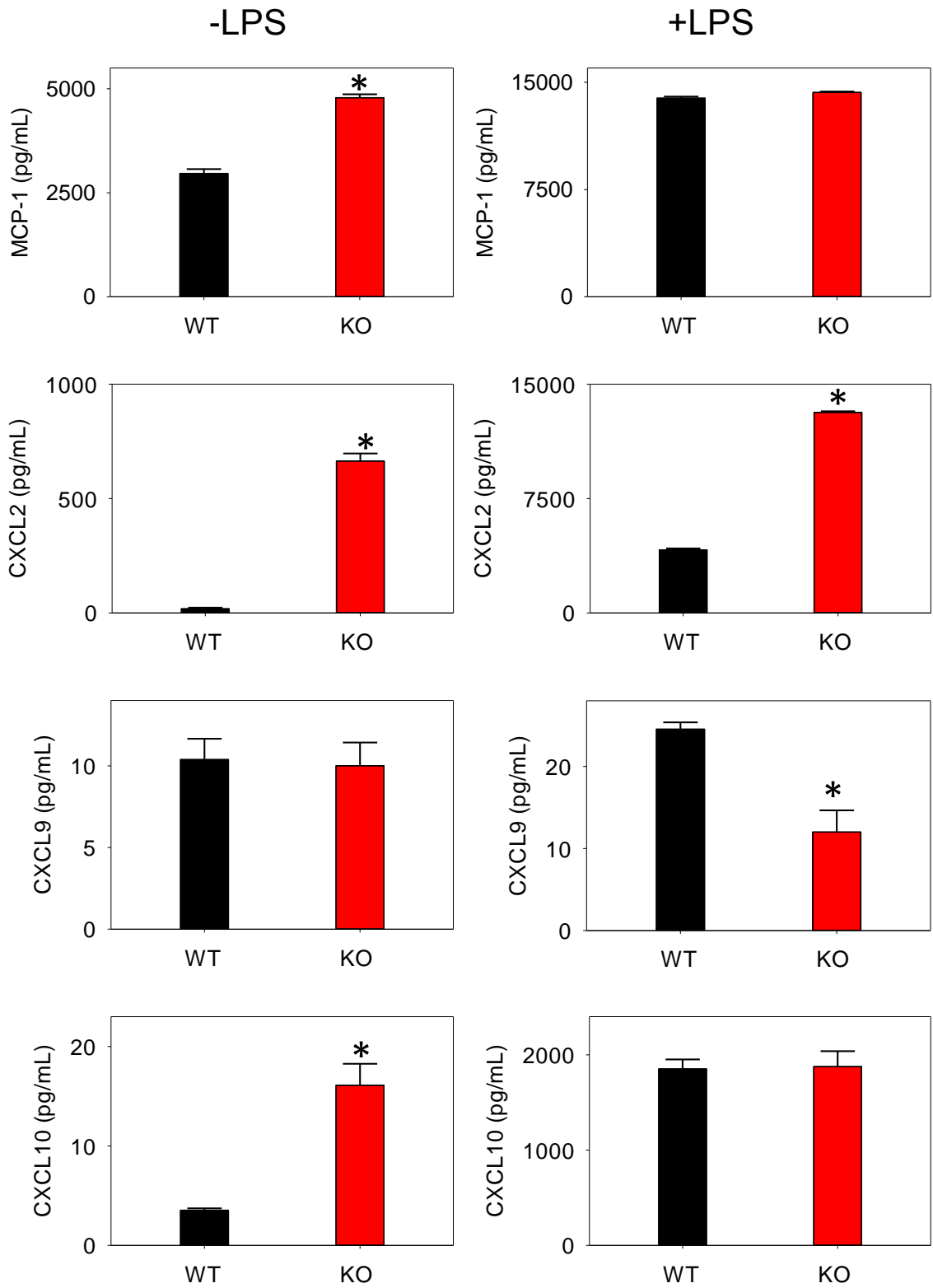
3.2.2. Effect of miR-21 deficiency on cytokine formation: Because vascular inflammation is a critical determinant of lesion nature and progression, we investigated how miR-21 affects inflammatory signaling in macrophages, the major driver of inflammation in atherosclerotic lesions. In the first series of experiments 0.5×10^6 WT and miR-21-KO BMDM were seeded in 12-well plates and incubated for 24h at 37°C. Incubated medium was then collected and analyzed for expression levels of 32 cytokines and chemokines by multiplex cytokine array. Levels of 8 analytes were too low to be reliably quantified. Data for the other cytokines are presented in (**Fig. 23**). As shown in **Fig. 23**, levels of CXCL2 were 38-fold ($P < 0.05$) higher in miR-21-KO than WT macrophages. Macrophage deficiency of miR-21 also increased the levels of TNF α by 7-fold, IL-6 by 4-fold, IL-9 by 1.8-fold, CXL10 by 3-fold, CCL3 by 2.4-fold and CCL4 by 3-fold ($P < 0.05$; **Fig. 23**). Basal levels of the other cytokines and chemokines in miR-21-KO macrophages were comparable with controls. These data suggest that basally, macrophage miR-21 deficiency increases the formation of several pro-inflammatory cytokines and chemokines.

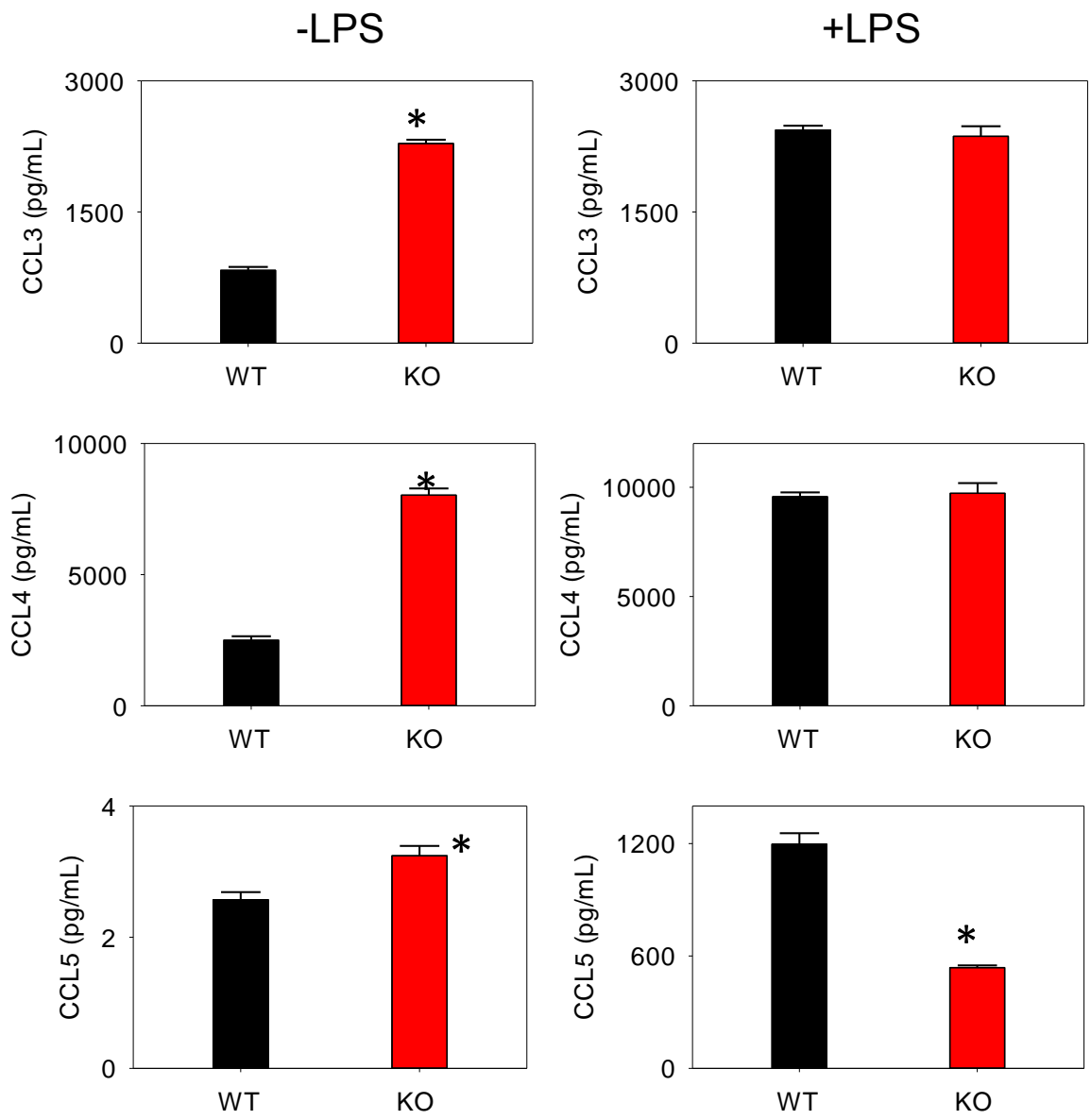
3.2.3. LPS induced cytokine formation in miR-21 deficient macrophages: Next, the effects of pro-inflammatory stimulants such as LPS on cytokine and chemokine formation in miR-21-KO macrophages were studied. As shown in **Fig. 23**, incubation of both WT and miR-21-KO BMDM with LPS (100 ng/mL) for 24h increased the formation of leukemia inhibiting factor (LIF; an IL-6 class of cytokine) by 24-fold, IL-1 β by 18-fold, IL1 α by 11-fold, and IL-2, IL-6, IL9, IL-12 (p40), TNF α , CXCL2, and G-CSF by 2.5-5-fold ($P < 0.05$). Levels of KC (murine analog of IL-8) and VEGF were also moderately (< 2 -fold; $P < 0.05$) increased by LPS in miR-21-KO BMDM. To confirm the multiplex data, A time course (4-24h) of LPS (100 ng/mL) induced IL-6 formation was also examined by ELISA in WT and miR-21-KO BMDM. As shown in **Fig. 24**, IL-6 formation in LPS stimulated

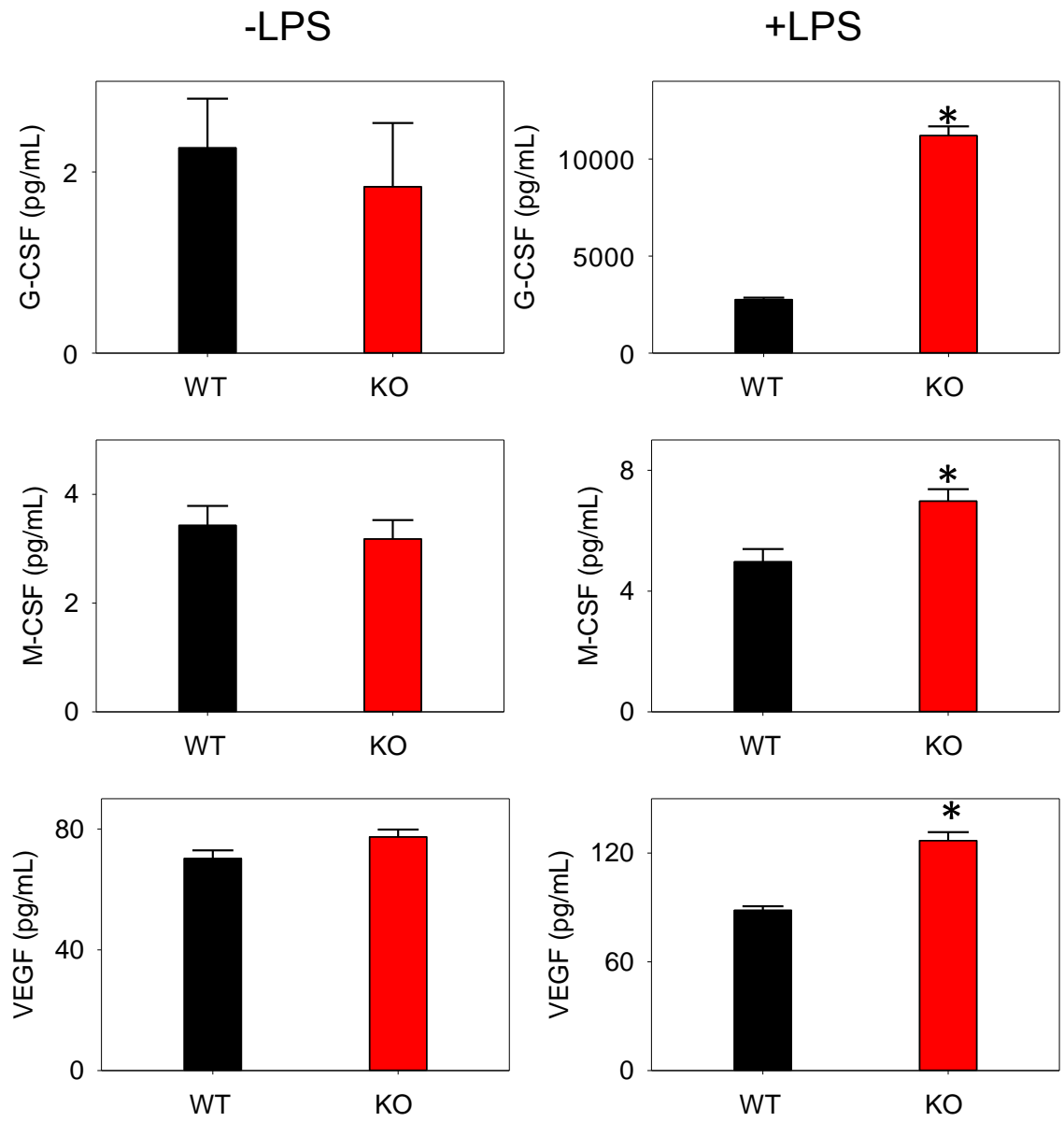












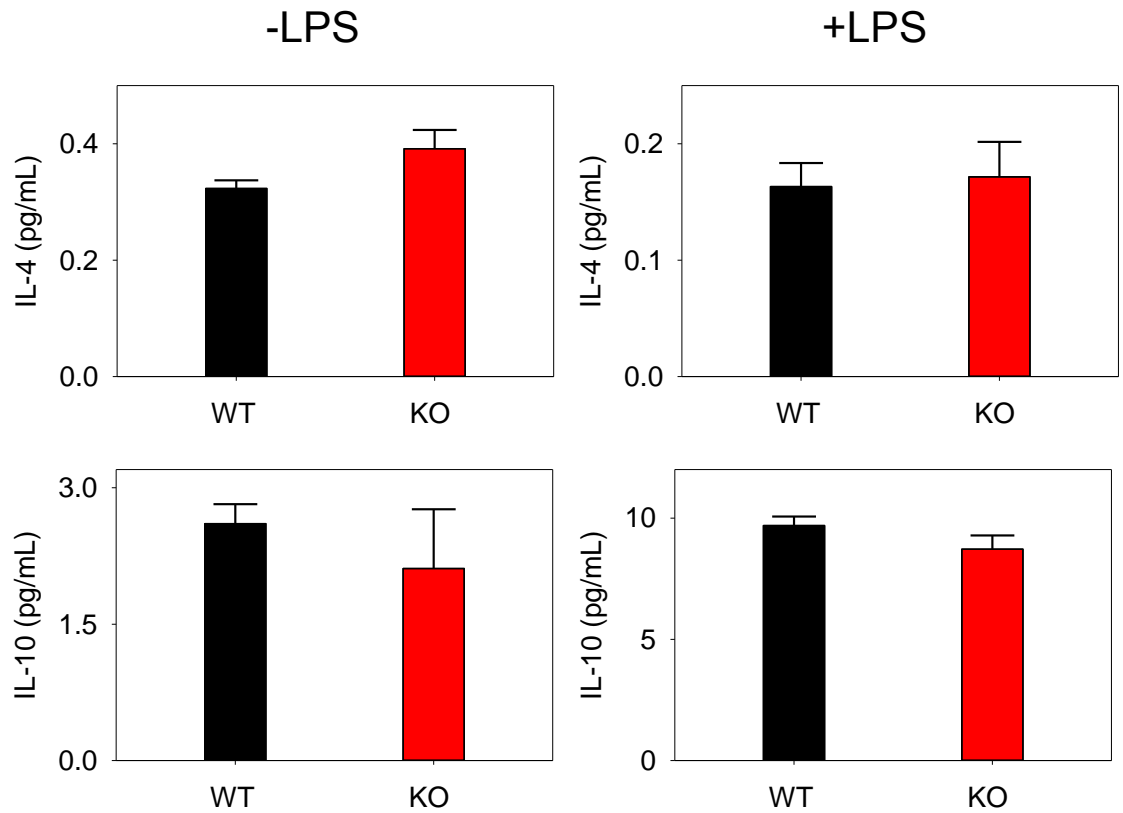


Figure 23. Cytokines and chemokine levels in LPS-stimulated miR-21-KO macrophages. MiR-21-KO and WT BMDM were incubated with 100ng/ml LPS or PBS (vehicle) for 24 hours and the cytokines secreted in the incubation medium were measured by multi-plex cytokine array. Data (n=6/group) are mean \pm SEM. *P<0.05 vs PBS group.

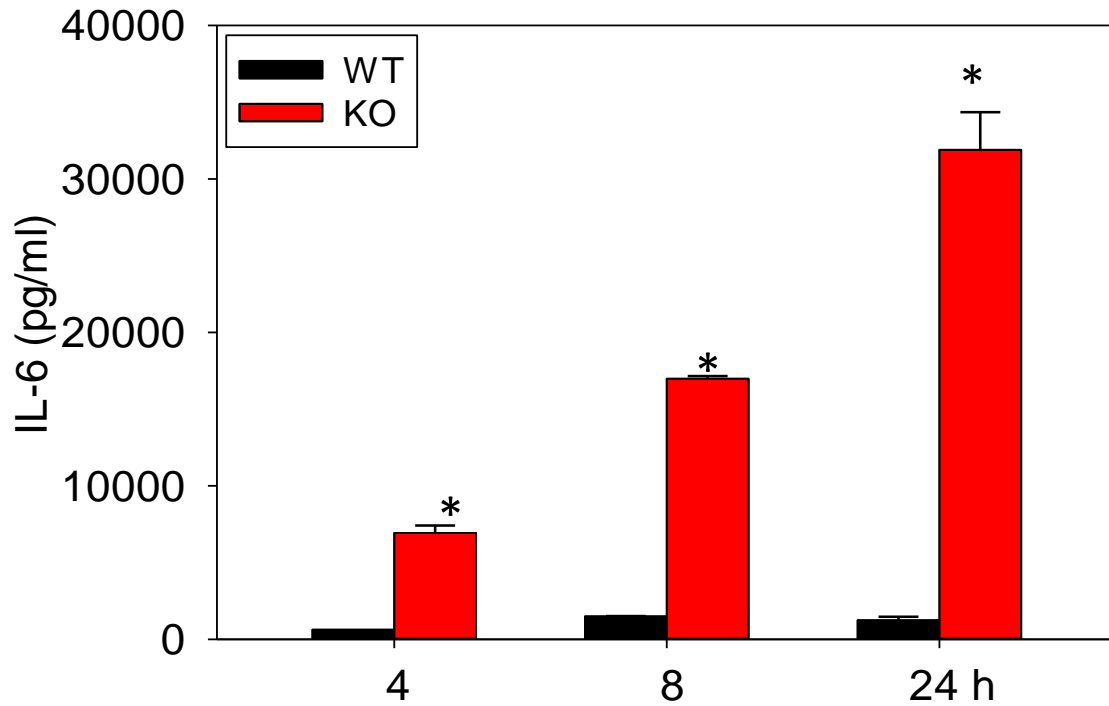


Figure 24. Formation of IL-6 in LPS-stimulated miR-21-KO macrophages. MiR-21-KO and WT BMDM were incubated with 100ng/ml LPS or PBS (vehicle) for 4, 8, and 24h, and IL-6 secreted in the incubation medium was measured by ELISA. Data (n=6/group) are mean \pm SEM. *P<0.05 vs PBS group.

miR-21-KO cells were significantly higher than WT macrophages at all time points examined. Collectively, these data suggest that miR-21 prevents the formation of pro-inflammatory cytokines in response to inflammatory molecules like LPS.

3.2.4. Inflammatory and atherogenic stimuli and expression of potential miR-21 targets in atherosclerotic lesions of chimeric miR-21-KO mice: Since formation of pro-inflammatory cytokines such as IL-1 β and IL-12 was significantly increased by LPS in miR-21-KO macrophages, examination of how deficiency of miR-21 affects the abundance of these cytokines in atherosclerotic lesions was conducted. As shown in **Fig. 25** and **Fig. 26**, staining for IL-1 β and IL-12 was much higher in the aortic valves of chimeric miR-21-KO than WT mice, suggesting that miR-21 is likely to be a critical regulator of vascular inflammation.

3.2.5. Effect of miR-21 deficiency on the activation of NF- κ B and p38 and ERK MAP kinases: To explore the mechanisms by which miR-21 inhibits the formation of pro-inflammatory cytokines, the effect of miR-21 deficiency on NF- κ B activation was first examined. For this, nuclear translocation of NF- κ B in cells treated with LPS was measured. As shown in **Fig. 27**, treatment of WT BMDM with LPS (100 ng/mL) led to a significant increase in the nuclear abundance of the NF- κ B p65-unit at 1h after treatment. The nuclear translocation of NF- κ B was much faster in miR-21-KO cells, and maximal activation was achieved 5min after stimulation. NF- κ B content in these cells returned to basal levels after 1h. After 5-30min of LPS stimulation NF- κ B activation was increased by ~2-fold in miR-21-KO BMDM (**Fig 27**). These data suggest that LPS-induced activation of NF- κ B is more robust and rapid in miR-21-KO macrophages than WT cells.

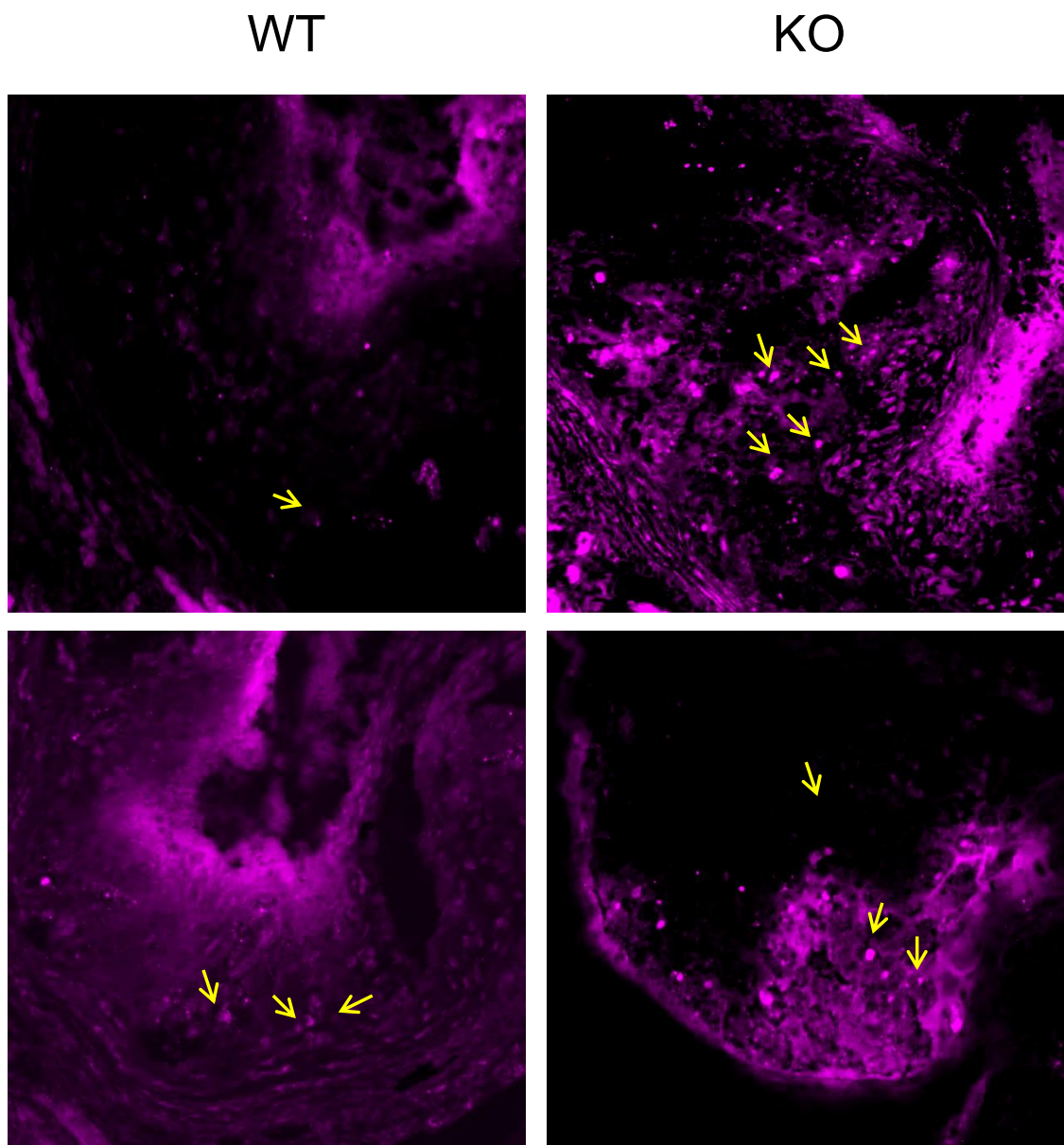


Figure 25. Abundance of IL-1 β in atherosclerotic lesions of miR-21-KO chimeric LDLR-KO mice. Representative photomicrographs of IL-1 β in the aortic valves of LDLR-KO mice transplanted with bone marrow cells from WT or miR-21 KO mice, and fed Western diet for 12 weeks.

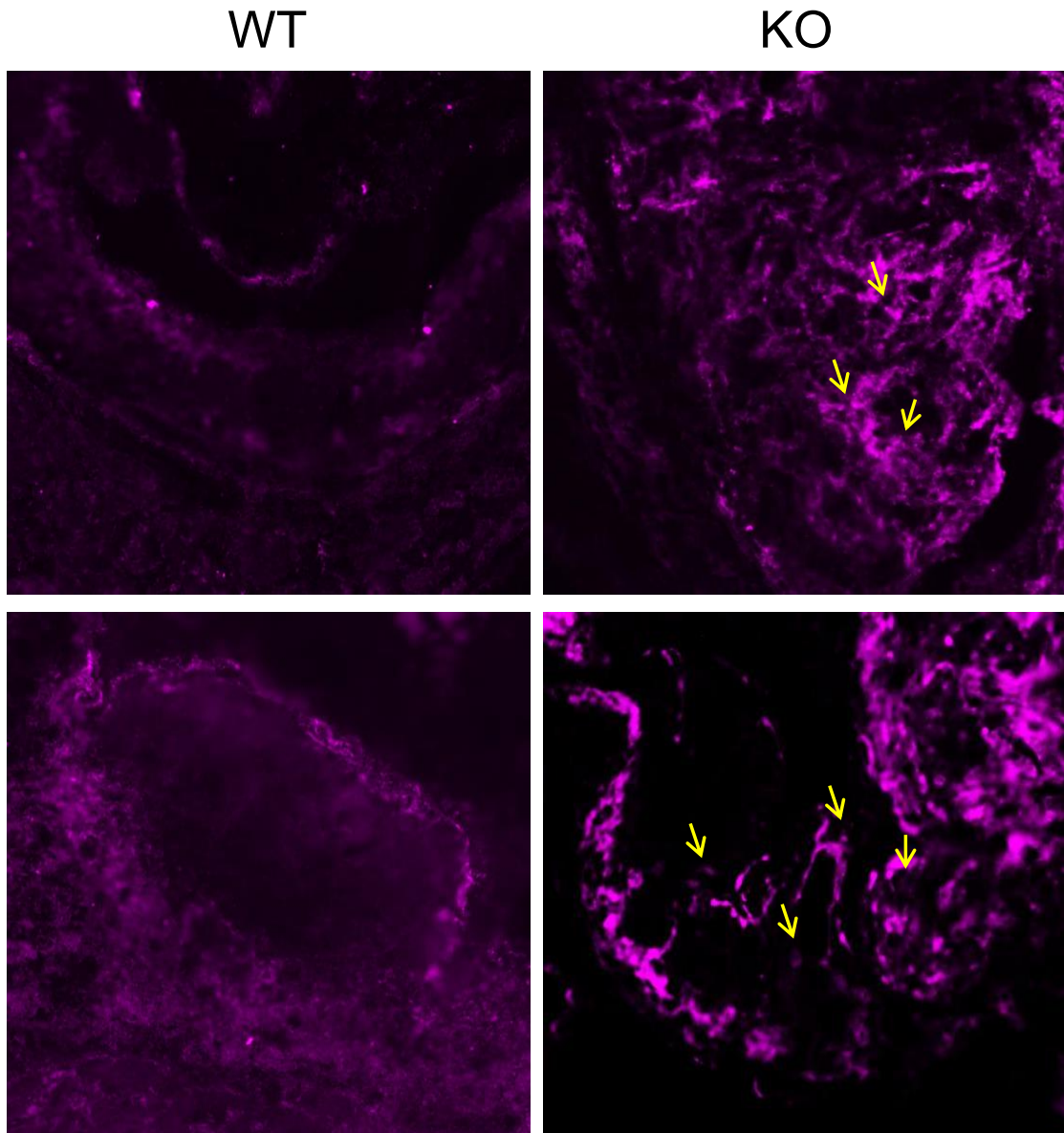
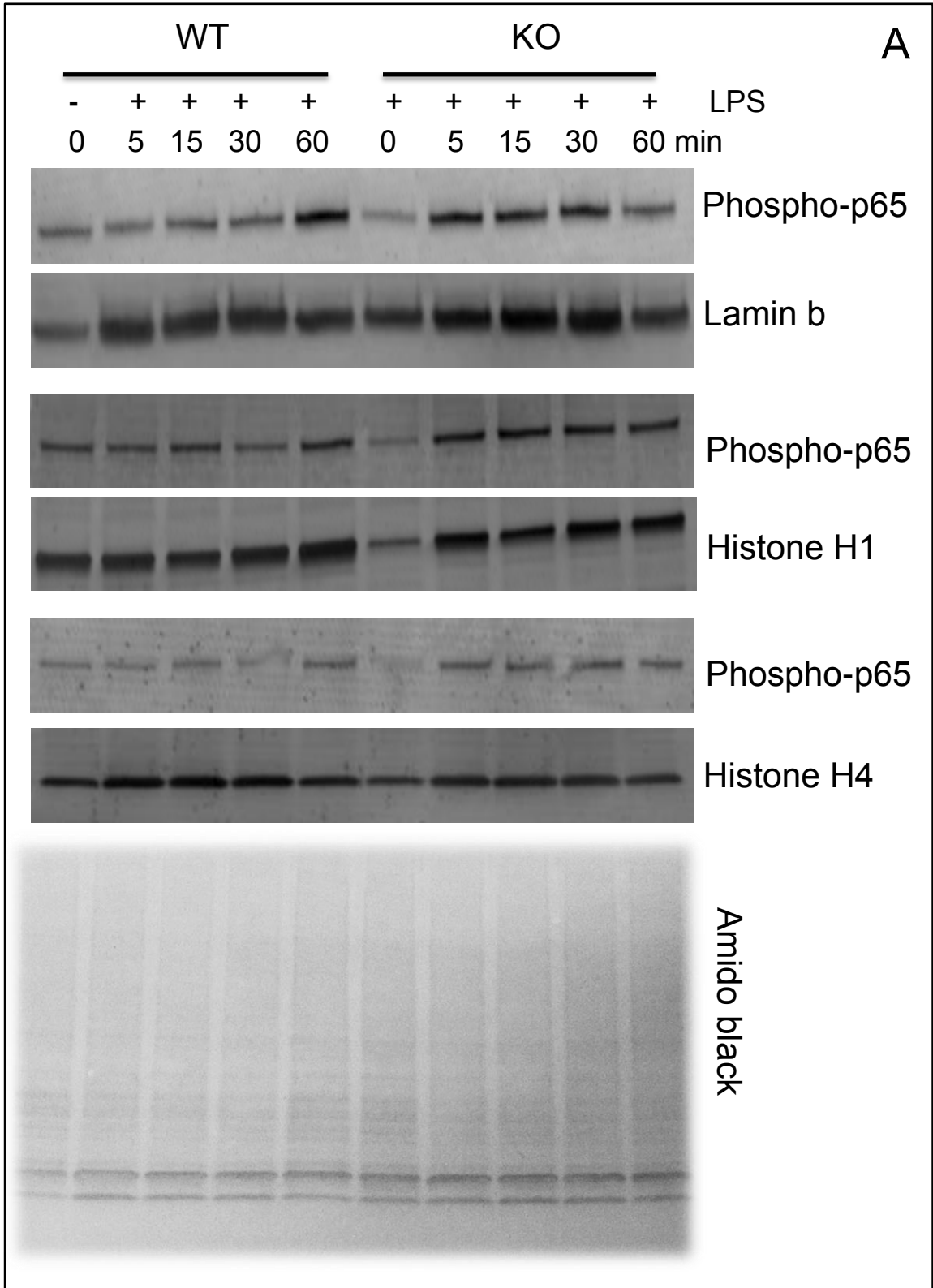


Figure 26. Abundance of IL-12 in atherosclerotic lesions of miR-21-KO chimeric LDLR-KO mice. Representative photomicrographs of IL-12 in the aortic valves of LDLR-KO mice transplanted with bone marrow cells from WT or miR-21 KO mice, and fed Western diet for 12 weeks.



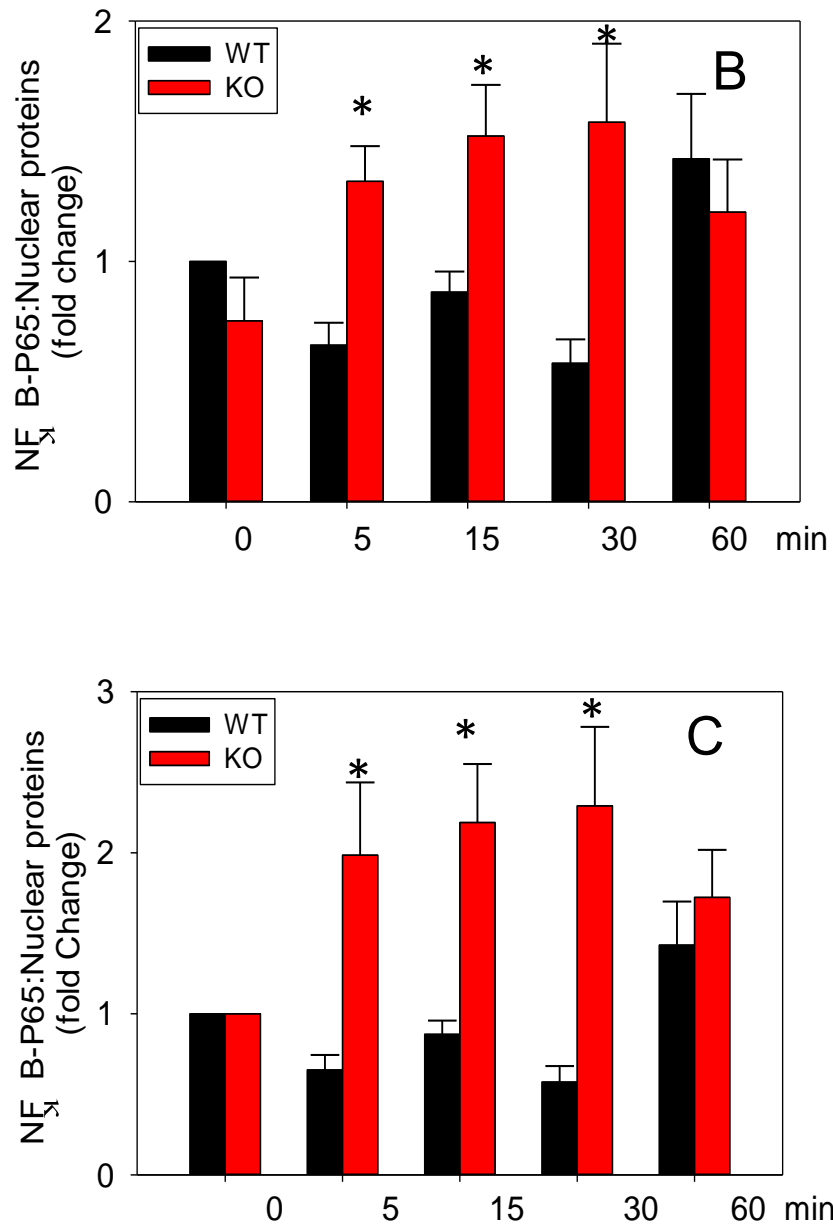


Figure 27. Effect of miR-21 deficiency on the activation of NF-κB. MiR-21-KO and WT BMDM were incubated with LPS (100 ng/ml) for 0-120 min, and activation of NF-κB (p65) was measured in the nuclear extract by Western blotting (A). Intensities of the bands were normalized to 0 min WT (B) or respective 0 min groups (C). Data are mean ± SEM. *P < 0.05 vs PBS group.

Apart from NF- κ B, TLR4 signaling can also be regulated by MAP kinases [246]. Therefore, we examined the effect of miR-21 deficiency on the activation of p38 and ERK in LPS-stimulated BMDM. As shown in **Fig. 28**, LPS activated p38 both in WT and miR-21-KO macrophages in a time-dependent manner. The maximum activation was achieved after 15 min of stimulation, and subsequently p38 phosphorylation diminished with time. Throughout the time course, LPS-induced p38 activation in miR-21-KO cells was comparable with WT macrophages. These data suggest that increased TLR4 activation by LPS in miR-21-KO macrophages is not mediated by p38 phosphorylation.

MiR-21 has been suggested to modulate the activation of ERK MAP kinase in response to a variety of stimuli [229, 247, 248]. My data show that appreciable ERK phosphorylation was visible after 5min of LPS stimulation in WT but not miR-21-KO macrophages (**Fig. 29**). The phosphorylation of ERK peaked at the 15min time point in the WT cells. MiR-21-KO cells also displayed ERK activation at this time point; however, it was much lower than the WT cells. ERK activation diminished in both WT and miR-21-KO cells after 30 min of LPS stimulation. Together, these data suggest that LPS induced phosphorylation of ERK was appreciably lower in miR-21-KO BMDM than WT cells.

3.2.6. Effect of miR-21 deficiency on the abundance of its predicted targets: Our data so far suggests that IL-12 is a target protein of miR-21 in LPS-stimulated macrophages, and cytokines such as IL-1 β , IL-6, and LIF are also the potential direct targets of miR-21. To have comprehensive analyses of miR-21 targets, I examined the effect of LPS on several of its predicted targets in macrophages. As shown in **Fig. 30**, LPS down-regulated PDCD4 and Vimentin in both WT and miR-21-KO BMDM, and the levels of PDCD4 and Vimentin in LPS-induced WT cells were comparable with LPS-induced miR-21-KO macrophages. LPS did not affect the levels of PTEN, FABP4,

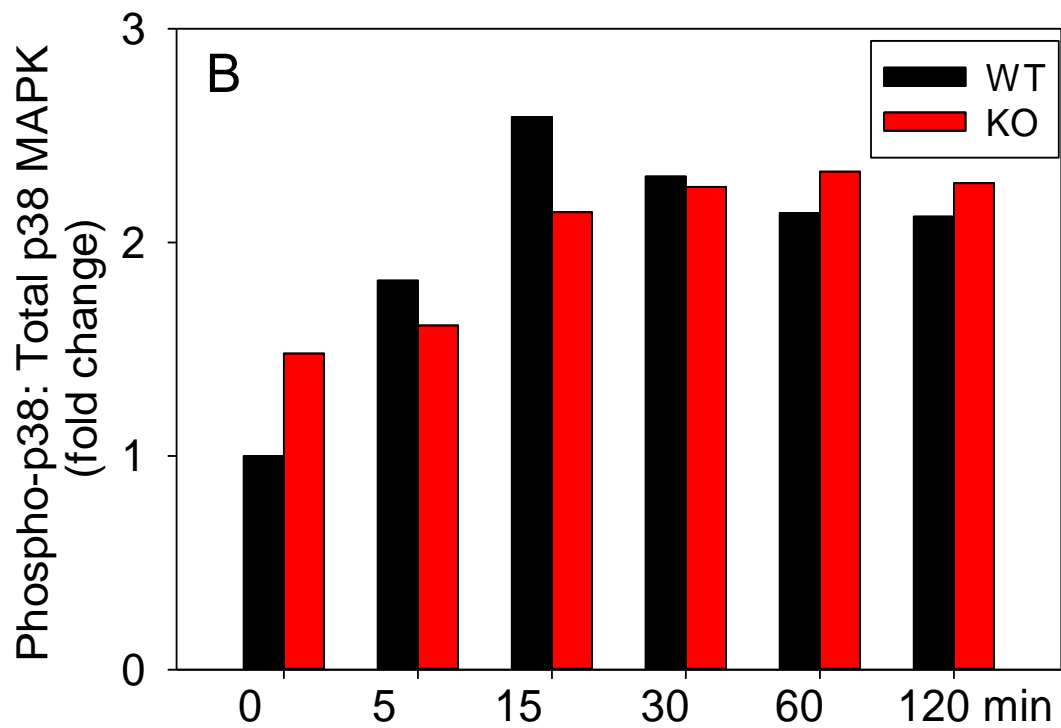
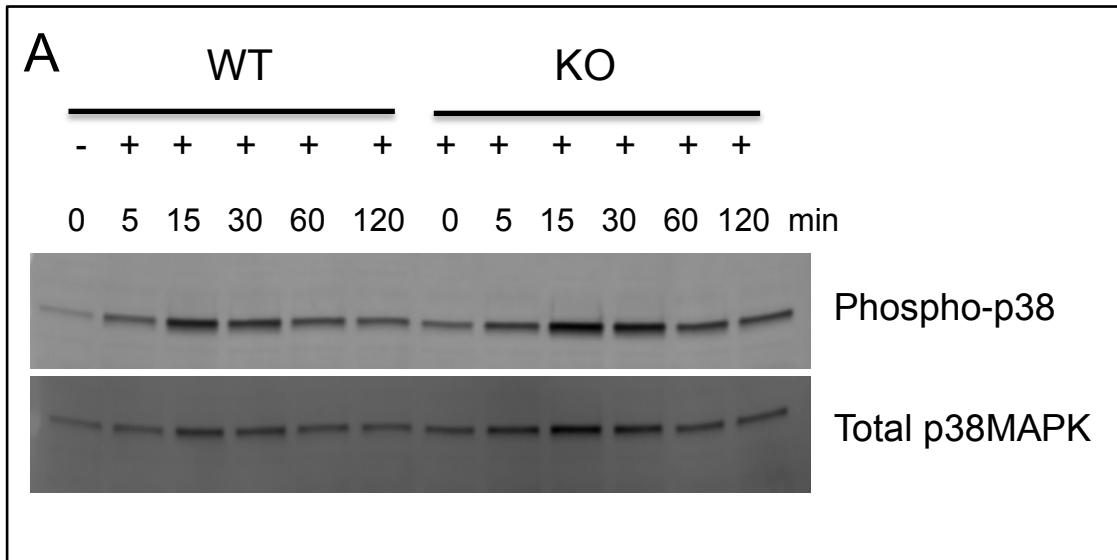


Figure 28. Effect of miR-21 deficiency on the phosphorylation of p38 MAP Kinase.

miR-21-KO and WT BMDM were incubated with LPS (100 ng/ml) for 0-120min and activation of p38 was measured by Western blotting (A). Panel B shows the data normalized to total p38.

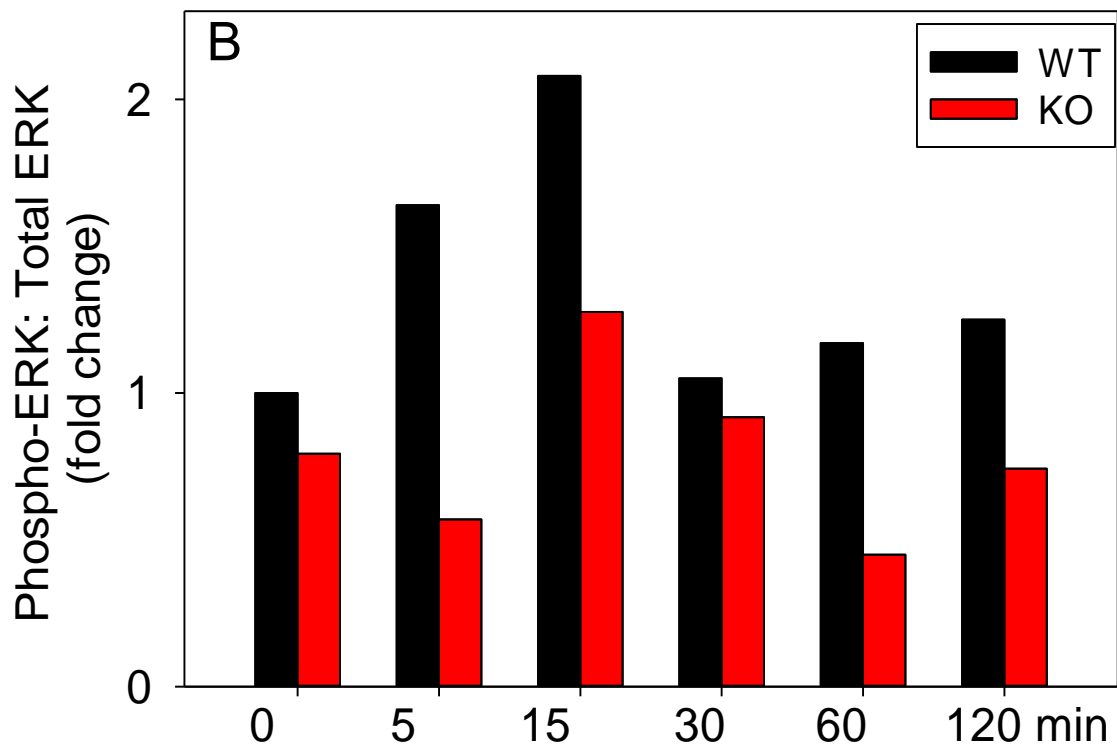
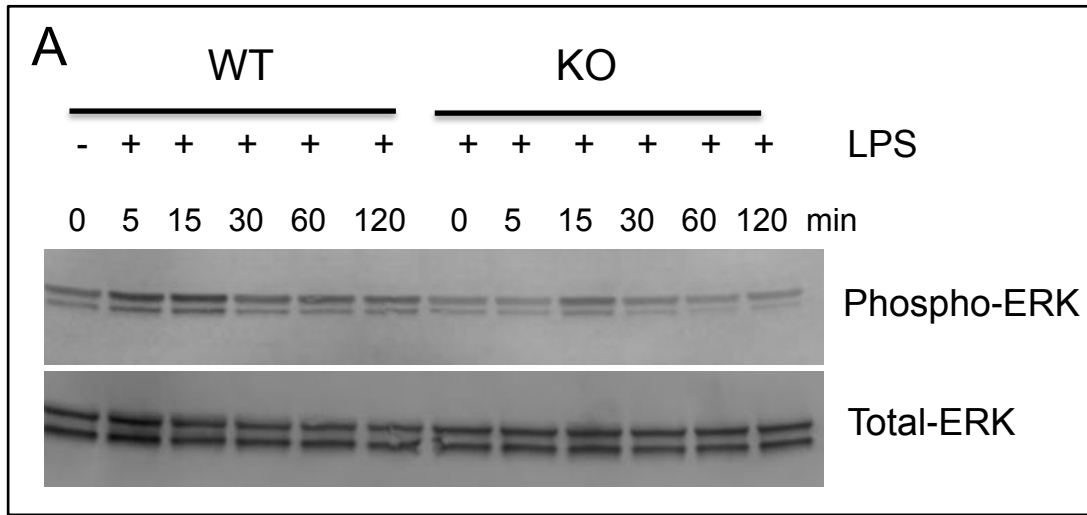


Figure 29. Effect of miR-21 deficiency on the ERK activation. miR-21 KO and WT BMDM were incubated with LPS (100 ng/ml) for 0-120min and activation of pERK was measured by Western blotting (A). Panel B shows the data normalized to total ERK.

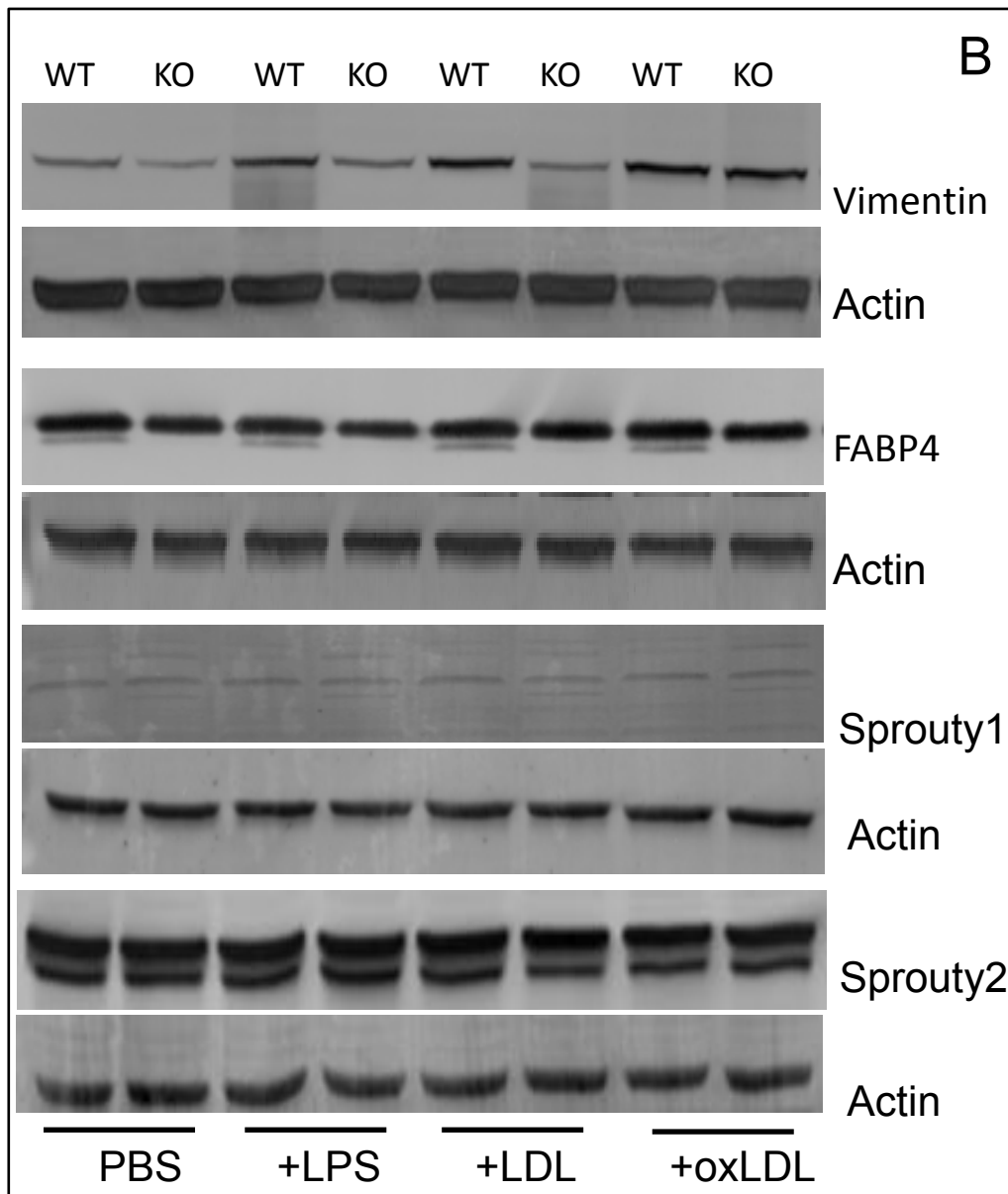
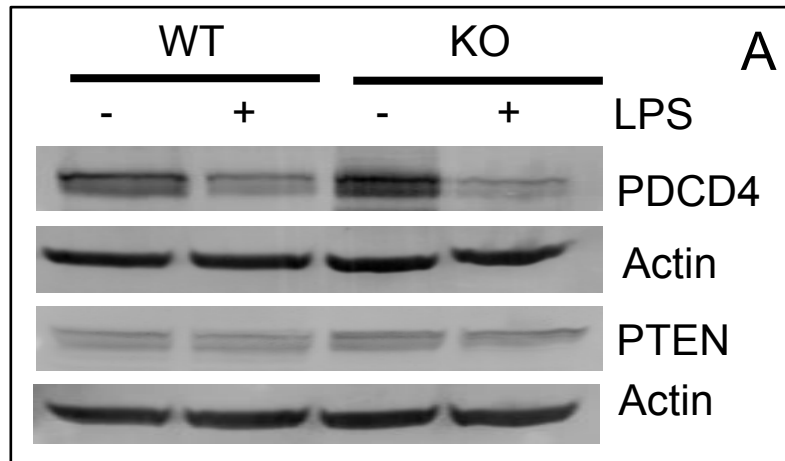


Figure 30. Effect of miR-21 deficiency on its target proteins. (A) miR-21 KO and WT BMDM were incubated with LPS (100 ng/ml) for 24h and expression of PDCD4 and PTEN was measured by Western blotting. (B) miR-21 KO and WT miR-21-KO and WT BMDM were incubated with PBS, LPS (100 ng/ml), LDL (50 µg/mL) or oxLDL (50 µg/mL) for 24h, and expression of vimentin, FABP4, Sprouty1 and Sprouty2 was measured by Western blotting.

Sprouty 1, and Sprouty 2 in both WT and miR-21-KO cells. Similarly LDL or oxidized LDL did not affect the quantity of Vimentin, FABP4, Sprouty 1, and Sprouty 2 in both WT and miR-21-KO macrophages.

3.2.7. miR-21 and macrophage apoptosis: Apart from inflammation, apoptosis is also a critical determinant of the nature and stability of atherosclerotic plaques. Therefore, the effect of miR-21 deficiency in macrophage apoptosis was measured. For these experiments, I first studied the apoptosis of unstimulated BMDM. WT and BMDM were seeded in 12-well plates and apoptosis was measured after 6h by flow cytometry following staining with Annexin V/propidium iodide. As illustrated in **Fig. 31**, both early and late apoptosis was significantly higher in miR-21-KO macrophages than WT cells. Next, we examined the effect of two well-known inducers of apoptosis, 4-hydroxynonenal (HNE) and staurosporine (STS) on apoptosis in miR-21 deficient macrophages. As shown in **Fig. 32** and **Fig. 33**, both HNE and STS significantly increased the early as well as late apoptosis in miR-21-KO macrophages. These data suggest that miR-21 protects against macrophage apoptosis.

3.2.8. MiR-21 and activation of caspases in macrophage: To study the mechanisms of miR-21-induced macrophage apoptosis, we probed the activation of caspases in miR-21-KO BMDM. Stimulation with STS led to increased levels of cleaved caspase-3 and caspase-7 in both WT and miR-21-KO cells; however, the magnitude of cleavage was 3-4-fold greater in miR-21-KO cells (**Fig. 34**). To examine whether the activation of caspases in miR-21-KO cells is triggered by the extrinsic or intrinsic pathway, I examined the effect of STS on the cleavage of caspase-8 and caspase-9. As shown in **Fig. 35**, STS did activate caspase-8 in WT and miR-21-KO cells. However, caspase-9 was cleaved by STS in WT macrophages and deficiency of miR-21 increased the STS-

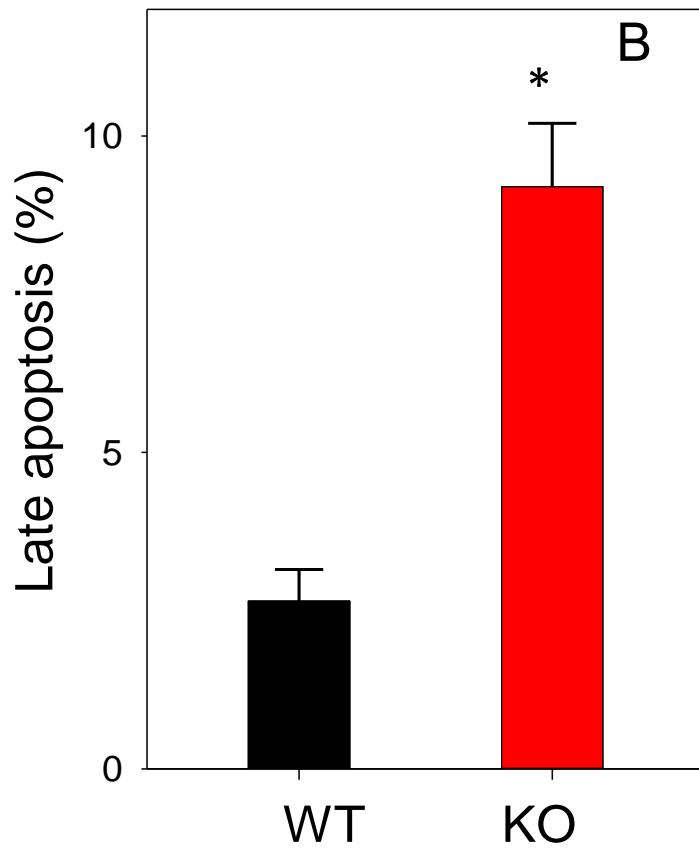
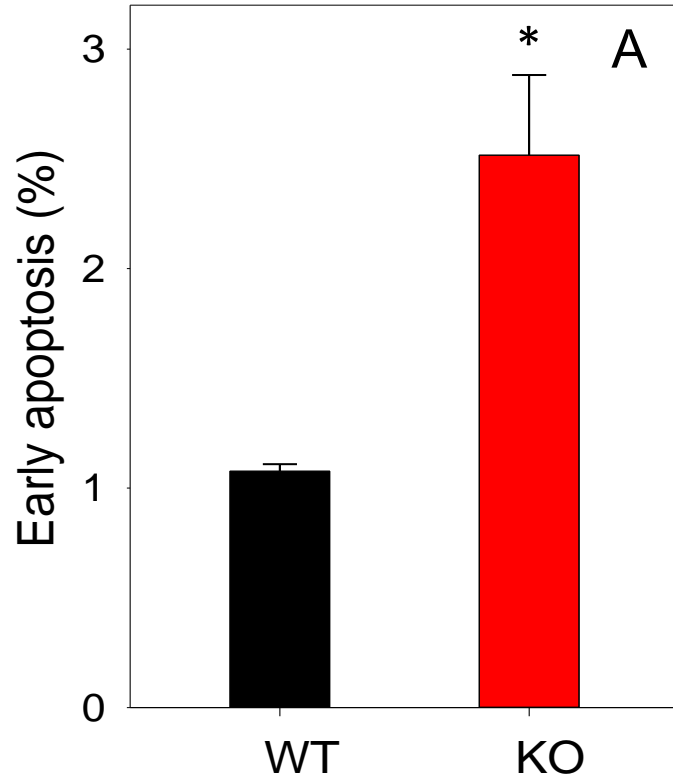


Figure 31. *MiR-21* deficiency increases macrophage apoptosis. WT and miR-21-KO BMDM were seeded in 12-well plate and incubated for 6h in RPMI cell culture medium at 37 °C. Cells were then harvested and stained with Annexin V/propidium iodide (PI) and analyzed by flow cytometry. (A) Percentages of Annexin V⁺, PI⁻ (early apoptosis) and (B) Percentage of PI⁺ cells (late apoptosis). Data (n=6/group) are mean ± SEM. *P = <0.05 vs WT.

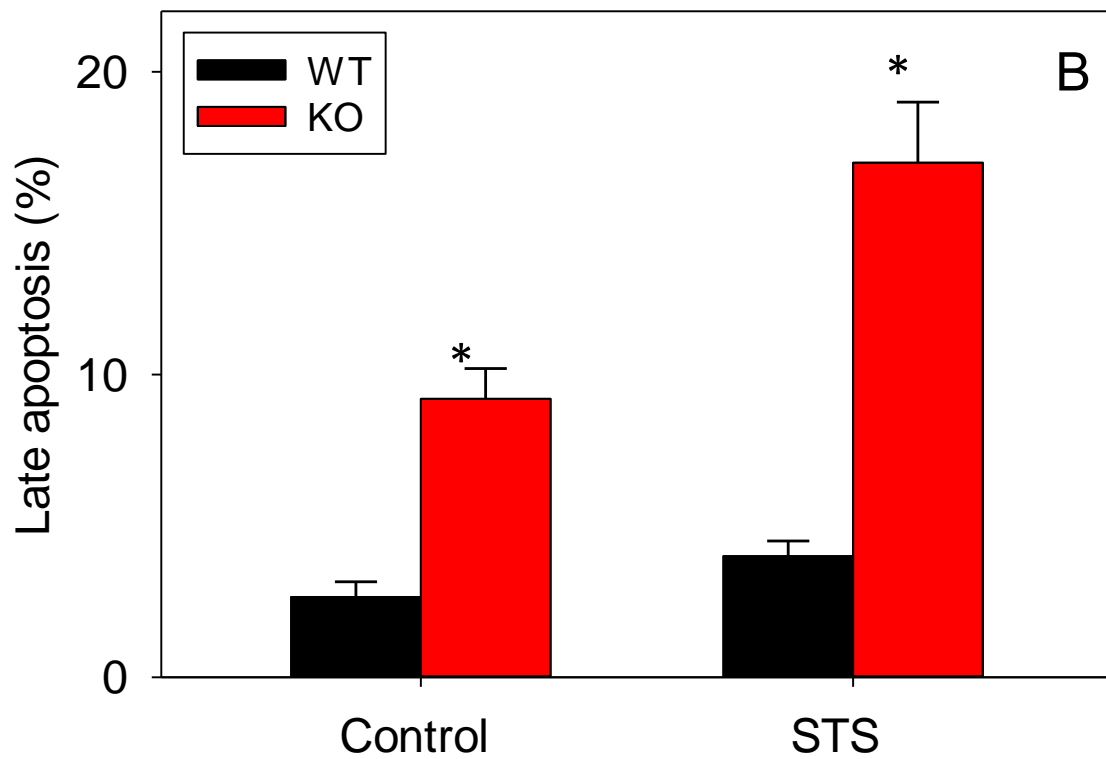
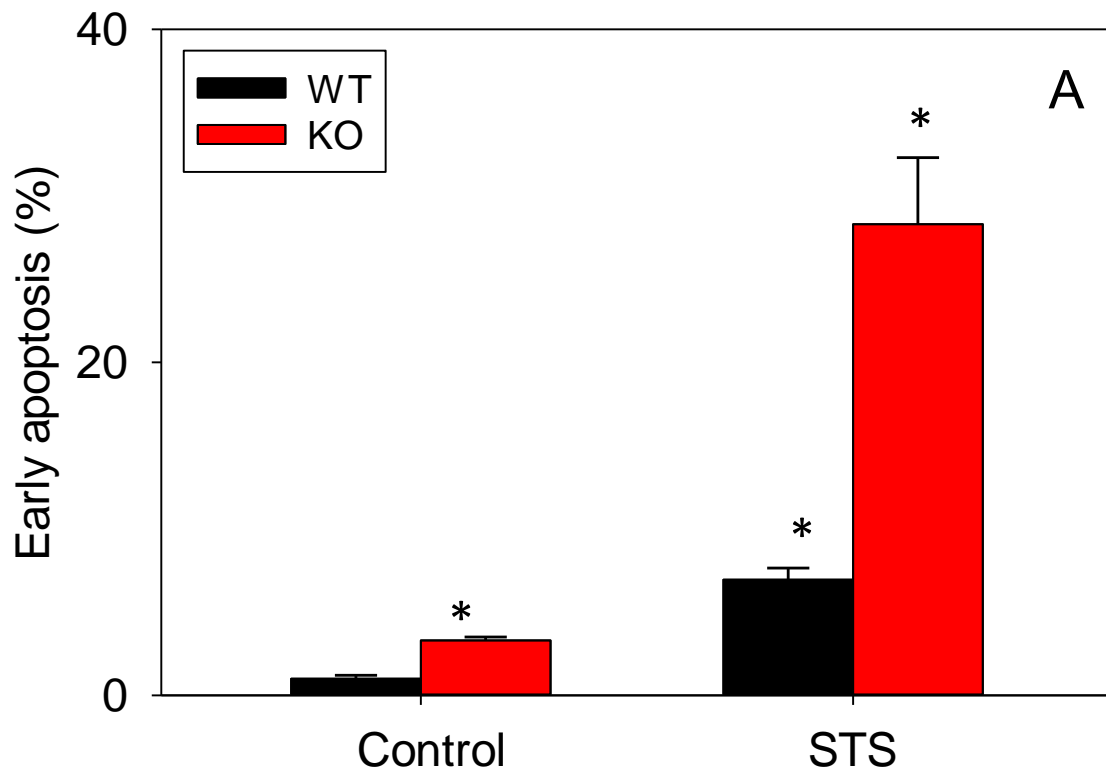


Figure 32. *miR-21* protects macrophages from staurosporine-induced apoptosis.

WT and miR-21-KO BMDM were incubated with staurosporine (500 nM) or DMSO (vehicle) for 6h. Cells were stained with Annexin V/propidium iodide (PI) and analyzed by flow cytometry. (A) Percentages of Annexin V⁺, PI⁻ (early apoptosis) and (B) percentage of PI⁺ cells (late apoptosis). Data (n=6/group) are mean ± SEM. *P = <0.05 vs WT.

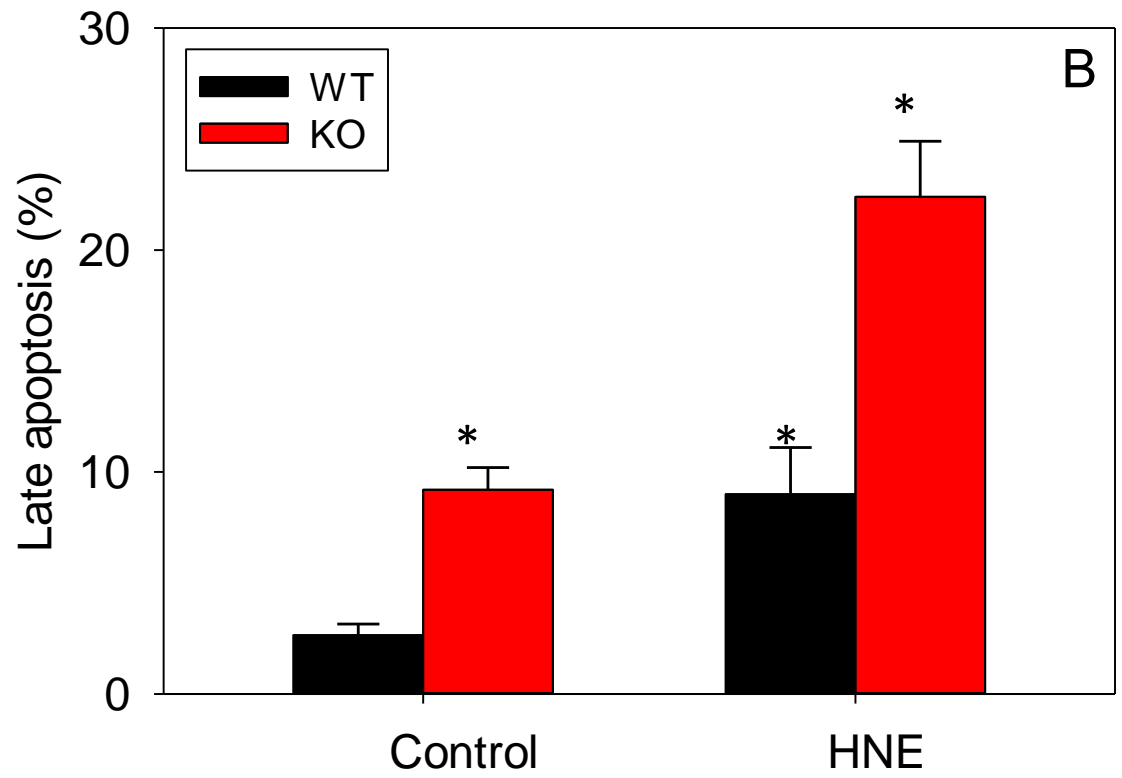
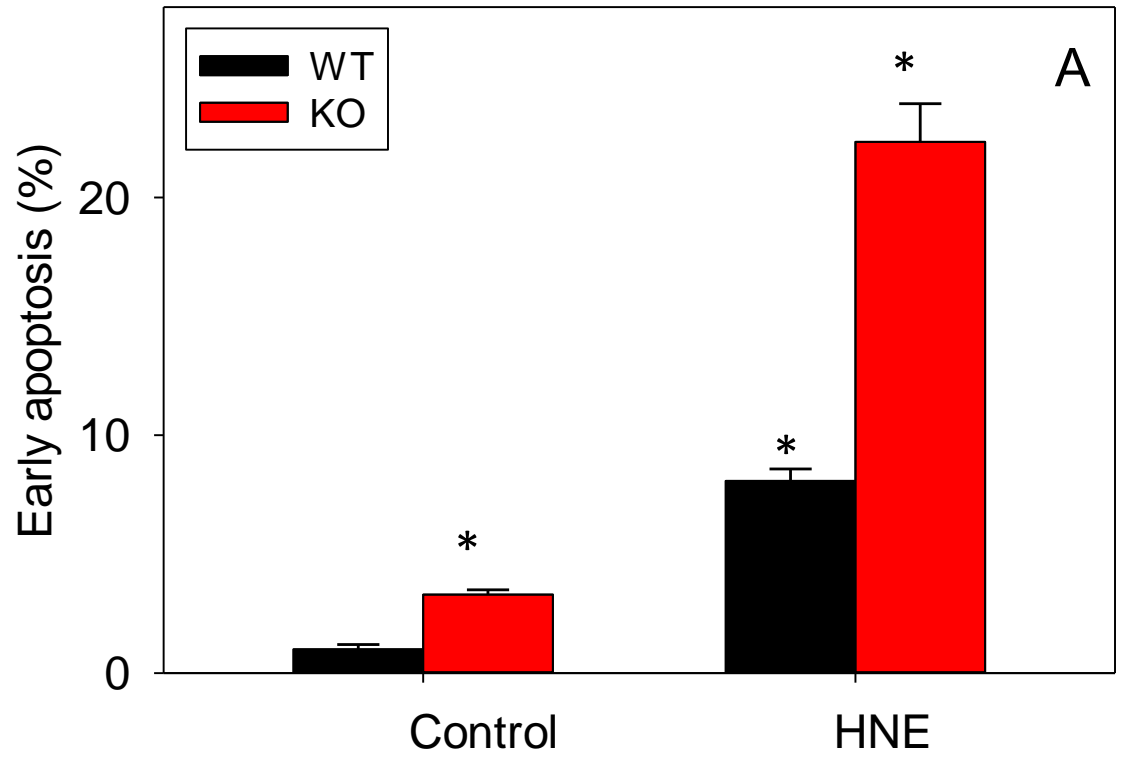


Figure 33. *miR-21* protects macrophages from HNE-induced apoptosis. WT and miR-21-KO BMDM were incubated without or with HNE (25 μ M) in HBSS for 2h. Cells were then incubated for 4h in RPMI medium and stained with Annexin V/propidium iodide (PI) and analyzed by flow cytometry. (A) Percentages of Annexin V⁺, PI⁻ (early apoptosis) and (B) percentage of PI⁺ cells (late apoptosis). Data (n=6/group) are mean \pm SEM. *P = <0.05 vs WT.

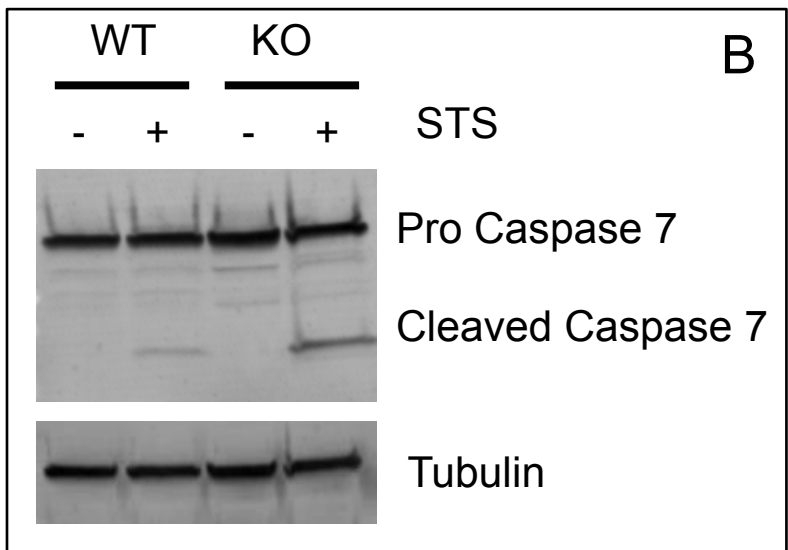
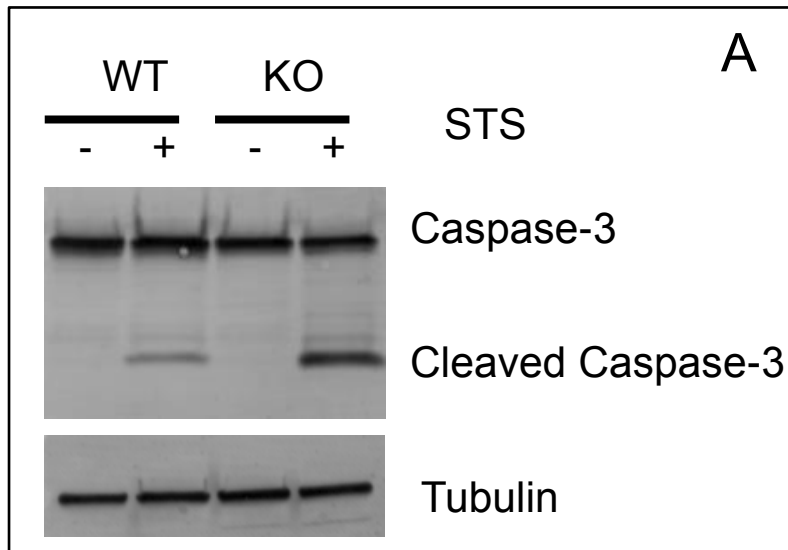


Figure 34. Effect of miR-21 on the activation of caspase-3 and caspase-7 in BMDM.

WT and miR-21-KO BMDM were incubated with 500 nM staurosporine (STS) or DMSO for 6h and cleaved caspase-3 and caspase-7 were measured by Western blotting.

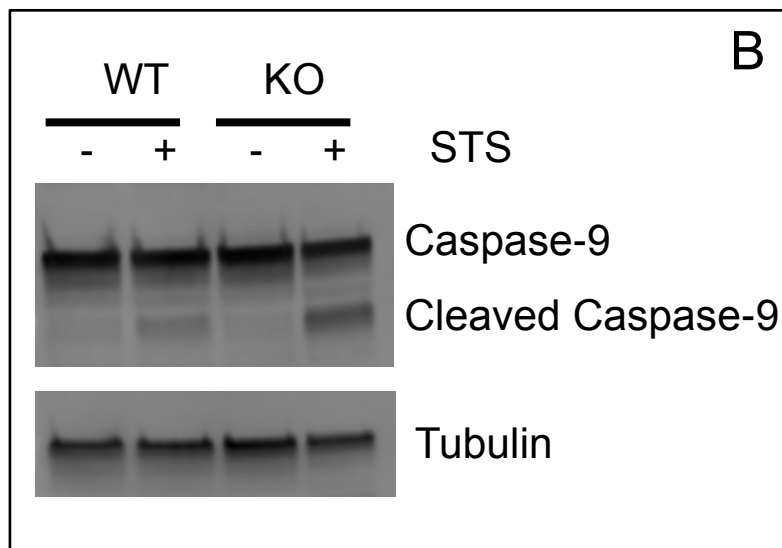
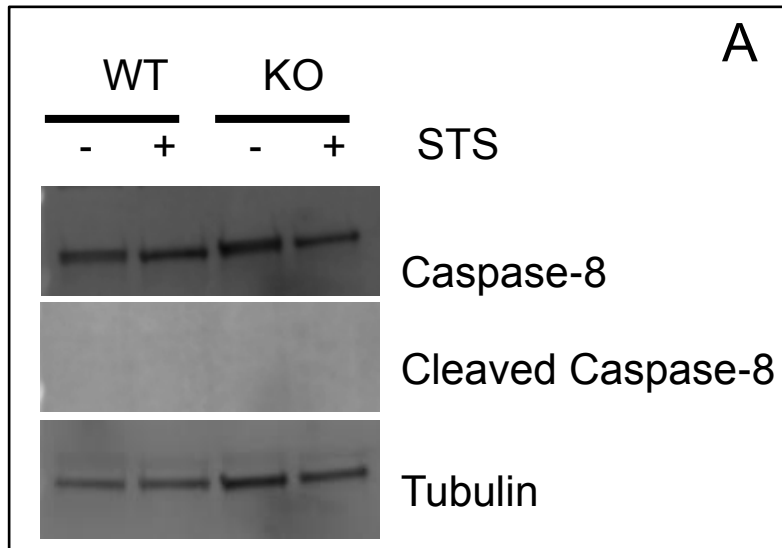


Figure 35. Effect of miR-21 deficiency on the activation of extrinsic and intrinsic pathways of apoptosis in BMDM. WT and miR-21-KO BMDM were incubated with 500 nM staurosporine (STS) or DMSO for 6 h and cleaved caspase-8 and caspase-9 were measured by Western blotting.

induced cleavage of caspase-9 by 4-fold. Together, these data suggest that miR-21 prevents macrophage apoptosis by preventing the activation of the caspase-9-driven intrinsic pathway.

To examine the role of miR-21 targets PDCD4 and PTEN on macrophage apoptosis, we measured the levels of these proteins in STS stimulated BMDM. As shown in **Fig. 36**, STS did not affect the abundance of PDCD4 or PTEN in both the WT and miR-21-KO cells, suggesting that these proteins do not regulate macrophage apoptosis, at least in response to STS.

3.2.9. Effect of miR-21 deficiency on apoptosis and necrosis in atherosclerotic plaques: To investigate whether miR-21 also protects from cell death in atherosclerotic lesions, apoptosis and necrosis in the aortic valves of WT and miR-21-KO chimeric mice was investigated. TUNNEL staining was utilized to examine apoptosis in the lesions. TUNNEL positive cells were visible in the lesions of both WT and KO-mice, but the abundance of TUNNEL positive cells was significantly higher in the lesions of miR-21-KO chimeric mice (**Fig. 37**). Staining for activated caspase-3 (**Fig. 38**) and caspase-9 (**Fig. 39**) was also greater in miR-21-KO chimeric mice.

In order to study lesion necrosis, sections of the aortic valves were stained with hematoxylin and eosin, and necrosis was measured by quantitating the anuclear, afibrotic, and eosin-negative areas. As shown in **Fig. 40**, 14% of the area in aortic lesions of WT mice was necrotic. Lesion necrosis was increased by 1.4-fold in miR-21-KO chimeric mice. Together these data suggest that the deficiency of miR-21 increases apoptosis and necrosis in atherosclerotic plaques.

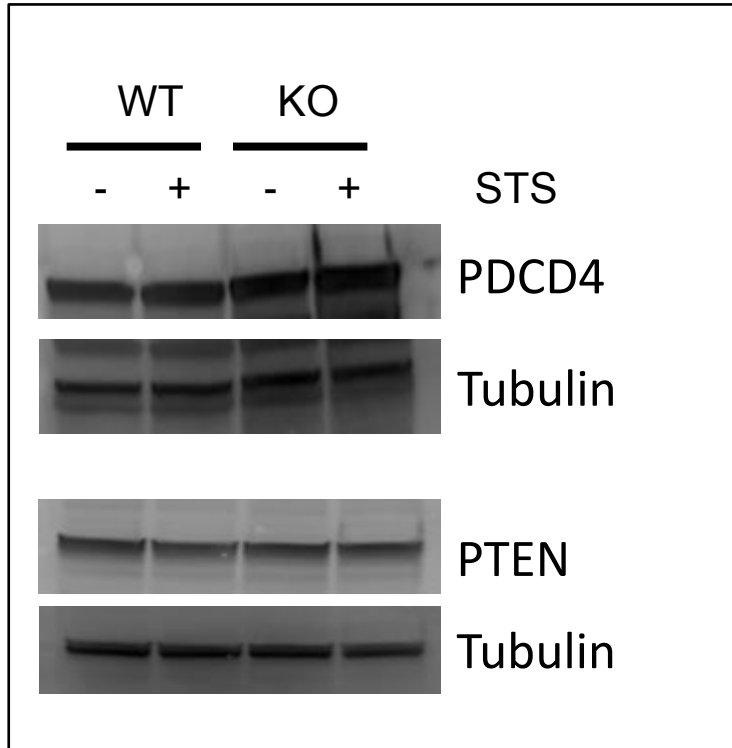
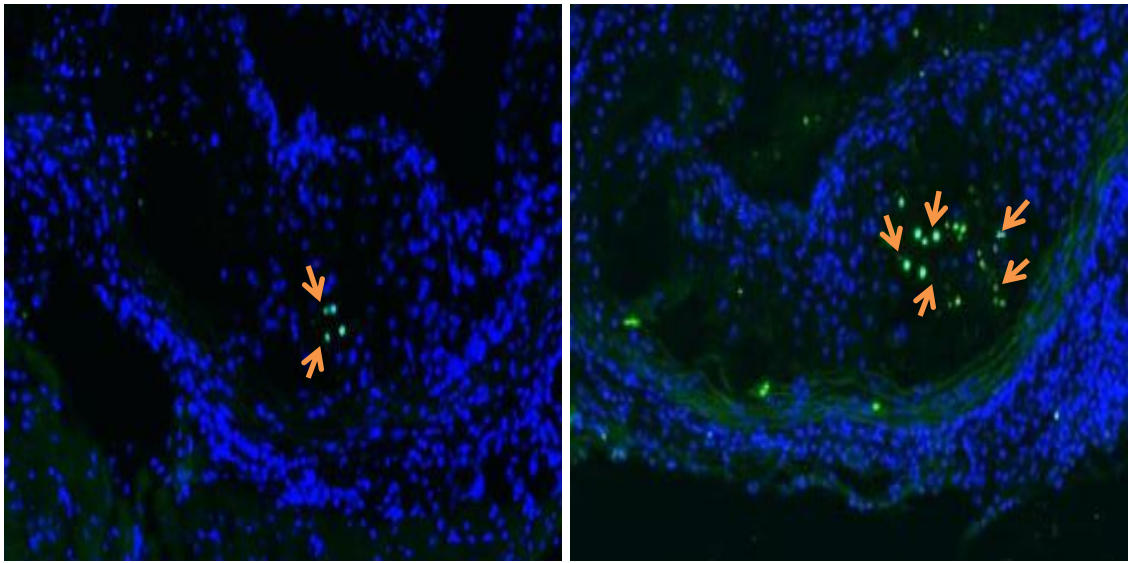


Figure 36. Effects of miR-21 deficiency on the abundance of PTEN and PDCD4. WT and miR-21-KO BMDM were incubated with 500 nM staurosporine (STS) or DMSO for 24 h, and levels of PTEN and PDCD4 were measured by Western blotting.



WT

KO

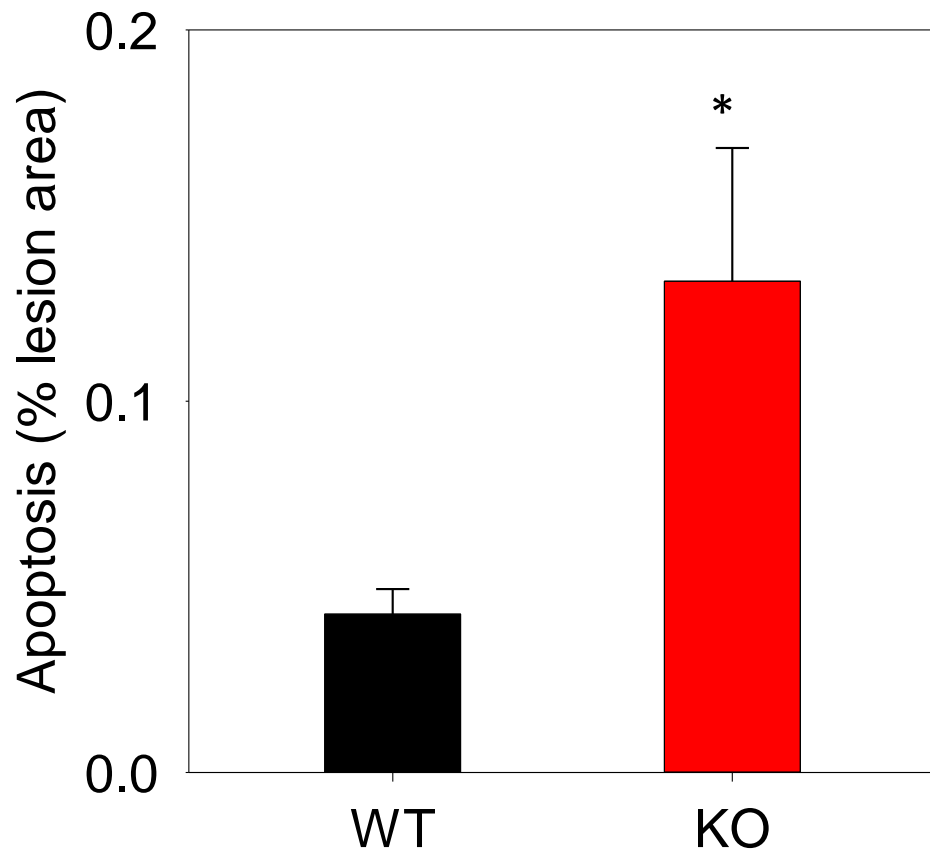


Figure 37. Apoptosis in the aortic valves of miR-21-KO chimeric LDLR-KO mice.

Sections of the aortic valves of LDLR-KO mice transplanted with bone marrow cells from WT or miR-21 KO mice (fed Western diet for 12 weeks) were stained to look for TUNEL-positive signals (green). Values (n=12/group) are mean \pm SEM. *P < 0.05 vs WT.

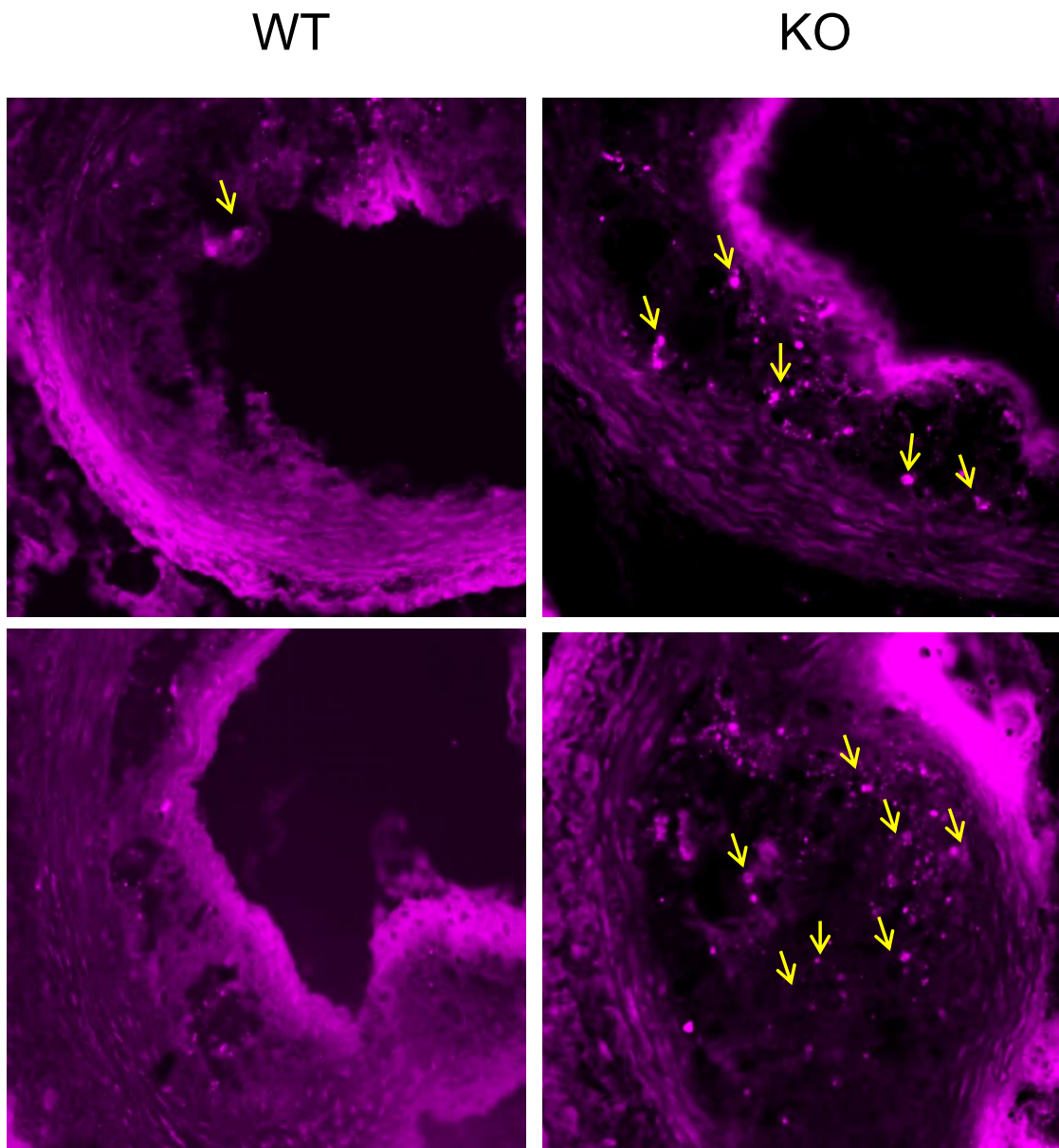


Figure 38. Abundance of activated caspase-3 in atherosclerotic lesions of miR-21-KO chimeric LDLR-KO mice. Representative photomicrographs of cleaved caspase-3 in the aortic valves of LDLR-KO mice transplanted with bone marrow cells from WT or miR-21 KO mice and fed Western diet for 12 weeks.

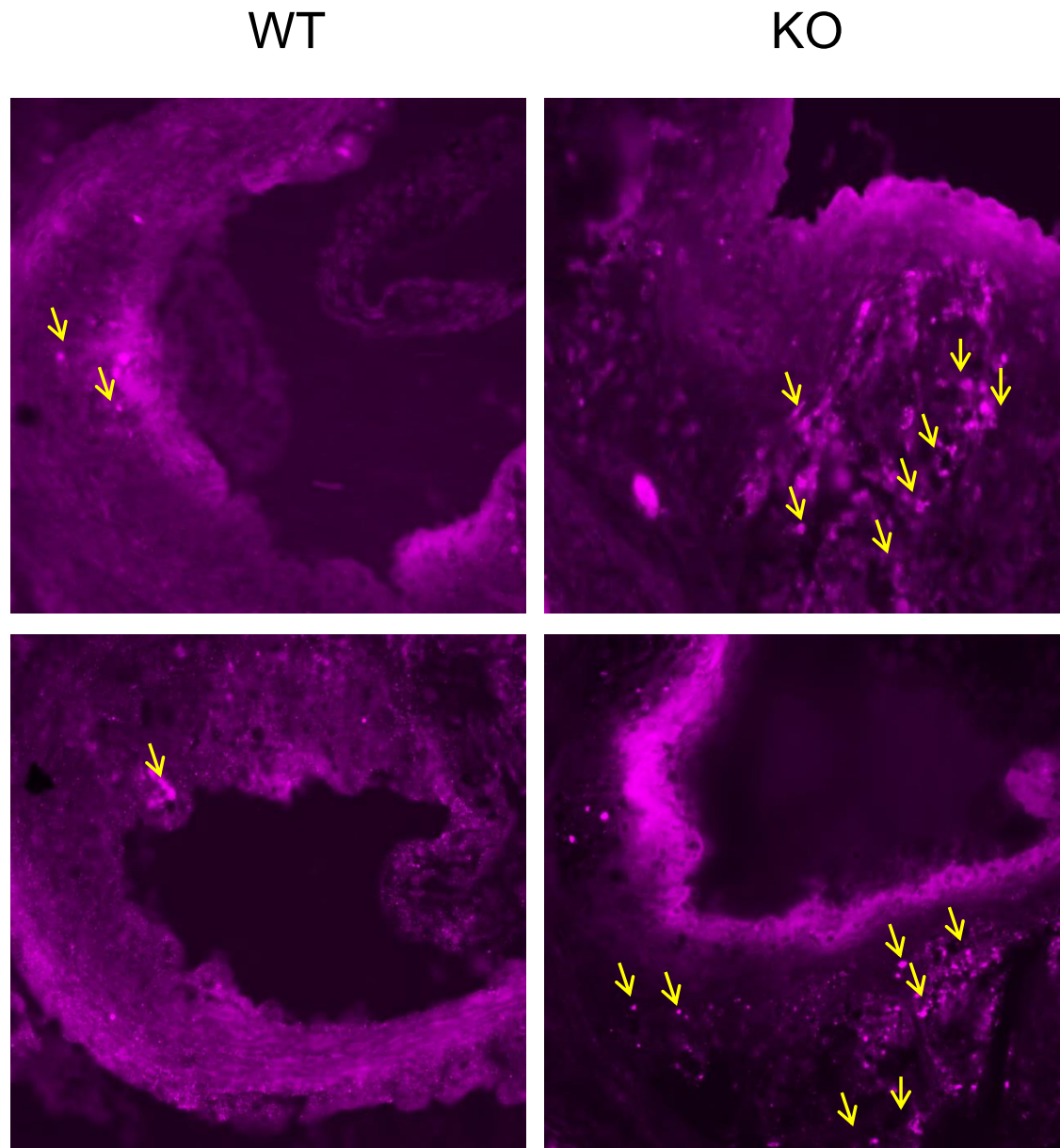
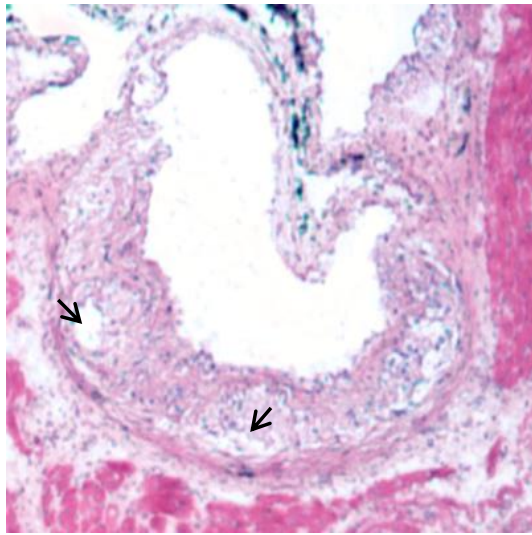
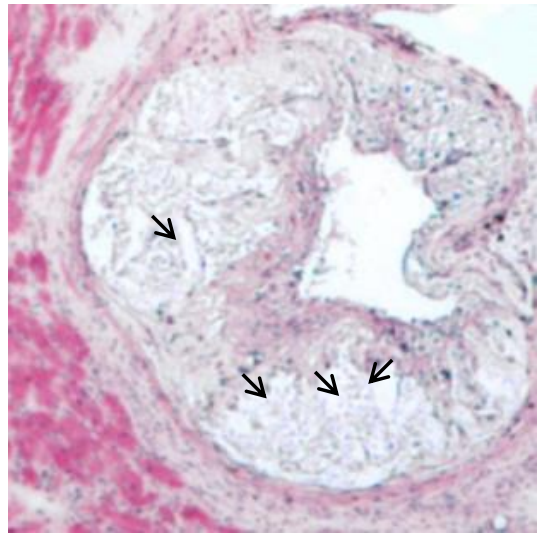


Figure 39. Abundance of activated caspase-9 in atherosclerotic lesions of miR-21-KO chimeric LDLR-KO mice. Representative photomicrographs of cleaved caspase-9 in the aortic valves of LDLR-KO mice transplanted with bone marrow cells from WT or miR-21 KO mice and fed Western diet for 12 weeks.



WT



KO

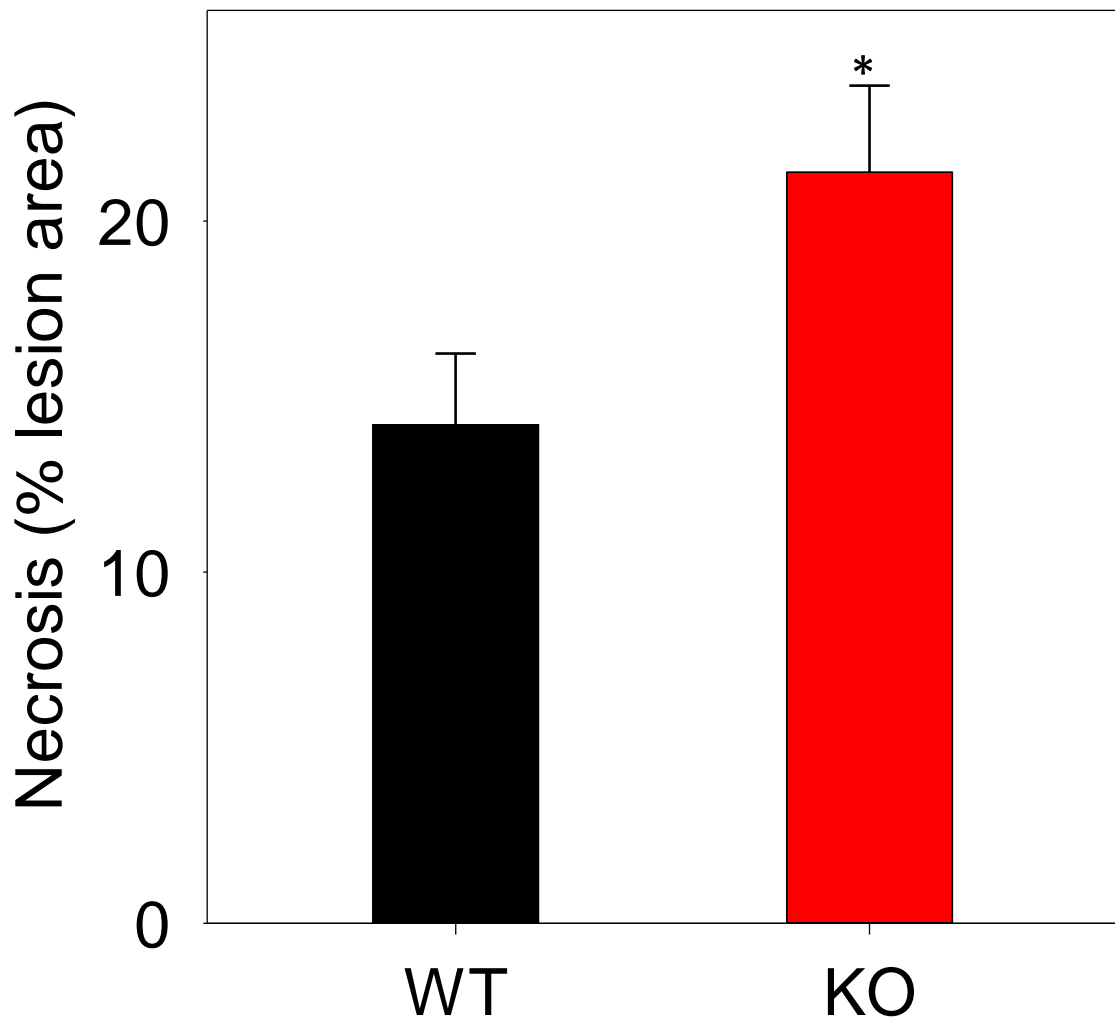


Figure 40. Effect of miR-21 deficiency on lesional necrosis. Sections of the aortic valves of LDLR-KO mice transplanted with bone marrow cells from WT or miR-21 KO mice (fed Western diet for 12 weeks) were stained with hematoxylin & eosin. Necrotic areas are anuclear, afibrotic, and eosin-negative. Values (n=6/group) are mean \pm SEM. *P < 0.05 vs WT.

3.3.0 DISCUSSION:

Data presented in this chapter show that: a) *in vitro* polarization of miR-21-KO macrophages by $\text{INF}\gamma$ +LPS induces the markers of the M1 phenotype; b) deficiency of miR-21 increases the formation of pro-inflammatory cytokines *in vitro* (basally, as well as in response to LPS), and in atherosclerotic lesions of LDLR-KO mice; c) NF- κ B and ERK are likely to induce a pro-inflammatory response in miR-21-KO macrophages; d) deficiency of miR-21 cause macrophage apoptosis *in vitro* and in atherosclerotic plaques; and e) anti-apoptotic effects of miR-21 could be mediated by the intrinsic pathway of apoptosis via the activation of caspase-9.

An interesting observation of my study was that basally, miR-21-KO macrophages profoundly increased the formation of pro-inflammatory cytokines and chemokines such as TNF α , KC (murine analog of IL-8), CCL3, CCL4, CXCL2, and CXCL10. Levels of anti-inflammatory cytokines IL-4 and IL-10 were not affected by miR-21 deficiency in LPS-stimulated cells. Further studies are required to examine the molecular mechanisms by which miR-21 deficiency basally increases the formation of these inflammatory mediators.

Macrophages mediate the innate immunity of atherosclerotic plaques. TLR4 are well known activators of innate immunity and play a key role in vascular inflammation and atherogenesis. TLR signaling is very active in human atherosclerotic plaques, and activation of TLR4 plays a vital role in the initiation and progression of atherogenesis [249]. My data suggest that the deficiency of miR-21 increases macrophage inflammation. Priming the cells with $\text{INF}\gamma$ followed by stimulation with a low dose of LPS, a TLR4 agonist, showed a significant upregulation of markers of pro-inflammatory “M1”

polarization-Cd11c and CD86, whereas abundance of CD80 was not affected. Further studies are required to investigate why miR-21 regulates the expression of some M1 markers and not others. Nonetheless, my data support the notion that miR-21 is an anti-inflammatory microRNA. It is further supported by the fact that a relatively higher dose of LPS robustly increased the formation of several pro-inflammatory cytokines and chemokines. LPS-induced formation of IL-6 and IL-12 is consistent with the published literature [250]. In dendritic cells, it has been shown that IL-12 is a direct target of miR-21 because it binds to the 3' UTR region of the gene [195, 203]. The massive increase in the formation of LIF, IL1 α , IL1 β , and CXCL2 in LPS-stimulated miR-21-KO macrophages suggests that these cytokines could be potential direct targets of miR-21. Induction of IL-1 β and IL-6 in atherosclerotic plaques exhibits the first direct evidence that miR-21 inhibits vascular inflammation.

While there are several pathways to generate IL-1 β , one of the areas of intense investigation is the contribution of inflammasome activation in IL-1 β formation. Accumulation of cholesterol in macrophages could lead to the formation of cholesterol crystals. These cholesterol crystals can activate the cytosolic-nucleotide binding domain and leucine-rich repeat gene family (NLRP3) activating its associated inflammasome and facilitate the formation of IL-1 β . The cholesterol crystals in atherosclerotic plaques can promote vascular inflammation by activating NLRP3 and increasing the formation of IL-1 β . Genetic deficiency of IL1 β or NLRP3 has been shown to decrease atherogenesis [251]. Additional studies are required to examine the potential role of miR-21 in inflammasome activation.

Anti-inflammatory functions of miR-21 could also be mediated by NF- κ B since several miRs have been reported to modulate inflammation by regulating NF- κ B. miR-146a and

146b are induced in macrophages in an NF- κ B-dependent manner and facilitate the resolution of inflammation by limiting TLR signaling and cytokine formation [252]. Similarly, miR-147 attenuates TLR signaling in macrophages in a negative feedback manner [137]. miR-155 mediated cytokine formation is suggested to be mediated by the activation of myeloid differentiation primary response gene 88 (MyD88)/NF- κ B signaling [140]. Moreover, miR-342-5p has been reported to increase iNOS and IL-6 via Akt1-mediated inhibition of miR-155 expression, while inhibition of miR-342-5p prevented atherosclerosis in ApoE-KO mice [95]. I observed a more rapid and higher activation of NF- κ B in LPS-stimulated macrophages. These observations are in agreement with Barnett *et. al.*, who recently reported that the deficiency of miR-21 increases LPS-induced IL-6 formation via NF- κ B activation [244]. Further studies are required to examine the effect of NF- κ B inhibition on cytokine production in miR-21-KO macrophages.

Cytokine formation in macrophages can also be facilitated by MAP Kinases such as ERK and p-38. miR-21-induced angiogenesis has been suggested to be mediated by AKT and ERK activation [253]. In this study ERK and AKT were induced by miR-21, and an antigomir of miR-21 blocked this process. MiR-21 has also been suggested to be regulated by reactive oxygen species-activated ERK/NF- κ B in arsenite-induced cell transformation [248]. Others have suggested that miR-21 is both a target and regulator of ERK/NF- κ B and JNK/c-jun axis [254]. My data show that LPS-induced ERK activation was diminished in miR-21-KO cells. P38 is a well-known contributor to LPS-induced cytokine formation. However, deficiency of miR-21 did not affect p38 activation. Therefore, these MAP Kinases are unlikely to mediate the LPS-induced cytokine formation in miR-21-KO macrophages. Deficiency of miR-21 in macrophages also did

not affect the abundance of several miR-21 targets including PTEN, PDCD4 and Sprouty 1 and 2. Together these data suggest that the pro-inflammatory signaling in miR-21-KO macrophages is likely to be regulated by NF- κ B.

My data also showed that prolonged incubation of miR-21-KO macrophages with IL-4 induced the markers of alternatively activated “M2” macrophages, CD206 and CD301. Delayed induction of these M2 markers suggests that inhibition of miR-21 may facilitate the resolution of inflammation in advanced lesions. Treatment with resolvin D1, a lipid mediator that facilitates the resolution of inflammation, has been suggested to induce miR-21 in peritonitis [240]. However, further studies are required to directly test the contribution of miR-21 in the resolution of inflammation, especially in advanced atherosclerotic lesions.

Another salient feature of my study was the activation of apoptotic signaling. My data showed apoptosis was significantly increased both basally, and in response to atherogenic stimulant HNE and the protein kinase inhibitor staurosporine, in miR-21-KO macrophages. Increased apoptosis in miR-21-KO cells was accompanied by enhanced activation of caspase-3 and caspase-7. miR-21 deficiency did not affect caspase-8 activation suggesting that miR-21 does not affect the extrinsic pathway of apoptosis. However, deficiency of miR-21 increased the cleavage of caspase-9 in response to staurosporine, suggesting the activation of the intrinsic pathway of apoptosis. Myeloid cell-specific deficiency of miR-21 also increased apoptosis and enhanced the abundance of active caspase-3 and caspase-9. These studies are quite novel because the contribution of miR-21 in macrophage apoptosis, in the context of atherosclerosis, has never been examined. My data suggest that one of the mechanisms by which miR-21 inhibits apoptosis is by inhibiting the activation of the intrinsic pathway of apoptosis.

Further studies are required to examine whether caspase-9 activation in miR-21-KO macrophages is involved in Apaf-1 expression and apoptosome formation, or these pathways do not contribute to caspase-9 activation in these cells. Staurosporine did not affect the abundance of PTEN and PDCD4, the well-known targets of apoptosis in cancer cells [220], in miR-21-KO macrophages. Further studies are required to identify the targets of miR-21-induced intrinsic apoptosis in macrophages, especially in response to atherogenic stimuli.

The effects of miR-21-mediated macrophage apoptosis are likely to be different at the various stages of atherogenesis. In early stages increased apoptosis is likely to decrease the lesion size because efferocytosis would remove the apoptotic cells [225]. An increase in apoptosis in intermediate, and advanced lesions would increase plaque necrosis and progression [225]. Indeed, I observed a significant increase in plaque necrosis in the lesions of miR-21 deficient chimeric LDLR-KO mice. These observations are contrary to the recent studies by Ma *et. al.* [230], which showed that miR-21-KO mice are protected from caerulein- or L-arginine-induced pancreatitis by inhibiting necrosis. The observed differences are likely to be due to local environment (lipid rich lesions in atherosclerosis) and cell specificity. Apoptosis of smooth muscle cells in the advanced atherosclerotic lesions would lead to the thinning of the necrotic core and compromise lesion stability. Therefore, caution should be exercised in interpreting the results.

CHAPTER 4

CONCLUSIONS AND FUTURE DIRECTIONS

The goal of this dissertation was to determine the role of miR-21 in atherogenesis and to delineate the molecular mechanisms by which miR-21 affects atherogenesis. To support the rationale of the study, I first performed a gene array analysis to identify the differential expression of miRs in murine aortic lesions. I identified 503 miRs in the lesions, out of which 50 miRs were downregulated and 100 miRs were upregulated in the plaques. Systematic, thorough, and rigorous analyses of these miRs identified 15 miRs expressed in macrophages and associated with inflammation and apoptosis, which drive the separation of the expression pattern of differentially expressed miRs in the plaque. miR-21 was identified as the fourth miR in that hierarchy. Expression of miR-21 was increased by >1.5-fold in atherosclerotic plaques and by 1.5-2.0-fold in the macrophages of atherogenic mice. *In vitro*, LDL, oxidized LDL, acetylated LDL, and LPS induced miR-21 by 2-4-fold in bone marrow-derived macrophages.

To examine the contribution of miR-21 in the manifestation of atherosclerosis, I first examined the effect of miR-21 deficiency on foam cell formation. Incubation of miR-21-KO macrophages with acetylated LDL increased the foam cell formation by >2-fold, suggesting the anti-atherogenic nature of miR-21. Additional studies are required to examine if this is mediated by the upregulation of CD-36, SRA-1 or both.

To examine the role of miR-21 in atherosclerotic plaque formation, bone marrow cells of LDLR-KO mice were lethally irradiated and re-populated with bone marrow cells of either WT or miR-21-KO mice. These chimeric mice were maintained on western diet for 12 weeks. This led to a 1.7-fold increase in the lesion size in the aortic valves of the chimeric miR-21-KO mice. These data clearly demonstrated the atheroprotective role of miR-21.

Since inflammation and apoptosis play critical roles in all phases of atherosclerosis, contribution of these processes in miR-21-mediated atherosclerosis was further examined. Basally, macrophages isolated from miR-21-KO mice showed induction of several cytokines and chemokines. Stimulation of miR-21-KO macrophages with interferon γ +LPS polarized them to the pro-inflammatory M1 phenotype (increased expression of CD11c and CD86). LPS increased the nuclear translocation of NF- κ B and robustly increased the formation of several pro-inflammatory cytokines including LIF, IL-6, IL-12, IL-1 α , IL-1 β , and CXCL-2, in miR-21-KO macrophages. This was accompanied by the activation of NF- κ B. Further studies are required to examine the causal role of NF- κ B in increasing the formation of these cytokines in miR-21-KO macrophages. This can be accomplished by knocking down NF- κ B p65 by siRNA and measuring the cytokine formation. To examine if these cytokines are direct targets of miR-21, luciferase activity should be performed in miR-21-KO cells.

Complimentary to *in vitro* experiments, abundance of IL-1 β and IL-12 was also increased in atherosclerotic lesions of miR-21-KO chimeric mice. While these studies support the notion that miR-21 inhibits lesion inflammation, additional experiments should be performed to isolate the macrophages from the aortae of atherogenic miR-21-KO chimeric mice in order to quantify the expression of these cytokines. This will provide quantitative evidence for the anti-inflammatory nature of miR-21 in the context of atherosclerosis. Expression of NF- κ B, and predicted miR-21 targets in these cells will delineate the mechanism by which miR-21 prevents vascular inflammation.

To examine the contribution of miR-21 in apoptosis, macrophage apoptosis was measured in cells treated with staurosporine and HNE-treated cells as well as unstimulated cells. Deficiency of miR-21 significantly increased both early and late apoptosis in miR-21-KO macrophages. Apoptosis in these cells was significantly increased by staurosporine and HNE. This was accompanied by the activation of caspase-3, caspase-7 and caspase-9. These data suggest that miR-21 prevents macrophage apoptosis by preventing the activation of the intrinsic pathway of activation. Further studies are required to examine the role of Apaf-1 and cytochrome C in the miR-21-dependent activation of caspase-9. Additional studies are also required to examine if this process is mediated by Bax, Bcl-xl, or other apoptotic mediators.

Increased TUNEL staining as well as increased staining for caspase-3 and caspase-9 in the lesions of miR-21-KO chimeric mice support the anti-apoptotic role of miR-21 in atherogenesis. This was accompanied by increased lesion necrosis. Since macrophage apoptosis has different roles at various stages of lesion progression, the role of miR-21

in macrophage apoptosis needs to be examined in early, intermediate, and advanced lesions. Moreover, smooth muscle cell apoptosis of the necrotic core should also be investigated because it is a critical determinant of lesion stability.

In summary, this dissertation has identified a novel anti-atherogenic role of miR-21, which is at least in part, due to anti-inflammatory and anti-apoptotic properties of miR-21, especially in macrophages.

REFERENCES

1. Mozaffarian, D., *et al.*, *Heart disease and stroke statistics--2015 update: a report from the American Heart Association*. *Circulation*, 2015. **131**(4): p. e29-322.
2. Heidenreich, P.A., *et al.*, *Forecasting the future of cardiovascular disease in the United States: a policy statement from the American Heart Association*. *Circulation*, 2011. **123**(8): p. 933-44.
3. Go, A.S., *et al.*, *Heart disease and stroke statistics--2013 update: a report from the American Heart Association*. *Circulation*, 2013. **127**(1): p. e6-e245.
4. Steinberg, D. and J.L. Witztum, *Oxidized low-density lipoprotein and atherosclerosis*. *Arterioscler Thromb Vasc Biol*, 2010. **30**(12): p. 2311-6.
5. Glass, C.K. and J.L. Witztum, *Atherosclerosis. the road ahead*. *Cell*, 2001. **104**(4): p. 503-16.
6. Libby, P., *Inflammation in atherosclerosis*. *Nature*, 2002. **420**(6917): p. 868-74.
7. Doran, A.C., N. Meller, and C.A. McNamara, *Role of smooth muscle cells in the initiation and early progression of atherosclerosis*. *Arterioscler Thromb Vasc Biol*, 2008. **28**(5): p. 812-9.
8. Keaney, J.F., Jr., *Atherosclerosis: from lesion formation to plaque activation and endothelial dysfunction*. *Mol Aspects Med*, 2000. **21**(4-5): p. 99-166.
9. Eddinger, T.J. and R.A. Murphy, *Developmental changes in actin and myosin heavy chain isoform expression in smooth muscle*. *Arch Biochem Biophys*, 1991. **284**(2): p. 232-7.
10. Galkina, E., *et al.*, *Lymphocyte recruitment into the aortic wall before and during development of atherosclerosis is partially L-selectin dependent*. *J Exp Med*, 2006. **203**(5): p. 1273-82.
11. Asakura, T. and T. Karino, *Flow patterns and spatial distribution of atherosclerotic lesions in human coronary arteries*. *Circ Res*, 1990. **66**(4): p. 1045-66.
12. Chatzizisis, Y.S., *et al.*, *Role of endothelial shear stress in the natural history of coronary atherosclerosis and vascular remodeling: molecular, cellular, and vascular behavior*. *J Am Coll Cardiol*, 2007. **49**(25): p. 2379-93.
13. Williams, K.J. and I. Tabas, *The response-to-retention hypothesis of early atherogenesis*. *Arterioscler Thromb Vasc Biol*, 1995. **15**(5): p. 551-61.
14. Camejo, G., *et al.*, *Association of apo B lipoproteins with arterial proteoglycans: pathological significance and molecular basis*. *Atherosclerosis*, 1998. **139**(2): p. 205-22.
15. Mestas, J. and K. Ley, *Monocyte-endothelial cell interactions in the development of atherosclerosis*. *Trends Cardiovasc Med*, 2008. **18**(6): p. 228-32.
16. Kamei, M. and C.V. Carman, *New observations on the trafficking and diapedesis of monocytes*. *Curr Opin Hematol*, 2010. **17**(1): p. 43-52.
17. Johnson, J.L. and A.C. Newby, *Macrophage heterogeneity in atherosclerotic plaques*. *Curr Opin Lipidol*, 2009. **20**(5): p. 370-8.
18. Perrotta, I., *Ultrastructural features of human atherosclerosis*. *Ultrastruct Pathol*, 2013. **37**(1): p. 43-51.
19. Newby, A.C. and A.B. Zaltsman, *Fibrous cap formation or destruction--the critical importance of vascular smooth muscle cell proliferation, migration and matrix formation*. *Cardiovasc Res*, 1999. **41**(2): p. 345-60.
20. Mason, D.P., *et al.*, *Matrix metalloproteinase-9 overexpression enhances vascular smooth muscle cell migration and alters remodeling in the injured rat carotid artery*. *Circ Res*, 1999. **85**(12): p. 1179-85.

21. Tousoulis, D., *et al.*, *Insight to the pathophysiology of stable angina pectoris*. *Curr Pharm Des*, 2013. **19**(9): p. 1593-600.
22. Amento, E.P., *et al.*, *Cytokines and growth factors positively and negatively regulate interstitial collagen gene expression in human vascular smooth muscle cells*. *Arterioscler Thromb*, 1991. **11**(5): p. 1223-30.
23. Clarke, M. and M. Bennett, *The emerging role of vascular smooth muscle cell apoptosis in atherosclerosis and plaque stability*. *Am J Nephrol*, 2006. **26**(6): p. 531-5.
24. Tabas, I., *Macrophage death and defective inflammation resolution in atherosclerosis*. *Nat Rev Immunol*, 2010. **10**(1): p. 36-46.
25. van der Wal, A.C. and A.E. Becker, *Atherosclerotic plaque rupture--pathologic basis of plaque stability and instability*. *Cardiovasc Res*, 1999. **41**(2): p. 334-44.
26. Libby, P., P.M. Ridker, and G.K. Hansson, *Progress and challenges in translating the biology of atherosclerosis*. *Nature*, 2011. **473**(7347): p. 317-25.
27. Gui, T., *et al.*, *Diverse roles of macrophages in atherosclerosis: from inflammatory biology to biomarker discovery*. *Mediators Inflamm*, 2012. **2012**: p. 693083.
28. Moore, K.J. and I. Tabas, *Macrophages in the pathogenesis of atherosclerosis*. *Cell*, 2011. **145**(3): p. 341-55.
29. Shibata, N. and C.K. Glass, *Regulation of macrophage function in inflammation and atherosclerosis*. *J Lipid Res*, 2009. **50** **Suppl**: p. S277-81.
30. Mullick, A.E., P.S. Tobias, and L.K. Curtiss, *Modulation of atherosclerosis in mice by Toll-like receptor 2*. *J Clin Invest*, 2005. **115**(11): p. 3149-56.
31. Stewart, C.R., *et al.*, *CD36 ligands promote sterile inflammation through assembly of a Toll-like receptor 4 and 6 heterodimer*. *Nat Immunol*, 2010. **11**(2): p. 155-61.
32. Lutgens, E., *et al.*, *Deficient CD40-TRAF6 signaling in leukocytes prevents atherosclerosis by skewing the immune response toward an antiinflammatory profile*. *J Exp Med*, 2010. **207**(2): p. 391-404.
33. de Winther, M.P., *et al.*, *Nuclear factor kappaB signaling in atherogenesis*. *Arterioscler Thromb Vasc Biol*, 2005. **25**(5): p. 904-14.
34. Brand, K., *et al.*, *Activated transcription factor nuclear factor-kappa B is present in the atherosclerotic lesion*. *J Clin Invest*, 1996. **97**(7): p. 1715-22.
35. Kanters, E., *et al.*, *Inhibition of NF-kappaB activation in macrophages increases atherosclerosis in LDL receptor-deficient mice*. *J Clin Invest*, 2003. **112**(8): p. 1176-85.
36. Martinez, F.O., L. Helming, and S. Gordon, *Alternative activation of macrophages: an immunologic functional perspective*. *Annu Rev Immunol*, 2009. **27**: p. 451-83.
37. Mantovani, A., A. Sica, and M. Locati, *Macrophage polarization comes of age*. *Immunity*, 2005. **23**(4): p. 344-6.
38. Mantovani, A., C. Garlanda, and M. Locati, *Macrophage diversity and polarization in atherosclerosis: a question of balance*. *Arterioscler Thromb Vasc Biol*, 2009. **29**(10): p. 1419-23.
39. Khallou-Laschet, J., *et al.*, *Macrophage plasticity in experimental atherosclerosis*. *PLoS One*, 2010. **5**(1): p. e8852.
40. Stoger, J.L., *et al.*, *Distribution of macrophage polarization markers in human atherosclerosis*. *Atherosclerosis*, 2012. **225**(2): p. 461-8.
41. Gautier, E.L., *et al.*, *Macrophage apoptosis exerts divergent effects on atherogenesis as a function of lesion stage*. *Circulation*, 2009. **119**(13): p. 1795-804.

42. Lamkanfi, M. and V.M. Dixit, *Manipulation of host cell death pathways during microbial infections*. Cell Host Microbe, 2010. **8**(1): p. 44-54.
43. Mitchinson, M.J., S.J. Hardwick, and M.R. Bennett, *Cell death in atherosclerotic plaques*. Curr Opin Lipidol, 1996. **7**(5): p. 324-9.
44. Kockx, M.M., *Apoptosis in the atherosclerotic plaque: quantitative and qualitative aspects*. Arterioscler Thromb Vasc Biol, 1998. **18**(10): p. 1519-22.
45. Tabas, I., *Apoptosis and plaque destabilization in atherosclerosis: the role of macrophage apoptosis induced by cholesterol*. Cell Death Differ, 2004. **11 Suppl 1**: p. S12-6.
46. Yao, P.M. and I. Tabas, *Free cholesterol loading of macrophages induces apoptosis involving the fas pathway*. J Biol Chem, 2000. **275**(31): p. 23807-13.
47. Yao, P.M. and I. Tabas, *Free cholesterol loading of macrophages is associated with widespread mitochondrial dysfunction and activation of the mitochondrial apoptosis pathway*. J Biol Chem, 2001. **276**(45): p. 42468-76.
48. Seimon, T. and I. Tabas, *Mechanisms and consequences of macrophage apoptosis in atherosclerosis*. J Lipid Res, 2009. **50 Suppl**: p. S382-7.
49. Bartel, D.P., *MicroRNAs: target recognition and regulatory functions*. Cell, 2009. **136**(2): p. 215-33.
50. Lee, R.C., R.L. Feinbaum, and V. Ambros, *The C. elegans heterochronic gene lin-4 encodes small RNAs with antisense complementarity to lin-14*. Cell, 1993. **75**(5): p. 843-54.
51. Bartel, D.P., *MicroRNAs: genomics, biogenesis, mechanism, and function*. Cell, 2004. **116**(2): p. 281-97.
52. Kim, V.N. and J.W. Nam, *Genomics of microRNA*. Trends Genet, 2006. **22**(3): p. 165-73.
53. Treiber, T., N. Treiber, and G. Meister, *Regulation of microRNA biogenesis and function*. Thromb Haemost, 2012. **107**(4): p. 605-10.
54. Ozsolak, F., et al., *Chromatin structure analyses identify miRNA promoters*. Genes Dev, 2008. **22**(22): p. 3172-83.
55. Faller, M. and F. Guo, *MicroRNA biogenesis: there's more than one way to skin a cat*. Biochim Biophys Acta, 2008. **1779**(11): p. 663-7.
56. Borchert, G.M., W. Lanier, and B.L. Davidson, *RNA polymerase III transcribes human microRNAs*. Nat Struct Mol Biol, 2006. **13**(12): p. 1097-101.
57. Han, J., et al., *The Drosha-DGCR8 complex in primary microRNA processing*. Genes Dev, 2004. **18**(24): p. 3016-27.
58. Han, J., et al., *Molecular basis for the recognition of primary microRNAs by the Drosha-DGCR8 complex*. Cell, 2006. **125**(5): p. 887-901.
59. Gregory, R.I., et al., *The Microprocessor complex mediates the genesis of microRNAs*. Nature, 2004. **432**(7014): p. 235-40.
60. Lund, E., et al., *Nuclear export of microRNA precursors*. Science, 2004. **303**(5654): p. 95-8.
61. Wang, X., et al., *Dynamic mechanisms for pre-miRNA binding and export by Exportin-5*. RNA, 2011. **17**(8): p. 1511-28.
62. Macrae, I.J., et al., *Structural basis for double-stranded RNA processing by Dicer*. Science, 2006. **311**(5758): p. 195-8.
63. Zhang, H., et al., *Single processing center models for human Dicer and bacterial RNase III*. Cell, 2004. **118**(1): p. 57-68.
64. Perron, M.P. and P. Provost, *Protein components of the microRNA pathway and human diseases*. Methods Mol Biol, 2009. **487**: p. 369-85.

65. Fazi, F. and C. Nervi, *MicroRNA: basic mechanisms and transcriptional regulatory networks for cell fate determination*. Cardiovasc Res, 2008. **79**(4): p. 553-61.
66. Drakaki, A. and D. Iliopoulos, *MicroRNA Gene Networks in Oncogenesis*. Curr Genomics, 2009. **10**(1): p. 35-41.
67. Lagos-Quintana, M., et al., *Identification of tissue-specific microRNAs from mouse*. Curr Biol, 2002. **12**(9): p. 735-9.
68. Elmen, J., et al., *LNA-mediated microRNA silencing in non-human primates*. Nature, 2008. **452**(7189): p. 896-9.
69. Esau, C., et al., *miR-122 regulation of lipid metabolism revealed by in vivo antisense targeting*. Cell Metab, 2006. **3**(2): p. 87-98.
70. Hsu, S.H., et al., *Essential metabolic, anti-inflammatory, and anti-tumorigenic functions of miR-122 in liver*. J Clin Invest, 2012. **122**(8): p. 2871-83.
71. Krutzfeldt, J., et al., *Silencing of microRNAs in vivo with 'antagomirs'*. Nature, 2005. **438**(7068): p. 685-9.
72. Wen, J. and J.R. Friedman, *miR-122 regulates hepatic lipid metabolism and tumor suppression*. J Clin Invest, 2012. **122**(8): p. 2773-6.
73. Tsai, W.C., et al., *MicroRNA-122 plays a critical role in liver homeostasis and hepatocarcinogenesis*. J Clin Invest, 2012. **122**(8): p. 2884-97.
74. Li, T., et al., *Identification of miR-130a, miR-27b and miR-210 as serum biomarkers for atherosclerosis obliterans*. Clin Chim Acta, 2011. **412**(1-2): p. 66-70.
75. Ji, R., et al., *MicroRNA expression signature and antisense-mediated depletion reveal an essential role of MicroRNA in vascular neointimal lesion formation*. Circ Res, 2007. **100**(11): p. 1579-88.
76. Raitoharju, E., et al., *miR-21, miR-210, miR-34a, and miR-146a/b are up-regulated in human atherosclerotic plaques in the Tampere Vascular Study*. Atherosclerosis, 2011. **219**(1): p. 211-7.
77. Bidzhakov, K., et al., *microRNA expression signatures and parallels between monocyte subsets and atherosclerotic plaque in humans*. Thromb Haemost, 2012. **107**(4): p. 619-25.
78. Karunakaran, D., et al., *Macrophage Mitochondrial Energy Status Regulates Cholesterol Efflux and Is Enhanced by Anti-miR33 in Atherosclerosis*. Circ Res, 2015. **117**(3): p. 266-78.
79. Cipollone, F., et al., *A unique microRNA signature associated with plaque instability in humans*. Stroke, 2011. **42**(9): p. 2556-63.
80. Nazari-Jahantigh, M., et al., *MicroRNA-155 promotes atherosclerosis by repressing Bcl6 in macrophages*. J Clin Invest, 2012. **122**(11): p. 4190-202.
81. Shan, Z., et al., *An Endocrine Genetic Signal Between Blood Cells and Vascular Smooth Muscle Cells: Role of MicroRNA-223 in Smooth Muscle Function and Atherogenesis*. J Am Coll Cardiol, 2015. **65**(23): p. 2526-37.
82. Di Gregoli, K., et al., *MicroRNA-24 regulates macrophage behavior and retards atherosclerosis*. Arterioscler Thromb Vasc Biol, 2014. **34**(9): p. 1990-2000.
83. Sun, X., et al., *Systemic delivery of microRNA-181b inhibits nuclear factor-kappaB activation, vascular inflammation, and atherosclerosis in apolipoprotein E-deficient mice*. Circ Res, 2014. **114**(1): p. 32-40.
84. Lv, Y.C., et al., *MicroRNA-19b promotes macrophage cholesterol accumulation and aortic atherosclerosis by targeting ATP-binding cassette transporter A1*. Atherosclerosis, 2014. **236**(1): p. 215-26.

85. Distel, E., et al., *miR33 inhibition overcomes deleterious effects of diabetes mellitus on atherosclerosis plaque regression in mice*. *Circ Res*, 2014. **115**(9): p. 759-69.
86. Horie, T., et al., *MicroRNA-33 deficiency reduces the progression of atherosclerotic plaque in ApoE^{-/-} mice*. *J Am Heart Assoc*, 2012. **1**(6): p. e003376.
87. Marquart, T.J., et al., *Anti-miR-33 therapy does not alter the progression of atherosclerosis in low-density lipoprotein receptor-deficient mice*. *Arterioscler Thromb Vasc Biol*, 2013. **33**(3): p. 455-8.
88. Ouimet, M., et al., *MicroRNA-33-dependent regulation of macrophage metabolism directs immune cell polarization in atherosclerosis*. *J Clin Invest*, 2015. **2015**.
89. Loyer, X., et al., *Inhibition of microRNA-92a prevents endothelial dysfunction and atherosclerosis in mice*. *Circ Res*, 2014. **114**(3): p. 434-43.
90. Zhou, J., et al., *Regulation of vascular smooth muscle cell turnover by endothelial cell-secreted microRNA-126: role of shear stress*. *Circ Res*, 2013. **113**(1): p. 40-51.
91. Sala, F., et al., *MiR-143/145 deficiency attenuates the progression of atherosclerosis in Ldlr^{-/-} mice*. *Thromb Haemost*, 2014. **112**(4): p. 796-802.
92. Hu, Y.W., et al., *An agomir of miR-144-3p accelerates plaque formation through impairing reverse cholesterol transport and promoting pro-inflammatory cytokine production*. *PLoS One*, 2014. **9**(4): p. e94997.
93. Lovren, F., et al., *MicroRNA-145 targeted therapy reduces atherosclerosis*. *Circulation*, 2012. **126**(11 Suppl 1): p. S81-90.
94. Meiler, S., et al., *MicroRNA 302a is a novel modulator of cholesterol homeostasis and atherosclerosis*. *Arterioscler Thromb Vasc Biol*, 2015. **35**(2): p. 323-31.
95. Wei, Y., et al., *The microRNA-342-5p fosters inflammatory macrophage activation through an Akt1- and microRNA-155-dependent pathway during atherosclerosis*. *Circulation*, 2013. **127**(15): p. 1609-19.
96. Son, D.J., et al., *The atypical mechanosensitive microRNA-712 derived from pre-ribosomal RNA induces endothelial inflammation and atherosclerosis*. *Nat Commun*, 2013. **4**: p. 3000.
97. Soh, J., et al., *MicroRNA-30c reduces hyperlipidemia and atherosclerosis in mice by decreasing lipid synthesis and lipoprotein secretion*. *Nat Med*, 2013. **19**(7): p. 892-900.
98. Schober, A., et al., *MicroRNA-126-5p promotes endothelial proliferation and limits atherosclerosis by suppressing Dlk1*. *Nat Med*, 2014. **20**(4): p. 368-76.
99. Li, K., et al., *Apolipoprotein E Enhances microRNA-146a in Monocytes and Macrophages to Suppress Nuclear Factor-kappaB-Driven Inflammation and Atherosclerosis*. *Circ Res*, 2015.
100. Chen, L.J., et al., *MicroRNA mediation of endothelial inflammatory response to smooth muscle cells and its inhibition by atheroprotective shear stress*. *Circ Res*, 2015. **116**(7): p. 1157-69.
101. Tian, G.P., et al., *The effects of miR-467b on lipoprotein lipase (LPL) expression, pro-inflammatory cytokine, lipid levels and atherosclerotic lesions in apolipoprotein E knockout mice*. *Biochem Biophys Res Commun*, 2014. **443**(2): p. 428-34.
102. Li, P., et al., *MicroRNA-663 regulates human vascular smooth muscle cell phenotypic switch and vascular neointimal formation*. *Circ Res*, 2013. **113**(10): p. 1117-27.

103. Donners, M.M., *et al.*, *Hematopoietic miR155 deficiency enhances atherosclerosis and decreases plaque stability in hyperlipidemic mice*. PLoS One, 2012. **7**(4): p. e35877.
104. Du, F., *et al.*, *MicroRNA-155 deficiency results in decreased macrophage inflammation and attenuated atherogenesis in apolipoprotein E-deficient mice*. Arterioscler Thromb Vasc Biol, 2014. **34**(4): p. 759-67.
105. Wei, Y., *et al.*, *Regulation of Csf1r and Bcl6 in macrophages mediates the stage-specific effects of microRNA-155 on atherosclerosis*. Arterioscler Thromb Vasc Biol, 2015. **35**(4): p. 796-803.
106. Zhang, R.N., *et al.*, *Tongxinluo inhibits vascular inflammation and neointimal hyperplasia through blockade of the positive feedback loop between miR-155 and TNF-alpha*. Am J Physiol Heart Circ Physiol, 2014. **307**(4): p. H552-62.
107. Tian, F.J., *et al.*, *Elevated microRNA-155 promotes foam cell formation by targeting HBP1 in atherogenesis*. Cardiovasc Res, 2014. **103**(1): p. 100-10.
108. Marquart, T.J., *et al.*, *miR-33 links SREBP-2 induction to repression of sterol transporters*. Proc Natl Acad Sci U S A, 2010. **107**(27): p. 12228-32.
109. Najafi-Shoushtari, S.H., *et al.*, *MicroRNA-33 and the SREBP host genes cooperate to control cholesterol homeostasis*. Science, 2010. **328**(5985): p. 1566-9.
110. Rayner, K.J., *et al.*, *MiR-33 contributes to the regulation of cholesterol homeostasis*. Science, 2010. **328**(5985): p. 1570-3.
111. Horie, T., *et al.*, *MicroRNAs and Lipoprotein Metabolism*. J Atheroscler Thromb, 2014. **21**(1): p. 17-22.
112. Rottiers, V., *et al.*, *Pharmacological inhibition of a microRNA family in nonhuman primates by a seed-targeting 8-mer antimiR*. Sci Transl Med, 2013. **5**(212): p. 212ra162.
113. Rayner, K.J., *et al.*, *Inhibition of miR-33a/b in non-human primates raises plasma HDL and lowers VLDL triglycerides*. Nature, 2011. **478**(7369): p. 404-7.
114. Davalos, A., *et al.*, *miR-33a/b contribute to the regulation of fatty acid metabolism and insulin signaling*. Proc Natl Acad Sci U S A, 2011. **108**(22): p. 9232-7.
115. Wang, D., *et al.*, *Gut microbiota metabolism of anthocyanin promotes reverse cholesterol transport in mice via repressing miRNA-10b*. Circ Res, 2012. **111**(8): p. 967-81.
116. Zhang, M., *et al.*, *MicroRNA-27a/b regulates cellular cholesterol efflux, influx and esterification/hydrolysis in THP-1 macrophages*. Atherosclerosis, 2014. **234**(1): p. 54-64.
117. Ramirez, C.M., *et al.*, *Control of cholesterol metabolism and plasma high-density lipoprotein levels by microRNA-144*. Circ Res, 2013. **112**(12): p. 1592-601.
118. de Aguiar Vallim, T.Q., *et al.*, *MicroRNA-144 regulates hepatic ATP binding cassette transporter A1 and plasma high-density lipoprotein after activation of the nuclear receptor farnesoid X receptor*. Circ Res, 2013. **112**(12): p. 1602-12.
119. Kang, M.H., *et al.*, *Regulation of ABCA1 protein expression and function in hepatic and pancreatic islet cells by miR-145*. Arterioscler Thromb Vasc Biol, 2013. **33**(12): p. 2724-32.
120. Vickers, K.C., *et al.*, *MicroRNA-223 coordinates cholesterol homeostasis*. Proc Natl Acad Sci U S A, 2014. **111**(40): p. 14518-23.
121. Ramirez, C.M., *et al.*, *MicroRNA-758 regulates cholesterol efflux through posttranscriptional repression of ATP-binding cassette transporter A1*. Arterioscler Thromb Vasc Biol, 2011. **31**(11): p. 2707-14.

122. Wang, L., et al., *MicroRNAs 185, 96, and 223 repress selective high-density lipoprotein cholesterol uptake through posttranscriptional inhibition*. Mol Cell Biol, 2013. **33**(10): p. 1956-64.
123. Sun, X., et al., *MicroRNA-181b regulates NF-kappaB-mediated vascular inflammation*. J Clin Invest, 2012. **122**(6): p. 1973-90.
124. Suarez, Y., et al., *Cutting edge: TNF-induced microRNAs regulate TNF-induced expression of E-selectin and intercellular adhesion molecule-1 on human endothelial cells: feedback control of inflammation*. J Immunol, 2010. **184**(1): p. 21-5.
125. Zhu, N., et al., *Endothelial enriched microRNAs regulate angiotensin II-induced endothelial inflammation and migration*. Atherosclerosis, 2011. **215**(2): p. 286-93.
126. Sun, H.X., et al., *Essential role of microRNA-155 in regulating endothelium-dependent vasorelaxation by targeting endothelial nitric oxide synthase*. Hypertension, 2012. **60**(6): p. 1407-14.
127. Cheng, H.S., et al., *MicroRNA-146 represses endothelial activation by inhibiting pro-inflammatory pathways*. EMBO Mol Med, 2013. **5**(7): p. 949-66.
128. Liao, Y.C., et al., *Let-7g improves multiple endothelial functions through targeting transforming growth factor-beta and SIRT-1 signaling*. J Am Coll Cardiol, 2014. **63**(16): p. 1685-94.
129. Harris, T.A., et al., *MicroRNA-126 regulates endothelial expression of vascular cell adhesion molecule 1*. Proc Natl Acad Sci U S A, 2008. **105**(5): p. 1516-21.
130. Sun, C., et al., *IRF-1 and miRNA126 modulate VCAM-1 expression in response to a high-fat meal*. Circ Res, 2012. **111**(8): p. 1054-64.
131. Kumar, S., et al., *Role of flow-sensitive microRNAs in endothelial dysfunction and atherosclerosis: mechanosensitive athero-miRs*. Arterioscler Thromb Vasc Biol, 2014. **34**(10): p. 2206-16.
132. Weber, M., et al., *MiR-21 is induced in endothelial cells by shear stress and modulates apoptosis and eNOS activity*. Biochem Biophys Res Commun, 2010. **393**(4): p. 643-8.
133. Zhou, J., et al., *MicroRNA-21 targets peroxisome proliferators-activated receptor-alpha in an autoregulatory loop to modulate flow-induced endothelial inflammation*. Proc Natl Acad Sci U S A, 2011. **108**(25): p. 10355-60.
134. Ni, C.W., H. Qiu, and H. Jo, *MicroRNA-663 upregulated by oscillatory shear stress plays a role in inflammatory response of endothelial cells*. Am J Physiol Heart Circ Physiol, 2011. **300**(5): p. H1762-9.
135. Chen, T., et al., *MicroRNA-125a-5p partly regulates the inflammatory response, lipid uptake, and ORP9 expression in oxLDL-stimulated monocyte/macrophages*. Cardiovasc Res, 2009. **83**(1): p. 131-9.
136. Yang, K., et al., *MiR-146a inhibits oxidized low-density lipoprotein-induced lipid accumulation and inflammatory response via targeting toll-like receptor 4*. FEBS Lett, 2011. **585**(6): p. 854-60.
137. Liu, G., et al., *miR-147, a microRNA that is induced upon Toll-like receptor stimulation, regulates murine macrophage inflammatory responses*. Proc Natl Acad Sci U S A, 2009. **106**(37): p. 15819-24.
138. Chen, T., et al., *MicroRNA-155 regulates lipid uptake, adhesion/chemokine marker secretion and SCG2 expression in oxLDL-stimulated dendritic cells/macrophages*. Int J Cardiol, 2011. **147**(3): p. 446-7.
139. Huang, R.S., et al., *MicroRNA-155 silencing enhances inflammatory response and lipid uptake in oxidized low-density lipoprotein-stimulated human THP-1 macrophages*. J Investig Med, 2010. **58**(8): p. 961-7.

140. Tang, B., *et al.*, Identification of MyD88 as a novel target of miR-155, involved in negative regulation of Helicobacter pylori-induced inflammation. FEBS Lett, 2010. **584**(8): p. 1481-6.
141. Naqvi, A.R., *et al.*, MicroRNAs responsive to Aggregatibacter actinomycetemcomitans and Porphyromonas gingivalis LPS modulate expression of genes regulating innate immunity in human macrophages. Innate Immun, 2014. **20**(5): p. 540-51.
142. Gantier, M.P., *et al.*, A miR-19 regulon that controls NF-kappaB signaling. Nucleic Acids Res, 2012. **40**(16): p. 8048-58.
143. Feng, J., *et al.*, miR-21 attenuates lipopolysaccharide-induced lipid accumulation and inflammatory response: potential role in cerebrovascular disease. Lipids Health Dis, 2014. **13**: p. 27.
144. Sheedy, F.J., *et al.*, Negative regulation of TLR4 via targeting of the proinflammatory tumor suppressor PDCD4 by the microRNA miR-21. Nat Immunol, 2010. **11**(2): p. 141-7.
145. Shang, Y.Y., *et al.*, MicroRNA-21, induced by high glucose, modulates macrophage apoptosis via programmed cell death 4. Mol Med Rep, 2015. **12**(1): p. 463-9.
146. Maegdefessel, L., *et al.*, Erratum: miR-24 limits aortic vascular inflammation and murine abdominal aneurysm development. Nat Commun, 2015. **6**: p. 6506.
147. Zhang, L., *et al.*, MicroRNA-26b Modulates the NF-kappaB Pathway in Alveolar Macrophages by Regulating PTEN. J Immunol, 2015. **195**(11): p. 5404-14.
148. Jennewein, C., *et al.*, MicroRNA-27b contributes to lipopolysaccharide-mediated peroxisome proliferator-activated receptor gamma (PPARgamma) mRNA destabilization. J Biol Chem, 2010. **285**(16): p. 11846-53.
149. Cai, Y., *et al.*, STAT3-dependent transactivation of miRNA genes following Toxoplasma gondii infection in macrophage. Parasit Vectors, 2013. **6**: p. 356.
150. Jiang, P., *et al.*, MiR-34a inhibits lipopolysaccharide-induced inflammatory response through targeting Notch1 in murine macrophages. Exp Cell Res, 2012. **318**(10): p. 1175-84.
151. Rodriguez-Ubreva, J., *et al.*, C/EBPa-mediated activation of microRNAs 34a and 223 inhibits Lef1 expression to achieve efficient reprogramming into macrophages. Mol Cell Biol, 2014. **34**(6): p. 1145-57.
152. Lai, L., *et al.*, MicroRNA-92a negatively regulates Toll-like receptor (TLR)-triggered inflammatory response in macrophages by targeting MKK4 kinase. J Biol Chem, 2013. **288**(11): p. 7956-67.
153. Banerjee, S., *et al.*, miR-125a-5p regulates differential activation of macrophages and inflammation. J Biol Chem, 2013. **288**(49): p. 35428-36.
154. Rajaram, M.V., *et al.*, Mycobacterium tuberculosis lipomannan blocks TNF biosynthesis by regulating macrophage MAPK-activated protein kinase 2 (MK2) and microRNA miR-125b. Proc Natl Acad Sci U S A, 2011. **108**(42): p. 17408-13.
155. Ren, D., *et al.*, SR-A deficiency reduces myocardial ischemia/reperfusion injury; involvement of increased microRNA-125b expression in macrophages. Biochim Biophys Acta, 2013. **1832**(2): p. 336-46.
156. Ruckerl, D., *et al.*, Induction of IL-4Ralpha-dependent microRNAs identifies PI3K/Akt signaling as essential for IL-4-driven murine macrophage proliferation in vivo. Blood, 2012. **120**(11): p. 2307-16.
157. Ying, H., *et al.*, MiR-127 modulates macrophage polarization and promotes lung inflammation and injury by activating the JNK pathway. J Immunol, 2015. **194**(3): p. 1239-51.

158. Lin, L., et al., *Type I IFN inhibits innate IL-10 production in macrophages through histone deacetylase 11 by downregulating microRNA-145*. J Immunol, 2013. **191**(7): p. 3896-904.
159. Prakhar, P., et al., *Ac2PIM-responsive miR-150 and miR-143 Target Receptor-interacting Protein Kinase 2 and Transforming Growth Factor Beta-activated Kinase 1 to Suppress NOD2-induced Immunomodulators*. J Biol Chem, 2015. **290**(44): p. 26576-86.
160. Wang, Z., et al., *Leukotriene B4 enhances the generation of proinflammatory microRNAs to promote MyD88-dependent macrophage activation*. J Immunol, 2014. **192**(5): p. 2349-56.
161. De Santis, R., et al., *miR-155 targets Caspase-3 mRNA in activated macrophages*. RNA Biol, 2015: p. 0.
162. Pierdomenico, A.M., et al., *MicroRNA-181b regulates ALX/FPR2 receptor expression and proresolution signaling in human macrophages*. J Biol Chem, 2015. **290**(6): p. 3592-600.
163. Qi, J., et al., *microRNA-210 negatively regulates LPS-induced production of proinflammatory cytokines by targeting NF-kappaB1 in murine macrophages*. FEBS Lett, 2012. **586**(8): p. 1201-7.
164. Zhao, L., et al., *The mutual regulation between miR-214 and A2AR signaling plays an important role in inflammatory response*. Cell Signal, 2015. **27**(10): p. 2026-34.
165. Ortega, F.J., et al., *Inflammation triggers specific microRNA profiles in human adipocytes and macrophages and in their supernatants*. Clin Epigenetics, 2015. **7**(1): p. 49.
166. Graff, J.W., et al., *Identifying functional microRNAs in macrophages with polarized phenotypes*. J Biol Chem, 2012. **287**(26): p. 21816-25.
167. Wang, J., et al., *miR-223 Inhibits Lipid Deposition and Inflammation by Suppressing Toll-Like Receptor 4 Signaling in Macrophages*. Int J Mol Sci, 2015. **16**(10): p. 24965-82.
168. Xi, X., et al., *MicroRNA-223 Is Upregulated in Active Tuberculosis Patients and Inhibits Apoptosis of Macrophages by Targeting FOXO3*. Genet Test Mol Biomarkers, 2015.
169. Ponomarev, E.D., et al., *MicroRNA-124 promotes microglia quiescence and suppresses EAE by deactivating macrophages via the C/EBP-alpha-PU.1 pathway*. Nat Med, 2011. **17**(1): p. 64-70.
170. Zhuang, G., et al., *A novel regulator of macrophage activation: miR-223 in obesity-associated adipose tissue inflammation*. Circulation, 2012. **125**(23): p. 2892-903.
171. Arranz, A., et al., *Akt1 and Akt2 protein kinases differentially contribute to macrophage polarization*. Proc Natl Acad Sci U S A, 2012. **109**(24): p. 9517-22.
172. Davis, B.N., et al., *Induction of microRNA-221 by platelet-derived growth factor signaling is critical for modulation of vascular smooth muscle phenotype*. J Biol Chem, 2009. **284**(6): p. 3728-38.
173. Chan, M.C., et al., *Molecular basis for antagonism between PDGF and the TGFbeta family of signalling pathways by control of miR-24 expression*. EMBO J, 2010. **29**(3): p. 559-73.
174. Liu, X., et al., *MicroRNA-31 regulated by the extracellular regulated kinase is involved in vascular smooth muscle cell growth via large tumor suppressor homolog 2*. J Biol Chem, 2011. **286**(49): p. 42371-80.

175. Sun, S.G., *et al.*, *miR-146a and Kruppel-like factor 4 form a feedback loop to participate in vascular smooth muscle cell proliferation*. EMBO Rep, 2011. **12**(1): p. 56-62.
176. Zhang, Y., *et al.*, *Insulin promotes vascular smooth muscle cell proliferation via microRNA-208-mediated downregulation of p21*. J Hypertens, 2011. **29**(8): p. 1560-8.
177. Leeper, N.J., *et al.*, *MicroRNA-26a is a novel regulator of vascular smooth muscle cell function*. J Cell Physiol, 2011. **226**(4): p. 1035-43.
178. Chen, J., *et al.*, *Induction of microRNA-1 by myocardin in smooth muscle cells inhibits cell proliferation*. Arterioscler Thromb Vasc Biol, 2011. **31**(2): p. 368-75.
179. Torella, D., *et al.*, *MicroRNA-133 controls vascular smooth muscle cell phenotypic switch in vitro and vascular remodeling in vivo*. Circ Res, 2011. **109**(8): p. 880-93.
180. Cordes, K.R., *et al.*, *miR-145 and miR-143 regulate smooth muscle cell fate and plasticity*. Nature, 2009. **460**(7256): p. 705-10.
181. Grundmann, S., *et al.*, *MicroRNA-100 regulates neovascularization by suppression of mammalian target of rapamycin in endothelial and vascular smooth muscle cells*. Circulation, 2011. **123**(9): p. 999-1009.
182. Yu, M.L., *et al.*, *Vascular smooth muscle cell proliferation is influenced by let-7d microRNA and its interaction with KRAS*. Circ J, 2011. **75**(3): p. 703-9.
183. Lin, Y., *et al.*, *Involvement of MicroRNAs in hydrogen peroxide-mediated gene regulation and cellular injury response in vascular smooth muscle cells*. J Biol Chem, 2009. **284**(12): p. 7903-13.
184. Li, Y., *et al.*, *MicroRNA-21 inhibits platelet-derived growth factor-induced human aortic vascular smooth muscle cell proliferation and migration through targeting activator protein-1*. Am J Transl Res, 2014. **6**(5): p. 507-16.
185. Fujita, S., *et al.*, *miR-21 Gene expression triggered by AP-1 is sustained through a double-negative feedback mechanism*. J Mol Biol, 2008. **378**(3): p. 492-504.
186. Jazbutyte, V. and T. Thum, *MicroRNA-21: from cancer to cardiovascular disease*. Curr Drug Targets, 2010. **11**(8): p. 926-35.
187. Fulci, V., *et al.*, *Quantitative technologies establish a novel microRNA profile of chronic lymphocytic leukemia*. Blood, 2007. **109**(11): p. 4944-51.
188. Lawrie, C.H., *et al.*, *MicroRNA expression distinguishes between germinal center B cell-like and activated B cell-like subtypes of diffuse large B cell lymphoma*. Int J Cancer, 2007. **121**(5): p. 1156-61.
189. Pichiorri, F., *et al.*, *MicroRNAs regulate critical genes associated with multiple myeloma pathogenesis*. Proc Natl Acad Sci U S A, 2008. **105**(35): p. 12885-90.
190. Sheedy, F.J., *Turning 21: Induction of miR-21 as a Key Switch in the Inflammatory Response*. Front Immunol, 2015. **6**: p. 19.
191. Roy, S. and C.K. Sen, *MiRNA in innate immune responses: novel players in wound inflammation*. Physiol Genomics, 2011. **43**(10): p. 557-65.
192. Cheng, Y. and C. Zhang, *MicroRNA-21 in cardiovascular disease*. J Cardiovasc Transl Res, 2010. **3**(3): p. 251-5.
193. Boldin, M.P. and D. Baltimore, *MicroRNAs, new effectors and regulators of NF-kappaB*. Immunol Rev, 2012. **246**(1): p. 205-20.
194. Loffler, D., *et al.*, *Interleukin-6 dependent survival of multiple myeloma cells involves the Stat3-mediated induction of microRNA-21 through a highly conserved enhancer*. Blood, 2007. **110**(4): p. 1330-3.
195. Lu, T.X., *et al.*, *MicroRNA-21 limits in vivo immune response-mediated activation of the IL-12/IFN-gamma pathway, Th1 polarization, and the severity of delayed-type hypersensitivity*. J Immunol, 2011. **187**(6): p. 3362-73.

196. Lu, J., *et al.*, *MicroRNA expression profiles classify human cancers*. *Nature*, 2005. **435**(7043): p. 834-8.
197. Monticelli, S., *et al.*, *MicroRNA profiling of the murine hematopoietic system*. *Genome Biol*, 2005. **6**(8): p. R71.
198. Cobb, B.S., *et al.*, *A role for Dicer in immune regulation*. *J Exp Med*, 2006. **203**(11): p. 2519-27.
199. Wu, H., *et al.*, *miRNA profiling of naive, effector and memory CD8 T cells*. *PLoS One*, 2007. **2**(10): p. e1020.
200. Kasashima, K., Y. Nakamura, and T. Kozu, *Altered expression profiles of microRNAs during TPA-induced differentiation of HL-60 cells*. *Biochem Biophys Res Commun*, 2004. **322**(2): p. 403-10.
201. Cekaite, L., T. Clancy, and M. Sioud, *Increased miR-21 expression during human monocyte differentiation into DCs*. *Front Biosci (Elite Ed)*, 2010. **2**: p. 818-28.
202. Hashimi, S.T., *et al.*, *MicroRNA profiling identifies miR-34a and miR-21 and their target genes JAG1 and WNT1 in the coordinate regulation of dendritic cell differentiation*. *Blood*, 2009. **114**(2): p. 404-14.
203. Lu, T.X., A. Munitz, and M.E. Rothenberg, *MicroRNA-21 is up-regulated in allergic airway inflammation and regulates IL-12p35 expression*. *J Immunol*, 2009. **182**(8): p. 4994-5002.
204. Landgraf, P., *et al.*, *A mammalian microRNA expression atlas based on small RNA library sequencing*. *Cell*, 2007. **129**(7): p. 1401-14.
205. Moschos, S.A., *et al.*, *Expression profiling in vivo demonstrates rapid changes in lung microRNA levels following lipopolysaccharide-induced inflammation but not in the anti-inflammatory action of glucocorticoids*. *BMC Genomics*, 2007. **8**: p. 240.
206. Sonkoly, E., *et al.*, *MicroRNAs: novel regulators involved in the pathogenesis of psoriasis?* *PLoS One*, 2007. **2**(7): p. e610.
207. Zhang, Y., *et al.*, *MicroRNA-21 controls the development of osteoarthritis by targeting GDF-5 in chondrocytes*. *Exp Mol Med*, 2014. **46**: p. e79.
208. Ruan, Q., *et al.*, *MicroRNA-21 regulates T-cell apoptosis by directly targeting the tumor suppressor gene Tipe2*. *Cell Death Dis*, 2014. **5**: p. e1095.
209. Wang, L., *et al.*, *Regulation of T lymphocyte activation by microRNA-21*. *Mol Immunol*, 2014. **59**(2): p. 163-71.
210. Sawant, D.V., *et al.*, *The Bcl6 target gene microRNA-21 promotes Th2 differentiation by a T cell intrinsic pathway*. *Mol Immunol*, 2013. **54**(3-4): p. 435-42.
211. Stagakis, E., *et al.*, *Identification of novel microRNA signatures linked to human lupus disease activity and pathogenesis: miR-21 regulates aberrant T cell responses through regulation of PDCD4 expression*. *Ann Rheum Dis*, 2011. **70**(8): p. 1496-506.
212. Gao, W., *et al.*, *A systematic-analysis of predicted miR-21 targets identifies a signature for lung cancer*. *Biomed Pharmacother*, 2012. **66**(1): p. 21-8.
213. Terrell, A.M., *et al.*, *Jak/STAT/SOCS signaling circuits and associated cytokine-mediated inflammation and hypertrophy in the heart*. *Shock*, 2006. **26**(3): p. 226-34.
214. Campbell, I.L., *Cytokine-mediated inflammation, tumorigenesis, and disease-associated JAK/STAT/SOCS signaling circuits in the CNS*. *Brain Res Brain Res Rev*, 2005. **48**(2): p. 166-77.
215. Case, S.R., *et al.*, *MicroRNA-21 inhibits toll-like receptor 2 agonist-induced lung inflammation in mice*. *Exp Lung Res*, 2011. **37**(8): p. 500-8.

216. Medina, P.P., M. Nolde, and F.J. Slack, *OncomiR addiction in an in vivo model of microRNA-21-induced pre-B-cell lymphoma*. Nature, 2010. **467**(7311): p. 86-90.
217. Hatley, M.E., et al., *Modulation of K-Ras-dependent lung tumorigenesis by MicroRNA-21*. Cancer Cell, 2010. **18**(3): p. 282-93.
218. Chan, J.A., A.M. Krichevsky, and K.S. Kosik, *MicroRNA-21 is an antiapoptotic factor in human glioblastoma cells*. Cancer Res, 2005. **65**(14): p. 6029-33.
219. Si, M.L., et al., *miR-21-mediated tumor growth*. Oncogene, 2007. **26**(19): p. 2799-803.
220. Buscaglia, L.E. and Y. Li, *Apoptosis and the target genes of microRNA-21*. Chin J Cancer, 2011. **30**(6): p. 371-80.
221. Cheng, Y., et al., *MicroRNA-21 protects against the H₂O₂-induced injury on cardiac myocytes via its target gene PDCD4*. J Mol Cell Cardiol, 2009. **47**(1): p. 5-14.
222. Dong, S., et al., *MicroRNA expression signature and the role of microRNA-21 in the early phase of acute myocardial infarction*. J Biol Chem, 2009. **284**(43): p. 29514-25.
223. Sayed, D., et al., *MicroRNA-21 is a downstream effector of AKT that mediates its antiapoptotic effects via suppression of Fas ligand*. J Biol Chem, 2010. **285**(26): p. 20281-90.
224. Smith, J.D., et al., *Decreased atherosclerosis in mice deficient in both macrophage colony-stimulating factor (op) and apolipoprotein E*. Proc Natl Acad Sci U S A, 1995. **92**(18): p. 8264-8.
225. Zeller, I. and S. Srivastava, *Macrophage functions in atherosclerosis*. Circ Res, 2014. **115**(12): p. e83-5.
226. Andreou, I., et al., *miRNAs in atherosclerotic plaque initiation, progression, and rupture*. Trends Mol Med, 2015. **21**(5): p. 307-18.
227. Nazari-Jahantigh, M., et al., *MicroRNA-specific regulatory mechanisms in atherosclerosis*. J Mol Cell Cardiol, 2014.
228. Hosin, A.A., et al., *MicroRNAs in atherosclerosis*. J Vasc Res, 2014. **51**(5): p. 338-49.
229. Ma, X., et al., *Loss of the miR-21 allele elevates the expression of its target genes and reduces tumorigenesis*. Proc Natl Acad Sci U S A, 2011. **108**(25): p. 10144-9.
230. Ma, X., et al., *The oncogenic microRNA miR-21 promotes regulated necrosis in mice*. Nat Commun, 2015. **6**: p. 7151.
231. Srivastava, S., et al., *Aldose reductase protects against early atherosclerotic lesion formation in apolipoprotein E-null mice*. Circ Res, 2009. **105**(8): p. 793-802.
232. Barski, O.A., et al., *Dietary carnosine prevents early atherosclerotic lesion formation in apolipoprotein E-null mice*. Arterioscler Thromb Vasc Biol, 2013. **33**(6): p. 1162-70.
233. Baba, S.P., et al., *Reductive metabolism of AGE precursors: a metabolic route for preventing AGE accumulation in cardiovascular tissue*. Diabetes, 2009. **58**(11): p. 2486-97.
234. Srivastava, S., et al., *Oral exposure to acrolein exacerbates atherosclerosis in apoE-null mice*. Atherosclerosis, 2011. **215**(2): p. 301-8.
235. Mukhopadhyay, A., et al., *Genetic deletion of the tumor necrosis factor receptor p60 or p80 abrogates ligand-mediated activation of nuclear factor-kappa B and of mitogen-activated protein kinases in macrophages*. J Biol Chem, 2001. **276**(34): p. 31906-12.

236. Libby, P., *Mechanisms of acute coronary syndromes and their implications for therapy*. N Engl J Med, 2013. **368**(21): p. 2004-13.
237. Cochain, C. and A. Zerneck, *Noncoding RNAs in vascular inflammation and atherosclerosis: recent advances toward therapeutic applications*. Curr Opin Lipidol, 2014. **25**(5): p. 380-6.
238. Iliopoulos, D., et al., *STAT3 activation of miR-21 and miR-181b-1 via PTEN and CYLD are part of the epigenetic switch linking inflammation to cancer*. Mol Cell, 2010. **39**(4): p. 493-506.
239. Shin, V.Y., et al., *NF-kappaB targets miR-16 and miR-21 in gastric cancer: involvement of prostaglandin E receptors*. Carcinogenesis, 2011. **32**(2): p. 240-5.
240. Recchiuti, A., et al., *MicroRNAs in resolution of acute inflammation: identification of novel resolvin D1-miRNA circuits*. FASEB J, 2011. **25**(2): p. 544-60.
241. Libby, P., A.H. Lichtman, and G.K. Hansson, *Immune effector mechanisms implicated in atherosclerosis: from mice to humans*. Immunity, 2013. **38**(6): p. 1092-104.
242. Nahid, M.A., M. Satoh, and E.K. Chan, *MicroRNA in TLR signaling and endotoxin tolerance*. Cell Mol Immunol, 2011. **8**(5): p. 388-403.
243. O'Connell, R.M., et al., *MicroRNA-155 is induced during the macrophage inflammatory response*. Proc Natl Acad Sci U S A, 2007. **104**(5): p. 1604-9.
244. Barnett, R.E., et al., *Anti-inflammatory effects of miR-21 in the macrophage response to peritonitis*. J Leukoc Biol, 2016. **99**(2): p. 361-71.
245. Feng, B., et al., *Niemann-Pick C heterozygosity confers resistance to lesional necrosis and macrophage apoptosis in murine atherosclerosis*. Proc Natl Acad Sci U S A, 2003. **100**(18): p. 10423-8.
246. Kueanjinda, P., S. Roytrakul, and T. Palaga, *A Novel Role of Numb as A Regulator of Pro-inflammatory Cytokine Production in Macrophages in Response to Toll-like Receptor 4*. Sci Rep, 2015. **5**: p. 12784.
247. Mei, Y., et al., *miR-21 modulates the ERK-MAPK signaling pathway by regulating SPRY2 expression during human mesenchymal stem cell differentiation*. J Cell Biochem, 2013. **114**(6): p. 1374-84.
248. Ling, M., et al., *Regulation of miRNA-21 by reactive oxygen species-activated ERK/NF-kappaB in arsenite-induced cell transformation*. Free Radic Biol Med, 2012. **52**(9): p. 1508-18.
249. Curtiss, L.K. and P.S. Tobias, *Emerging role of Toll-like receptors in atherosclerosis*. J Lipid Res, 2009. **50 Suppl**: p. S340-5.
250. O'Neill, L.A., F.J. Sheedy, and C.E. McCoy, *MicroRNAs: the fine-tuners of Toll-like receptor signalling*. Nat Rev Immunol, 2011. **11**(3): p. 163-75.
251. Duewell, P., et al., *NLRP3 inflammasomes are required for atherogenesis and activated by cholesterol crystals*. Nature, 2010. **464**(7293): p. 1357-61.
252. Taganov, K.D., et al., *NF-kappaB-dependent induction of microRNA miR-146, an inhibitor targeted to signaling proteins of innate immune responses*. Proc Natl Acad Sci U S A, 2006. **103**(33): p. 12481-6.
253. Liu, L.Z., et al., *MiR-21 induced angiogenesis through AKT and ERK activation and HIF-1alpha expression*. PLoS One, 2011. **6**(4): p. e19139.
254. Shen, H., et al., *Alteration in Mir-21/PTEN expression modulates gefitinib resistance in non-small cell lung cancer*. PLoS One, 2014. **9**(7): p. e103305.

CURRICULUM VITAE

NAME: Rihab Hamed- Berair

ADDRESS: University of Louisville
Diabetes and Obesity Center
580 South Preston Street, Room 211
(502) 852-4216
Louisville, KY 40202

EDUCATION: B.S., Microbiology
Alahlia University, Sudan
1994-1998

M.S., Molecular Biology
University of Khartoum, Sudan
2000-2002

Ph.D., Biochemistry and Molecular Genetics
University of Louisville
2010-2016

TRAINING: Postgraduate research in genetic susceptibility to Leishmaniosis,
Wellcome Center for Molecular Mechanisms in Diseases (MMD),
Cambridge University, UK.
2000-2001

Medical genetics for developing countries, International Center for
Genetic Engineering and Biotechnology, Trieste, Italy
2003

Research in Y-chromosome and sickle cell disease, Stanford
University, USA
2004

AWARDS: Travel and research grant, Wellcome Trust, University of
Cambridge, Cambridge, UK
2000

Integrated Programs in Biomedical Sciences (IPIBS)
University of Louisville, Louisville, KY
Graduate Fellowship Recipient
August 2010- August 2012

Pre-doctoral Graduate Fellowship
University of Louisville
August 2010 – 2016

NIH/NHLBI supported Pre-doctoral Supplement Grant
(5R01HL055477)
Title: Toxicity and Detoxification of 4-Hydroxyalkenals in Heart
August 2013- May 2015

Arteriosclerosis, Thrombosis and Vascular Biology (ATVB)
meeting, San Francisco, May 6-8, 2015. Abstract was selected
“among the top 10 percent of the accepted abstracts”

PROFESSIONAL MEMBERSHIP:

American Heart Association (AHA). Council on Arteriosclerosis,
Thrombosis and Vascular Biology

National Black Graduate Student Association (NBGSA)

PUBLICATIONS:

Berair REH, Mohamed HS, Seielstad M, El Hassan AM, Khalil EAG, Peacock CS, Blackwell JM, Ibrahim ME (2003) Allele frequency and genotype distribution of polymorphism within disease-related genes is influenced by ethnic population sub-structuring in Sudan. *Genetica*; 119(1): 57-63.

Mohamed HS, Ibrahim ME, Miller EN, Peacock CS, Khalil EA, Cordell HJ, Howson JM, El Hassan AM, **Berair REH**, Blackwell JM. (2003). Genetic susceptibility to visceral leishmaniasis in the Sudan: Linkage and Association with IL4 and IFNGR1. *Gene and Immunity* 4(5): 351-5.

Rihab E. Bereir, Hisham Y Hassan, Niven A Salih, Peter A Underhill, Luigi L Cavalli-Sforza, Ayman A Hussain, Dominic Kwiatowski, Muntaser E Ibrahim (2007). Co-intrgression of Y-chromosome haplogroups and the sickle cell gene across Africa's Sahel. *European journal of human genetics* 15:1183-1185.

Ibrahim ME, Mahdi MA, **Bereir RE**, Giha RS, Wasunna C (2008). Evolutionary conservation of RNA editing in the genus *Leishmania*. *Infection, genetics and evolution* 8(3): 378-80.

Srinivas D. Sithu, Marina Malovichko, Krista A. Riggs, Nalinie S. Wickramasinghe, Millicent G. Winner, Abhinav Agarwal, **Rihab E.**

Hamid-Berair, Daniel W. Riggs, Aruni Bhatnagar, and Sanjay Srivastava. Atherogenesis and metabolic dysregulation in LDL receptor knockout rats. (Circ Res in Revision).

ABSTRACT AND POSTER

Berair REH, Mohamed HS, Peacock CS, Blackwell JM, Ibrahim ME. Polymorphism in Disease-related Genes and Ethnic Population Sub-structuring. Oral presentation at the second Genetics Meeting on: The genetics of the population of East Africa, Sudan, 2002.

Rihab Hamed-Berair, Srinivas D Sithu, Krista A Riggs, Millicent G Winner, Daniel W Riggs, Nalinie S Wickramasinghe, Abhinav Agarwal, Aruni Bhatnagar, Sanjay Srivastava. Circulating MicroRNAs as Biomarkers of Atherosclerosis in LDL Receptor Knockout Rats. Poster Presentation at Research Louisville, Louisville, KY. 2012.

Rihab E Hamed-Berair, Pawel Lorkiewicz, Srinivas D Sithu, Krista A Riggs, Marina Malovichko, Millicent G Winner, Abhinav Agarwal, Daniel W Riggs, Aruni Bhatnagar, Sanjay Srivastava. Dyslipidemia, Obesity, Insulin Resistance and Atherosclerosis in LDL-Receptor Deficient Rats. Poster Presentation at ATVB meeting, San Francisco, CA, 2015.

* Abstract was selected to re-present at AHA Scientific Session 2015.

Rihab E. Hamed-Berair, Abhinav Agarwal, Marcin Wysoczynski, Srinivas D. Sithu, Nalinie Wickramasinghe, Millicent G. Winner, Aruni Bhatnagar, Yong Li and Sanjay Srivastava. Anti-atherogenic effects of microRNA-21. Poster Presentation at AHA meeting, Orlando, FL, 2015.

EXPERTISE

Research

Molecular Biology and Biochemistry laboratory techniques including Western Blot, ELISA, immunohistochemistry, cell culture, transfection, flow cytometry, confocal microscopy, RNA and DNA purification, PCR, QRT-PCR.

Computer-based data analysis including Excel, Sigma Plot, FloJo, Photoshop, ImageJ, BD FACSDiva Software

Teaching

Teaching Assistant – Advanced Biochemistry, One-on-one teaching to graduate students and graded papers, UofL 2012.

Teaching Assistant - Immunology Department, Alahlia University, 2003. Prepared and gave lectures

Communication

Writing skills through preparation of manuscripts, grant proposals, and posters.

Presentations including departmental seminars and international conference poster presentations